

EMFO
EMISSIONSFORSKNINGSPROGRAMMET

WEAREM

Wear particles from road traffic

- a field, laboratory and
modelling study

Final report

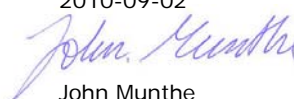
Åke Sjödin, Martin Ferm, Anders Björk, Magnus Rahmberg, IVL
Anders Gudmundsson, Erik Swietlicki, Lund University
Christer Johansson, SLB analys
Mats Gustafsson, Göran Blomqvist, VTI

B1830
June 2010



Organization IVL Swedish Environmental Research Institute Ltd.	Report Summary
Address P.O. Box 5302 SE-400 14 Göteborg	Project title Trafikgenererade inandningsbara slitagepartiklar: bildningsprocesser, emissionsfaktorer och förekomst ur åtgärdsperspektiv - EMFO dnr AL90 B 2004:01351 Project sponsor Emissionsforskningsprogrammet (www.pff.nu) Stiftelsen IVL (www.ivl.se)
Telephone +46 (0)31-725 62 00	
Authors Åke Sjödin, Martin Ferm, Anders Björk, Magnus Rahmberg, IVL Anders Gudmundsson, Erik Swietlicki, Lund University Christer Johansson, SLB analys Mats Gustafsson, Göran Blomquist, VTI	
Title and subtitle of the report Wear particles from road traffic - a field, laboratory and modeling study	
Summary The present report forms the final report from a major research project within the Swedish National Road Vehicle Emission Research Programme EMFO, carried out during the period 2005-2008. The project was carried out in collaboration between IVL, Lund University, SLB analys and VTI. Within the project extensive data have been collected by a variety of methods for measuring, sampling and analysing the chemical composition of different fractions of airborne particulate matter, with emphasis on the PM ₁₀ fraction. Collected data originate from indoor measurements in controlled runs with a circular road simulator as well as ambient air measurements at both street and roof level in a variety of Swedish cities. Based on elemental (metals etc.) source profiles of various sources to the different particle fractions, derived from the literature or from measurements carried out within the project, several different receptor models (e.g. COPREM, PMF) were applied to the collected data to derive the contribution from exhaust, brake wear, tyre wear, road surface wear, long-range transport etc., to the measured concentrations of PM ₁₀ and other particle fractions in urban environments. An important result of the project is the evidence for the great importance of studded tyres for the high PM ₁₀ concentration levels that occur in many Swedish cities during winter and early spring. According to the controlled indoor experiments with the road simulator studded tyres give rise to ten times higher emissions of PM ₁₀ than non-studded (friction) winter tyres, while PM ₁₀ emissions caused by summer tyres is almost negligible.	
Keyword PM, PM ₁₀ , PM _{2.5} , PM ₁ , particles, particulate matter, road traffic, emissions, urban air, road wear, tyre wear, brake wear, exhaust, modeling, models, COPREM, PMF, PCA	
Bibliographic data IVL Report B1830	
The report can be ordered via Homepage: www.ivl.se , e-mail: publicationservice@ivl.se , fax+46 (0)8-598 563 90, or via IVL, P.O. Box 21060, SE-100 31 Stockholm Sweden	

This report approved
2010-09-02



John Munthe
Scientific Director

Foreword

The present report forms the final report from the research project "Traffic generated inhalable wear particles: Formation processes, emission factors and occurrence from the viewpoint of measures" (in Swedish: "Trafikgenererade inandningsbara slitagepartiklar: bildningsprocesser, emissionsfaktorer och förekomst ur åtgärdsperspektiv", EMFO dnr AL90 B 2004:01351), carried out within the Swedish National Road Vehicle Emission Research Programme EMFO (Emissionsforskningsprogrammet - <http://www.pff.nu/>) during the period 2005-2008. The project was carried out in collaboration between IVL Swedish Environmental Research Institute, Department of Design Sciences at Lund University, SLB · analys at the Environment and Health Administration of the City of Stockholm, and VTI - Swedish National Road and Transport Research Institute. The funding organisations within EMFO of the project were the Swedish Road Administration and the Swedish Environmental Protection Agency. Also, the Foundation of the Swedish Environmental Research Institute (SIVL) provided additional funding to the project.

Summary

This report is an outcome of a major research effort within the Swedish National Road Vehicle Emission Research Programme EMFO, carried out 2005-2008 in collaboration between IVL, Lund University, the City of Stockholm and VTI. The aims of the project were:

- to determine the chemical and physical composition (i.e. the source profile) of road traffic generated airborne particles through both measurements in field and indoor measurements using a circular road simulator,
- to clarify the role of different factors which influence the formation of airborne particles from vehicle tyres and road surface interactions by experimental studies in a road simulator and by measurements in urban environments, and determine the emission factors for various combinations of these factors,
- to determine the traffic contribution to airborne particles in urban air and traffic environments and identify their origin (brake wear, tyre wear, road surface wear etc.),
- to develop a scientific basis for proposals for cost-effective measures to reduce the occurrence of wear particles in urban air.

Within the project extensive data have been collected by a variety of methods for measuring, sampling and analysing the chemical composition of primarily three different fractions of particulate matter - PM_{10} , $PM_{2.5}$, PM_1 . Emphasis has been on the PM_{10} fraction, in the case of which preferably the major Swedish cities experience significant problems with complying with the legally binding air quality standards. The collected data originate from indoor measurements in controlled runs with the VTI circular road simulator as well as ambient air measurements at both street and roof level in a variety of Swedish cities.

Based on elemental (metals etc.) source profiles of various sources to the different particle fractions, derived from the literature or from measurements carried out within the project, several different receptor models (e.g. COPREM, PMF) were applied to the collected data to derive the contributions from exhaust, brake wear, tyre wear, road surface wear, long-range transport etc., to the measured concentrations of PM_{10} and other particle fractions in urban environments.

Furthermore, from the measurements, emission factors (expressed in grams per vehkm) for the various particle fractions, as well as for a large number of contained metals (about 30 metals) were derived for a major city street in Stockholm. Total emission factors as well as emission factors for each of the different source types (exhaust, brake wear, tyre wear and road surface wear) have also been derived from the measurements.

Corresponding emission factors for the two source types tyre wear and road surface wear have been derived from the measurements in the circular road simulator. From these measurements, emission factors have also been derived for different particle size (aerodynamic particle diameter) as well as for different speeds in the range 30-70 km/h and different types of tyres (studded tyres, friction tyres, summer tyres). The road pavement in the road simulator applied in these measurements was the same as the pavement of the city street in Stockholm where ambient air measurements of particulate matter were made. According to the road simulator experiments, studded tyres give rise to ten times higher emissions of PM_{10} than friction tyres, while PM_{10} emissions caused by summer tyres are almost negligible.

The emission factor for PM_{10} derived from the road simulator experiments corresponds reasonably well with that derived from measurements in street canyons. The main sources of PM_{10} are road surface and tyre wear, while for $PM_{2.5}$ the dominant contribution is often from long-range transport. The applied receptor models are complementary and partly yield different results. Regarding PM_{10} , there is a large uncertainty especially as regards the contribution of tyre wear, due to a lack of knowledge regarding source profiles for different types of tyres.

Sammanfattning

EMFO:s projekt *Trafikgenererade inandningsbara slitagepartiklar: bildningsprocesser, emissionsfaktorer, och förekomst ur åtgärdspektiv* har genomförts under perioden 2005-2008 som ett samarbete mellan IVL, Lunds tekniska högskola, SLB analys vid Miljöförvaltningen i Stockholm samt VTI.

Projektets syfte har varit att:

- bestämma den kemiska och fysikaliska sammansättningen (dvs källprofilen) på trafikgenererade inandningsbara partiklar genom både mätningar i fält och under kontrollerade former med utnyttjande av VTI:s provvägsmaskin (PVM),
- klarlägga betydelsen av olika faktorer som påverkar bildningen av inandningsbara partiklar vid däck-vägbaneslitage genom experimentella studier i PVM respektive mätningar i urban miljö, och bestämma emissionsfaktorer för olika kombinationer av dessa faktorer,
- bestämma trafikens bidrag till inandningsbara partiklar i trafiknära miljöer och identifiera deras ursprung (bromsar, däck, vägbana etc.),
- ta fram ett vetenskapligt underlag för förslag till kostnadseffektiva åtgärder för att minska förekomsten av inandningsbara partiklar i tätortsluft och trafiknära miljöer.

Inom projektet har omfattande data samlats in med en rad olika metoder för mätning, provtagning samt analys av den kemiska sammansättningen av primärt tre olika fraktioner av partiklar - PM₁₀, PM_{2.5}, PM₁. Tonvikten har legat på PM₁₀, för vilken framför allt de svenska storstäderna har betydande problem med överskridanden av gällande miljö kvalitetsnormer, baserade på EU:s luftkvalitetsdirektiv. Insamlade data härrör från mätningar dels i VTI:s provvägsmaskin, dels i gatu- eller takmiljö i såväl större som mindre tätorter i Sverige över hela landet.

Med utgångspunkt från källprofiler för olika källor till de olika partikelfraktionerna, baserade dels på mätningar utförda inom projektet, dels på data hämtade från den senaste litteraturen, har flera olika receptormodeller (COPREM, PMF m.fl.) applicerats på insamlade data för att härleda bidraget från avgaser, bromsslitage, däckslitage, vägslitage samt långdistanstransport till observerade halter av PM₁₀ och övriga partikelfraktioner i olika tätortsmiljöer.

Vidare har ur mätningarna emissionsfaktorer (uttryckta i gram per fordonskm) för dels de olika partikelfraktionerna, dels för i partikelmassan ingående metaller (ca. 30 metaller) härletts för Hornsgatan i Stockholm. Såväl totala emissionsfaktorer som emissionsfaktorer för var och en av de olika källtyperna (avgaser, bromsslitage, däckslitage respektive vägslitage) har kunnat härledas ur mätningarna.

Motsvarande emissionsfaktorer för källtyperna däck- och vägslitage har härletts ur mätningarna i PVM. Ur dessa har emissionsfaktorer också kunnat härledas för olika partikelstorlek (aerodynamisk partikeldiameter), dels för olika hastighet i intervallet 30-70 km/h, dels för olika typer av däck (dubbdäck, friktionsdäck, sommardäck). Beläggningen i PVM i dessa mätningar var densamma som beläggningen på Hornsgatan i Stockholm. Enligt PVM-mätningarna ger dubbdäck upphov till ca 10 ggr högre emissioner av PM₁₀ än friktionsdäck, medan sommardäck ger upphov till i det närmaste försumbara PM₁₀-emissioner.

Emissionsfaktorn för PM₁₀ härledd ur PVM-mätningarna överensstämmer relativt väl med den som kan härledas ur mätningarna på Hornsgatan. De viktigaste källorna till PM₁₀ är väg- och däckslitage, medan för PM_{2.5} utgörs det dominerande bidraget ofta av långdistanstransport.

De tillämpade receptormodellerna är komplementära och ger delvis olika resultat. Beträffande PM₁₀ råder särskilt stor osäkerhet kring bidraget från däckslitage. För att förbättra precisionen i bidragsberäkningarna behövs framför allt bättre kunskap om källprofiler för olika däckstyper.

Table of contents

1	Introduction	7
2	Objectives and approach.....	8
3	Methods	9
3.1	Road simulator set-up.....	9
3.1.1	The VTI circular road simulator	9
3.1.2	Pavement and tyres	10
3.1.3	Test cycle	11
3.1.4	Wear measurements	11
3.1.5	Airborne wear particle sampling	11
3.2	Monitoring and sampling methods	12
3.2.1	SAM – Stationary Aerosol Sampler.....	12
3.2.2	IVL samplers	12
3.2.3	TEOM.....	13
3.2.4	DustTrak (DT).....	13
3.2.5	Scanning Mobility Particle Sizer (SMPS)	14
3.2.6	Aerodynamic Particle Sizer (APS) and Small Deposit Cascade Impactor (SDI)	14
3.2.7	Stacked Filter Units (SFU)	14
3.3	Analytical methods.....	15
3.3.1	PIXE.....	15
3.3.2	ICP-MS.....	15
3.3.3	Ion Chromatography (IC).....	15
3.3.4	PAH.....	15
3.3.5	SEM/EDS.....	16
3.4	Models.....	16
3.4.1	Principal Component Analysis, PCA	17
3.4.2	COPREM	17
3.4.3	PMF	18
4	Measurements	19
4.1	Road simulator.....	19
4.1.1	Emission factor calculation.....	19
4.2	Measurements in Malmö.....	20
4.3	Measurements in Stockholm	21
4.3.1	Campaign measurements.....	21
4.3.2	Continuous/permanent measurements	23
4.4	Measurements within the Swedish Urban Air Quality Network.....	24
5	Results	25
5.1	Road simulator.....	25
5.1.1	The influence of tyres and speed	25
5.1.2	The influence of pavement	27
5.1.3	Morphology of wear particles.....	28
5.1.4	The influence of ambient parameters.....	29
5.1.5	Emission factors	31
5.1.6	Source profiles	33
5.1.7	PCA models.....	35
5.2	Mass closure/mass balance of measured data.....	40
5.2.1	Stockholm.....	40
5.2.3	Road simulator.....	44
5.2.4	Swedish Urban Air Quality Network	45

5.3	Receptor modeling of field data.....	46
5.3.1	Source profiles	46
5.3.2	COPREM - Base results for PM ₁₀ , Hornsgatan	49
5.3.3	COPREM-results for PM _{2.5}	53
5.3.4	COPREM-results for PM ₁	54
5.3.5	COPREM – Variation of contribution due to source profiles	54
5.3.6	PMF modelling results.....	56
5.3.8	Swedish Urban Air Quality Network	61
5.3.9	Comparison of results from different receptor models	61
5.4	PM and trace element emission factors.....	63
5.4.1	Stockholm.....	63
5.4.2	Malmö	67
5.5	Methods comparison.....	71
5.5.1	PM mass measurements	71
5.5.2	Elemental and chemical speciation.....	72
5.6	Sites comparison.....	73
5.6.1	ICP-MS.....	73
5.6.2	PM emission factor determination	74
6	Discussion	75
7	Conclusions	77
8	References	79

Appendix 1. Calculated source contributions for the PM₁₀, PM_{2.5} and PM₁ fractions at Hornsgatan according to PMF

Appendix 2. Calculated (COPREM) source contributions to PM₁₀ in 4 cities within the Swedish Urban Air Quality Network

1 Introduction

Extensive air quality monitoring shows that national and EU air quality standards for PM₁₀ are exceeded in several Swedish cities, especially during dry weather conditions in winter and early spring. No doubt, traffic-generated wear particles play a major role for these exceedances, especially since studded tyres are frequently used in Sweden during the winter season, and may be used without restrictions until May or even longer in the northern part of Sweden. Studded tyres have been proven to increase road wear and/or resuspension drastically and hence the concentrations of fine particles in curbside and urban environments.

Although the violation of PM₁₀ air quality standards in Swedish cities as such presents a major problem, not least legally, recent air pollution and health studies indicate that health is more strongly linked to the finer particle fractions (e.g., PM_{2.5}, PM₁) than to PM₁₀. Therefore, just recently a new air quality directive directed towards PM_{2.5} has been launched within the European Union.

While the knowledge of the different sources to PM₁₀ in urban air may be considered to be fairly good, corresponding knowledge regarding finer fractions PM_{2.5} and PM₁ is generally poor. This especially applies to the contribution from road traffic to occurring ambient concentration levels in urban and curbside environments. This makes it difficult to identify and prioritize the actions needed when it comes to reduce the health risks and health impacts of airborne particulate matter in general.

For the road traffic sector the demand of measures against particulate pollution is hard to define, since the contribution from road traffic to the overall emissions of various particle size fractions as well as to their concentrations in various environments cannot be quantified with sufficient accuracy by conventional methods (via emission models based on emission measurements on individual vehicles in laboratory experiments). Instead, "inverse" methods such as source receptor modeling via chemical characterization of particles sampled from ambient air are useful for determining the actual contribution from traffic to airborne particulate matter, and may also be used for the validation of dispersion models involving particulate matter.

A sound basis for decisions on measures requires a deep knowledge of the factors that affect the generation of airborne particles. In order to study wear-related particulate matter characteristics, and to understand their formation processes associated with different types of road pavement material, tyres, friction material, etc., controlled experiments are also needed. For this purpose the VTI circular road simulator - PVM – possesses a high capability. Previous studies in PVM have revealed major differences in PM₁₀ generation between different combinations of road pavement, tyres and friction materials (Gustafsson et al., 2008, Gustafsson et al., 2009). These differences are considered to be related mainly to the stone material strength properties, but also the binder and the ability of the tyres to form PM₁₀ at different wear combinations. Similarly, for reducing slipperiness by the use of friction material, the relations between the properties of stone materials in the road pavement and the friction material are of great importance. Results indicate a great potential to minimize emissions of wear particles during the critical winter period by an appropriate choice of road pavement, tyres and strategies applied for reducing slipperiness during winter. This may particularly be valid for congested traffic environments in urban areas where also the population PM exposure tends to be high. The knowledge of how the emissions and concentrations of smaller particles such as PM_{2.5} and PM₁ are influenced by these different wear parameters is rather limited.

Thus, knowledge of the relevance of various parameters for the generation and dispersion of traffic wear particles of different size is crucial for designing cost-effective measures. Despite numerous efforts in earlier studies there is still a lack of knowledge regarding the influence of temperature, moisture, road surface texture, surface wear, stone strength of the material properties, and not least the relationship to the total wear, salting, dust binding, etc., remains to be clarified. Furthermore, measures designed to minimize particulate emissions must be assessed against sustainability, friction characteristics (road safety), noise and economic considerations.

2 Objectives and approach

The aims of the project were:

- to determine the chemical and physical composition (i.e. the source profile) of road traffic generated airborne particles through both measurements in field and indoor measurements with the use of a circular road simulator,
- to clarify the role of different factors that influence the formation of airborne particles from vehicle tyre and road surface interactions by experimental studies in the road simulator and measurements in urban environments, and determine the emission factors for various combinations of these factors,
- to determine the traffic contribution to airborne particles in urban air and traffic environments and identify their origin (brake wear, tyre wear, road surface wear etc.),
- to develop a scientific basis for proposals for cost-effective measures to reduce the occurrence of airborne particles in urban air and traffic environments.

Thus, the approach to reach these objectives relied on the coordinated use of mainly three principally different methodologies: 1) an indoor circular road simulator, 2) various sampling methods for different size fractions of airborne particles, some of which allowing for elemental and chemical speciation of particle composition, and 3) receptor models. As far as known, it is the first time ever that such a broad approach has been applied in traffic wear particle generation studies.

3 Methods

3.1 Road simulator set-up

3.1.1 The VTI circular road simulator

Particle sampling in the road simulator hall (with dimensions $10 \times 8 \times 5 \text{ m} = 400 \text{ m}^3$) makes it possible to sample wear particles with very low contamination from surrounding sources and no influence from tail-pipe emissions. The road simulator consists of four wheels that run along a circular track with a diameter of 5.3 m, cf. Figure 3.1. 1. A separate DC motor is driving each wheel and the speed can be varied up to 70 km h^{-1} . At 50 km h^{-1} a radial movement of the vertical centre axis is started to force the tyres to wear evenly on the pavement. Any type of pavement can be applied to the simulator track and any type of tyre can be mounted on the axles. During measurements the simulator hall is not actively ventilated although pressure gradients might cause minor self-ventilation. An internal air cooling system is used to temperate the simulator hall down to sub-zero temperatures. The hall is also equipped with a large filter fan, acting as a sink to simulate outdoor mixing and more natural sampling conditions.



Figure 3.1.1 The VTI circular road simulator.

3.1.2 Pavement and tyres

The pavement used for the tests were a stone mastic asphalt (SMA) with maximum stone size = 16 mm. The stone matrix material was quartzite from Dalbo in western Sweden. This pavement is similar to the existing pavement at the monitoring site at Hornsgatan in Stockholm, cf. chapter 4.3. Three tyre types were used – summer tyres (Nokian NRHi Ecosport), Nordic, unstudded winter tyres (Nokian Hakkapeliitta RSi) and studded winter tyres (Nokian Hakkapeliitta 4).

New tyres need to be worn to get rid of their protective surface layer. The tyres were worn using the road simulator according to VTI standard methods:

Studded tyres:

- Tyres and pavement are cooled to below zero temperature
- Cooling is used also during the wear-in routine
- The routine is run on dry pavement
- Axle load: 450 kg.
- Wheel air pressure: 2,5 bar
- Routine:
 1. 20 km/h for 1 h without eccentric movement
 2. 30 km/h for 1 h without eccentric movement
 3. 50 km/h for 4 hrs with eccentric movement
 4. 60 km/h for 2 hrs with eccentric movement
- Pavement temperature are not to exceed 0°C during the routine

Nordic unstudded winter tyres:

- Tyres and pavement are cooled to below zero temperature
- Cooling is used also during the wear-in routine.
- The routine is run on dry pavement
- Axle load: 450 kg
- Wheel air pressure: 2,5 bar
- Routine:
 1. 50 km/h for 1 h with eccentric movement
 2. 70 km/h for 1 h with eccentric movement
 3. Pavement temperature is not to exceed 0°C during the routine

Summer tyres:

- Pavement is kept at room temperature
- The routine is run on dry pavement
- Axle load: 450 kg
- Wheel air pressure: 2,5 bar
- Routine: 60 km/h for 2 hrs with eccentric movement

During the routine for studded tyres, stud protrusion was measured on 18 studs on each tyre before the start of the routine, after step 3 and after step 4.

3.1.3 Test cycle

The road simulator test cycle that is normally used is described as:

1. 1,5 hrs at 30 km/h
2. 1,5 hrs at 50 km/h with eccentric movement
3. 2 hrs at 70 km/h with eccentric movement

If particle sampling at high concentrations are to be performed, the above cycle is completed with

4. 1 h at 70 km/h with eccentric movement and filter fan activated

By using a standardized test cycle, measurements using different combinations can easily be compared.

3.1.4 Wear measurements

The depth of the worn track caused by studded tyres can be measured using a laser profilometer, cf. Figure 3.1.2. This instrument measures the track depth in a cross section perpendicular to the track in almost 200 measurement points (Wågberg, 2003).



Figure 3.1.2 Laser profilometer applied to the road simulator.

3.1.5 Airborne wear particle sampling

During the test cycle the generated wear particles were characterized using different methods (for a detailed description of these methods see chapter 3.2):

- Mass concentration: TEOM, DustTrak
- Particle size distribution: APS and SMPS
- Chemical composition: SDI and SFU with subsequent analysis using PIXE

During all tests, the background aerosol in the road simulator hall was measured before starting the road simulator using TEOM, DustTrak, APS and SMPS.

To exclude effects of contamination from the electrical motors powering the road simulator, measurements of size distributions close to a ventilation opening were made using the SMPS. The ventilation air proved to be even cleaner than the background air of the simulator hall. Further, reference measurements were conducted on summer tyres and the measured particle concentrations were then always lower than in the background air, hence the emissions of particles from the road simulator itself are very low.

3.2 Monitoring and sampling methods

3.2.1 SAM – Stationary Aerosol Sampler

The ambient aerosol was sampled using a PM₁₀-inlet (Ruprecht & Patashnik) and with a flow rate of 5 lpm into the Stationary Aerosol Sampler (SAM), designed by the Department of Nuclear Physics at Lund University (Hansson and Nyman, 1985). Inside the SAM a coarse fraction (PM₁₀-PM_{2.5}) was sampled on a NuclePore[®] filter using an impactor with an aerodynamic cut-off diameter at 2.5 µm, and then the aerosol was sucked through a Nuclepore[®] filter for sampling of the PM_{2.5} fraction. The filters were subsequently analyzed on their content of a number of elements by means of the PIXE method (see below). Measurements with the SAM were only made at Amiralsgatan in the city of Malmö.

3.2.2 IVL samplers

PM₁, PM_{2.5} and PM₁₀ were all sampled using sampling heads developed at IVL in collaboration with the Department of Design Sciences at Lund University. All sampling heads are made of polyoxymethylene and have a greased impactor. The flow rate is 18 lpm. All parts are turned in an automatic lathe. The sampling head for PM₁₀ (Ferm et al., 2001) has been tested with good results against reference methods in Norway (Marsteen and Schaug, 2007). The PM₁ is similar to the PM_{2.5} sampler except for a small tube inserted in the jet that changes the 50 % cut-off from 2.5 µm aerodynamic diameter to 1.0 µm. The PM_{2.5} and PM₁ samplers have been tested against the EU-approved reference sampler “KleinfILTERGERÄT” with good results (Ferm et al., 2008). Teflon filters were used in the PM₁₀ sampler (47 mm Zefluor, pore size 2 µm) as well as in the PM_{2.5} and PM₁ samplers (25 mm TF-1000, pore size 1 µm). The samplers are shown in Figure 3.2.1.

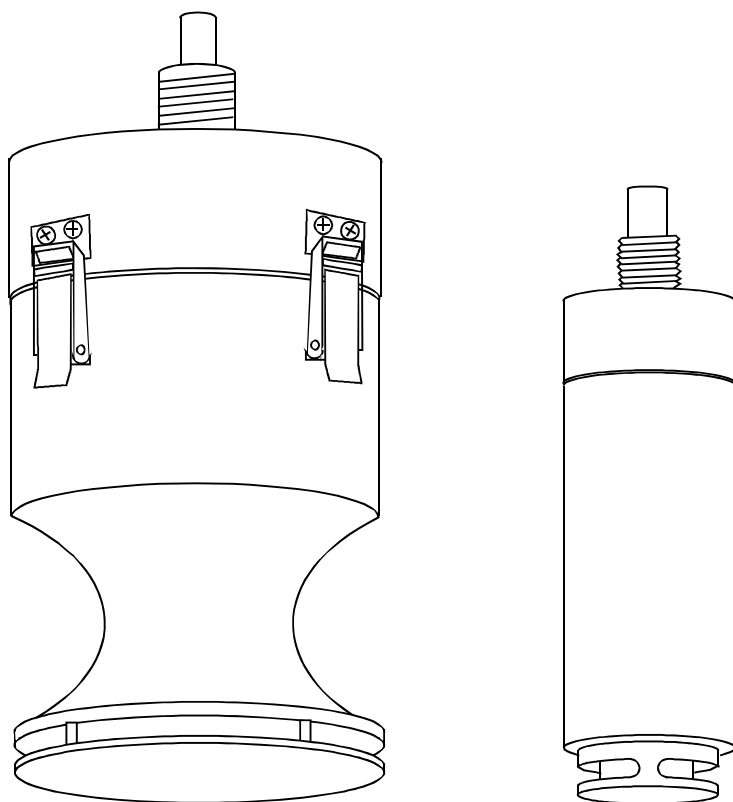


Figure 3.2.1 Sampling heads of the IVL samplers for PM₁₀ (left) and PM_{2.5} and PM₁ (right).

3.2.3 TEOM

The Tapered Element Oscillating Microbalance – TEOM - instrument (Rupprecht and Pataschnik) is based on gravimetric technique using a microbalance. A value of the mass concentration of PM₁₀ is provided every five minutes. The method is certified for air quality standard monitoring within the EU. The aerosol is sampled using a PM₁₀-inlet and then preheated to about 50 degrees Celcius before it is sucked and sampled through a filter placed on the top of a tapered rod of glass. Changing of the oscillating frequency of the filter is proportional to the mass of particles collected on the filter.

PM₁₀ and PM_{2.5} were measured automatically using TEOM model 1400. Concentrations from the instrument were multiplied with 1.2 to account for losses of volatile compounds by the heating of the microbalance (+40 C) in the TEOM-instrument (Johansson, 2003).

3.2.4 DustTrak (DT)

DustTrak (TSI Inc) is a fast optical particle instrument, which in this study was used for comparison of concentrations of PM₁₀ and PM_{2.5} between the road wear simulator runs. Although it is not approved for air quality surveillance against air quality guidelines, it is useful for monitoring of fast courses of events in homogeneous aerosols. For protection the DustTrak instruments were placed in environmental enclosures with omni-directional inlets for sampling of PM_{2.5} and PM₁₀.

3.2.5 Scanning Mobility Particle Sizer (SMPS)

A Scanning Mobility Particle Sizer (SMPS, TSI Inc., USA) was used to measure the number distribution for particles below 1 μm . The SMPS consisted of a Differential Mobility Analyzer (DMA, model 3071, TSI Inc., USA) and a Condensation Particle Counter (CPC, model 3010, TSI Inc., USA). The aerosol and the sheath air flow rates were set to 1 lpm and 10 lpm, respectively. Using an up and down scan timings of 120 s and 60 s, a detectable size range of 7 to 297 nm was achieved. The SMPS system was placed outside the closed room housing the road simulator and the aerosol was sampled from the road simulator hall using a 2.0 m $\frac{1}{4}$ " copper tube. For calculating mass concentrations a density of 1000 kg m^{-3} was used for the SMPS measurements.

3.2.6 Aerodynamic Particle Sizer (APS) and Small Deposit Cascade Impactor (SDI)

The APS and the cascade impactor were sampling the wear particles in the road simulator hall using an omni-directional PM_{10} inlet (Ruprecht & Patachnik), with a sampling flow of 16.7 lpm. Downstream the PM_{10} -inlet an aerosol splinter distributed 1 lpm to the APS and 10 lpm to the SDI and the remaining flow 5.7 lpm was sucked using an external pump. When the SDI not was used the 5.7 lpm was increased to 15.7 lpm. The sampling efficiency in the splinter and the transport losses for the SDI and the APS measurements were calculated. The entire difference was less than 10% for all aerodynamic particle sizes less than 10 μm . The PM_{10} -inlet was placed about 2 m from the edge of the pavement of the road simulator and the height of the inlet was about 2 m from the floor (1 m above the pavement).

The particle size distribution of the coarse fraction ($> 0.5 \mu\text{m}$) was measured using an Aerodynamic Particle Sizer (APS, model 3321, TSI Inc., USA), which measures the number concentration as a function of the aerodynamic particle diameter in the range 0.5 to 20 μm . The time resolution was 20 s. For calculating mass concentrations a density of 2 800 kg m^{-3} was used for the APS measurements.

An SDI (Small Deposit Impactor) multi-jet low-pressure cascade impactor (Maenhaut et al., 1996) was used to collect highly size-resolved aerosol particle samples in 12 size fractions (aerodynamic cut-off diameter between 0.045 and 8.39 μm). The particles was collected on NuclePore© polycarbonate membrane filters coated with a thin layer of grease. The wear particles were often sampled when the velocity of the road simulator was 70 km/h, but for summer tyres the sampling time was extended to the whole test cycle (30, 50 and 70 km/h), about 6 hours, to obtain sufficient amounts of particle mass on the filters.

The samples were analyzed using the PIXE method and for each cascade impactor sampling two blanks (also greased) were taken and analyzed and proper corrections were performed.

3.2.7 Stacked Filter Units (SFU)

Fine and coarse fraction samples for subsequent PIXE analysis were collected on 47 mm diameter Nuclepore© polycarbonate membrane filters mounted in Stacked Filter Units (SFU; Norwegian Institute for Air Research, NILU, Kjeller, Norway). By using two consecutive filters with different pore sizes (8 μm for the first coarse fraction filter and 0.4 μm for the second fine fraction filter), the SFU configuration can separate aerosol particles according to size (Cahill et al., 1979). The PM_{10} inlet in front of the SFU was of the Gent type (Hopke et al., 1997).

3.3 Analytical methods

3.3.1 PIXE

The SFU and SDI samples from the road simulator runs and the SAM samples from Amiralsgatan were analyzed for their elemental content by means of PIXE (Particle Induced X-ray Emission) at the ion beam analytical facility of the Division of Nuclear Physics at Lund University (Shariff et al., 2003). The PIXE method determines all elements with atomic number larger than 13 (=aluminum).

The elemental source profiles from the SFU samples expressed as enrichment factors were calculated versus a commonly used soil reference composition describing the proportions of the elements occurring in igneous rocks of the continents (Kaye and Laby, 1959). Titanium (Ti) was used as tracer element for soil. These enrichment factors were calculated in the traditional way as:

$$EF(Ti) = \frac{[X_{PIXE}] / [Ti_{PIXE}]}{[X_{REF}] / [Ti_{REF}]} \quad \text{Eq. (3.1)}$$

Here, square brackets denote elemental concentrations of elements X and Ti in the PIXE sample and the soil reference, respectively. The calculated enrichment factors can be used to assist source receptor modeling based on urban PM samples.

3.3.2 ICP-MS

The aerosol filter samples were carefully placed by plastic tweezers in the bottom of a test-tube. 0.5 ml HF (suprapure, 40%) and 1.5 ml HNO₃ (suprapure, 65%) were added to the test tubes to cover the filter samples. Test tubes were capped, agitated and allowed to stand at room temperature for 48 hrs. 8 ml of water was added to the samples. The samples were agitated and allowed to stand for another 48 hrs at room temperature. The samples were shaken well and an aliquot was measured by ICP-MS (Perkin-Elmer Sciex Elan 6000).

3.3.3 Ion Chromatography (IC)

The filters were leached in deionised water. Due to the hydrophobic character of the filters they float on the water. The 25 mm filters were leached in 4 ml water and were forced under the water surface in a small vial and shaken in a machine. The 10 mm filters were placed with the exposed side facing the water surface in a wide vial with 10 ml water. The leaching was made in an ultrasonic bath. The ions were analysed using electrically suppressed ion chromatography. The column Dionex AG22 was used to separate anions and Dionex CG 12 to separate cat ions.

3.3.4 PAH

The particles on the Teflon filters were Soxhlet-extracted with acetone during 24 hours.

An internal standard was added to the acetone extract for correction of losses during clean up. The acetone extract was diluted with water and extracted twice with a pentane and ether mixture.

The pentane/ether extracts were combined and concentrated under a nitrogen flow.

Further clean-up of the PAH extract was made on a deactivated silica gel column to remove more polar substances which interfere with the chromatography. A fraction containing aliphatic and aromatic compounds was collected.

Before analyses the PAH fraction was converted to a more polar solvent and analysed with High Performance Liquid Chromatography (HPLC) with a fluorescence detector. Identification and quantification were made using a certified standard. The yield was calculated using the internal standard and used to correct the obtained concentrations. A reference mixture was analysed for quality control.

3.3.5 SEM/EDS

A SEM (scanning electron microscope, LEO Gemini 1550) equipped with EDX (emission dispersive x-ray spectroscopy, Link ISIS) was used for studies of morphology and elemental composition of sampled PM₁₀ particles, cf. Figure 3.3.1.



Figure 3.3.1 SEM (scanning electron microscope, LEO Gemini 1550) equipped with EDX (emission dispersive x-ray spectroscopy, Link ISIS) at the Institution of thin film technique at Linköping University.

3.4 Models

In this report we have used both empirical knowledge and statistical models. The pure empirical models were mass closure/balance models and the pure statistical model was Principal Component Analysis, PCA. Further we have used receptor models that are based on statistical procedures and

empirical knowledge in different degree and height for identifying and quantifying the sources of particulate matter at any given location. The assumption is that that the receptor site concentrations can be adequately explained by a linear combination of contributions from various relevant sources with constant source profiles. Receptor modeling aims to determine the number, composition and magnitude of sources that contribute to the sampled aerosol. The methodology uses the fact that the sources exhibit different characteristics with respect to chemical composition and temporal variation. Two different models have been used; COPREM (Constrained Physical Receptor Model) and PMF (Positive Matrix Factorization). Both models solve the bi-linear equation iteratively by a weighted least square method in which the chi-square is minimized. Chi-square is the total squared distance between the measurements and the model values. Constraints exclude non-physical solutions (negative components in the source profiles and source strengths), and in both models additional constraints can be included to obtain the “best” solution. The main difference between PMF and COPREM is that in COPREM the user sets the source profiles, while in PMF these are estimated from the data. When the source profiles are not carefully selected in the COPREM model an error can be introduced, however, these source profiles can simplify the interpretation of the source variations. Thus, COPREM can be seen as an improved mass closure/balance model.

3.4.1 Principal Component Analysis, PCA

PCA is a tool that can be used for many types of data. In this project data on the content of metals and PAH on particle samples have been evaluated (Martens and Naes, 1989; Wold et. al 1987).

PCA is a technique that reduces the multidimensional data set to lower dimensions by calculating so-called principal components (PCs) that describe the data. A PCA model is based on measured data (i.e. content of different elements in PM samples) and operated in such a way that it describes as much variance as possible in the data. Results from PCA are often interpreted in score plots and loading plots. Score plots show how the samples are distributed and loading plots display the relationships between the variables (e.g. between different elements). Figure 3.4.1 shows an example of the result from a PCA model run.

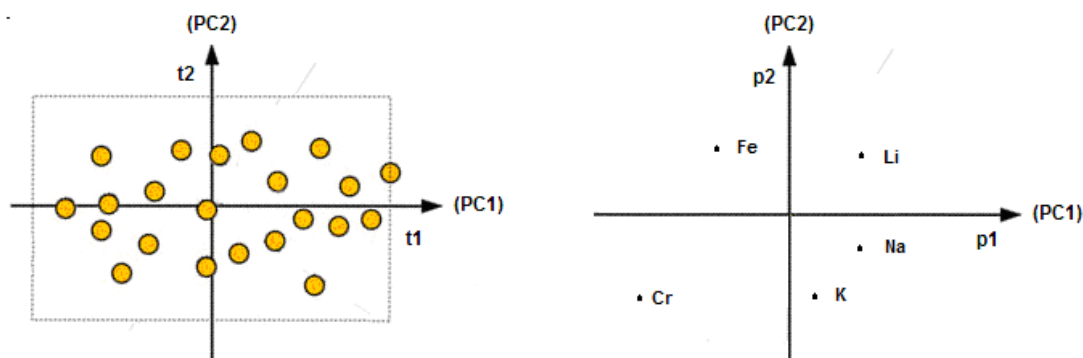


Figure 3.4.1 The score plot to the left shows the projection of the samples on the PC plane and the loading plot to the right shows the influence of each variable on the PCs.

3.4.2 COPREM

A general problem with factor analysis is to separate all the possible sources without mixing them, making it difficult to interpret the solutions. Different sources with some degree of co-variation often mix into common factors (e.g. ‘traffic’, ‘secondary’ or ‘continental air’, ‘oceanic air’), which

are hard to interpret. COPREM (Wählén, 2003) is a hybrid model in which the solutions can be controlled by “fixing” or “freeing” certain parameters. An initial profile matrix is set up in which the columns have the main characteristics of known sources, and constraints are set up to maintain these characteristics, or to prevent the profiles from mixing together during the iteration. In this way, a solution is obtained which is based on best knowledge of the local sources and with a sufficient number of sources.

The uncertainties (expressed as the standard deviation) of the elements in the source profiles are calculated based on a weighted multiple linear regression analysis. The results depend particularly on the uncertainties of the fitted data and should be considered as lower limits of the uncertainties. In principle, the upper limit of the uncertainty interval cannot be defined in a scientific way, because the result depends upon the user’s subjective decisions about the number of sources and the constraints. The rotational ambiguity of the solution can also be assessed. In this way a kind of uncertainty interval can be estimated. The problem of defining the uncertainty of source apportionments is common for receptor modeling.

3.4.3 PMF

For analysing the data for Hornsgatan in Stockholm Positive Matrix Factorization (PMF) was also used. The theory and algorithm of PMF are described in the literature (Paatero and Tapper, 1994; Paatero, 1997). Using the robust mode of PMF means that a limited number of outliers can be tolerated in the data without sacrificing the model stability (Paatero and Hopke 2003). Data below the detection limit were treated with the mechanism offered for this purpose by the algorithm. A number of so-called factors are extracted from the data. Each factor represents one or a combination of sources. For each factor, the temporal variation and the relative compositions are determined.

Two types of uncertainty are present in the PMF results. The uncertainty that is caused by propagation of the measurement uncertainty is calculated by PMF. The other type of uncertainty, usually denoted rotational ambiguity, is caused by the fact that it is not possible to completely distinguish between sources that do not vary independently. An approximate approach was used to estimate the magnitude of the rotational ambiguities (Paatero, 1997). This method determines a range of mathematically feasible solutions. Some parts of this range may be considered less realistic because of the physical interpretation and knowledge, e.g. about source compositions, but this is not accounted for in the uncertainty intervals determined and reported in the results chapter.

4 Measurements

4.1 Road simulator

Each pavement/tyre combination was tested according to the test cycle described in chapter 3.1.3. Three tests were performed: studded tyres, friction tyres and summer tyres were tested in the standardized road simulator test cycle, using three different speeds (30, 50 and 70 km/h).

4.1.1 Emission factor calculation

The smooth shifts in particle concentration during the tests are used to estimate the emission factors versus particle diameter. For each particle diameter the concentration in the road simulator hall can be described by the common ventilation equation:

$$c = \frac{\dot{m}}{Q_{dep}} \left(1 - e^{-\frac{Q_{dep}}{V}t}\right) + c_0 \left(1 - e^{-\frac{Q_{dep}}{V}t}\right)$$

$$c = \frac{\dot{m}}{k} (1 - e^{-kt}) + c_0 (1 - e^{-kt}) \quad \text{Eq (4.1)}$$

where

c = particle concentration, kg/m³

\dot{m} = particle source, kg/sm²

k = particle loss rate through deposition, s⁻¹

The different parts of the test cycles were fitted using Eq 4.1 and the unknown values of \dot{m} and k were derived. The derived k -values are unique for this experimental set-up and for each speed (30, 50 and 70 km/h). This means that derived k -values are theoretically equal for all different combinations of for instance pavement and tyres. When the k -values have been determined they could then be used for all experiments to calculate the emission factors. In this project the k -values were derived from the experiments with studded tyres and then used to calculate the emission factors also for the friction and summer tyres.

Emission factors (EF) were calculated using:

$$EF = \frac{\dot{m} \cdot V}{v} \quad \text{Eq (4.2)}$$

where

V = the volume of the road simulator hall

v = speed of the tyres, ms⁻¹

The emission factors were calculated per vehicle (=4 tyres) and per kilometer.

4.2 Measurements in Malmö

In Malmö in southern Sweden measurements at street level were performed at Amiralsgatan and urban background measurements were made on the roof of the nearby town hall (cf. Figures 4.2.1 and 4.2.2). PM_{10} and $PM_{2.5}$ were measured by means of two TEOM instruments. The internal correction algorithm in the TEOM instruments was removed and the mass concentration obtained was then multiplied with a factor 1.3. NO_x was measured with two chemiluminescence instruments.

The coarse ($PM_{10} - PM_{2.5}$) and fine ($PM_{2.5}$) fractions were collected using the SAM (see chapter 3.2.1). The SAM sampled the ambient aerosol using a PM_{10} -inlet.

The measurements were carried out from January (SAM) and March (TEOM) until June 2005.



Figure 4.2.1 The urban background station on the roof of the town hall in Malmö.



Figure 4.2.2 Measurements at street level (Amiralsgatan) in Malmö.

4.3 Measurements in Stockholm

Stockholm is the capital and the largest city in Sweden, located on the east coast of middle Sweden. The site at Hornsgatan has been described in several papers earlier (Gidhagen et al., 2003; Johansson et al., 2009; Omstedt et al., 2005; Ketznel et al., 2007; Olivares et al., 2007). Hornsgatan is a 24 m wide, four lane street surrounded by 24 m high buildings on both sides, thus being a rather symmetric street canyon with a unity width/height ratio. Traffic intensity is about 35 000 vehicles per day during weekdays, with an average of 5 % heavy duty vehicles, mostly buses, almost exclusively running on ethanol. Of the light duty vehicles, there is an average of 5% diesel fueled cars, mainly taxis. The traffic rhythm is determined by the traffic light crossing at the eastern end of the block. The cars heading westwards from the traffic lights pass the monitors under acceleration and they also have to run up a 2.3% slope. In contrast, the traffic heading eastwards are running downhill towards the traffic light, typically in a deceleration phase.

The urban background site is located at Torkel Knutssonsgatan, on the roof of a 25 m high building. This is 600 m east of Hornsgatan in a less trafficked area.

4.3.1 Campaign measurements

Measurements of PM_{10} , $PM_{2.5}$ and occasionally PM_1 were performed at street level (Hornsgatan) as well as roof level (Torkel Knutssonsgatan). Since the content of elements, PAH as well as ions in the PM samples should be analysed duplicate sampling had to be made. Sampling was made on a 24h basis changing at midnight. Six auto-changers were used at each site. Each auto-changer was

connected to eight sampling heads. The stations as well as the sampling heads are shown in Figures 4.3.1 - 4.3.3. Four campaigns were performed, see Table 4.3.1.



Figure 4.3.1 The sampling and monitoring station at Hornsgatan.



Figure 4.3.2 The 48 sampling heads for the campaign sampling of PM₁₀, PM_{2.5} and PM₁ at Hornsgatan in Stockholm.



Figure 4.3.3 Sampling heads for the campaign sampling of PM₁₀, PM_{2.5} and PM₁ at roof level at Torkel Knutssonsgatan in Stockholm.

Table 4.3.1 Time intervals of the four measurement campaigns. The numbers indicate duplicate or single sampling.

start	stop	Hornsgatan			Torkel Knutssonsgatan		
		PM ₁₀	PM _{2.5}	PM ₁	PM ₁₀	PM _{2.5}	PM ₁
2006-04-05	2006-04-19	2	2	2	2	2	1
2006-11-02	2006-11-08	2	2	2	2	2	1
2007-03-09	2007-03-23	2	2	2	2	2	
2007-05-21	2007-05-29	2	2	2	2	2	

4.3.2 Continuous/permanent measurements

PM was sampled on the north side of Hornsgatan at 3 m above street level and at the urban background site.

Air intakes for NO_x monitoring (chemiluminescence, Thermo Electron) were placed at both sides 1.5 from the façades, at 3 m height and also at the urban background site. Close to the NO_x air intake at the north side of the street, a trailer was parked with a CPC3022 instrument (TSI Inc.) measuring total number concentrations. An identical instrument was located at the urban background station.

PM₁₀ concentrations recorded by the TEOM instrument were multiplied with 1.2 to account for losses of volatile compounds in this instrument (Johansson, 2003). Span and zero checks of the NO_x instruments using certified calibration gases with NO in nitrogen were performed

automatically every day. Conversion efficiency for reduction of NO₂ to NO was also checked every day by converting NO to NO₂ through O₃ titration.

A DMPS instrument yields particle number concentrations in 6 size intervals, from 20 to >200 nm in diameter. In parallel the aforementioned CPC 3022 instrument measured the total number of particles (ToN) with a lower cutoff of 7 nm.

Meteorological data – wind speed and wind direction - were collected from a 10 m mast situated on the roof of Torkel Knutssongatan.

4.4 Measurements within the Swedish Urban Air Quality Network

The Swedish Urban Air Quality Network was launched in 1986. It is a cooperation between IVL and a large number of preferably small to medium-size municipalities in Sweden. Air quality parameters such as SO₂, soot, NO₂ and PM₁₀ are measured using volumetric techniques (24h sampling) mostly during the winter season (October-April). Furthermore, ozone and VOC are occasionally monitored by means of diffusive samplers. The analysis techniques are accredited by SWEDAC (the Swedish Board for Accreditation and Conformity Assessment). Besides PM₁₀ also PM_{2.5} or PM₁ are occasionally measured using the IVL samplers described in chapter 3.2.2. Teflon filters are used for the PM sampling, which enables subsequent analysis of e.g. metals and PAH. Within the scope of this project PM₁₀ filters from the following stations were analysed for their content of metals by means of ICP-MS:

- Jönköping: Sampling was made at an urban background site near a downtown pedestrian street (Smedjegatan). Also measurements at street level were made at Barnarpsgatan.
- Västerås: Sampling was made at street level (Stora gatan).
- Örebro: Sampling was made at street level.
- Piteå: Sampling was made at a downtown urban background site (Rådhusorget).
- Kävlinge: The sampling station was situated near the market centre in Löddeköping and the motorway E6 to Malmö. Sampling of PM_{2.5} was also made.

5 Results

5.1 Road simulator

5.1.1 The influence of tyres and speed

The resulting PM_{10} concentrations for the use of different types of tyres in the road simulator runs are presented in Figure 5.1.1. As can be seen studded tyres gives rise to very high concentrations compared to the two other tyre types. The road simulator speed was 30, 50 and 70 km/h (at the time periods 11:30-13:00, 13:00-14:30 and 14:30-16:30, respectively). For the studded tyres, the concentration development with time can be described as: At the start of the simulator, the particle concentration rises, reaches a peak and then slowly decreases. When the speed is raised to 50 km/h, concentration increases and levels of before the speed is raised to 70 km/h. Then a sharp concentration peak occurs, followed by a decrease in concentration, levelling out at a constant concentration. Studded tyres cause extremely high concentrations of PM_{10} , about ten times higher than those associated with Nordic non-studded winter tyres. PM_{10} generated by summer tyres are almost negligible.

Figure 5.1.1 shows the measured mass concentration in the road simulator hall using the DustTrak. The TEOM and DustTrak show the same typical pattern. Before the start of the road simulator the mass concentration is low. Increasing the speed from 30 to 50 km/h an even and smooth increase in mass concentration is observed, contrary to the speed changes from 0 to 30 and 50 to 70 km/h, respectively. These show high peak values that decrease after a while. The peaks are caused by resuspension of particles. The peak at 30 km/h is caused by particles that have not been removed from the track/pavement despite careful cleaning. The peak at 70 km/h is caused by resuspension of particles deposited onto the pavement that can be airborne again when the speed is increased. However, in all cases an almost/virtual steady-state mass concentration is obtained after approximately 1 hour. The first rapid decrease in concentration occurs after the start of the filter fan, and the other three by the reduction of speed to 50 km/h, 30 km/h and finally when the road simulator is brought to a complete stop. In all these cases a smooth exponential decrease of the mass concentration is observed.

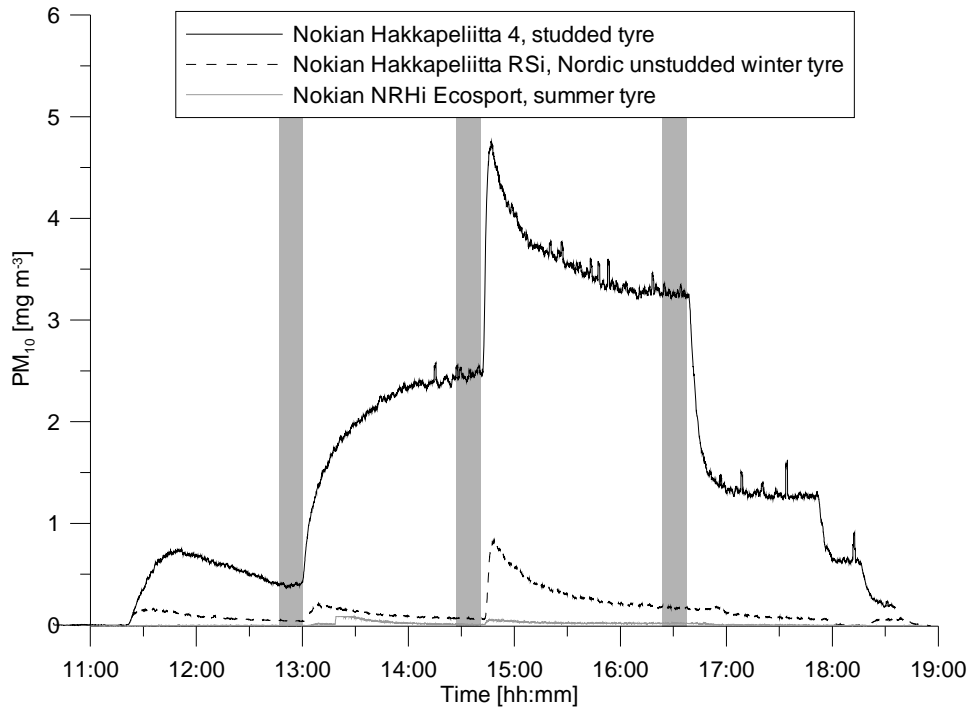


Figure 5.1.1 PM_{10} concentrations (measured by DustTrak) in the road simulator hall, resulting from runs with different types of tyres (studded winter tyres, non-studded winter tyres and summer tyres). The road simulator speed was set to 30, 50 and 70 km/h, see the description of test cycles in chapter 3.1.3. The grey shaded 15 minute periods are used for mean value calculations for each speed (see Figure 5.1.2).

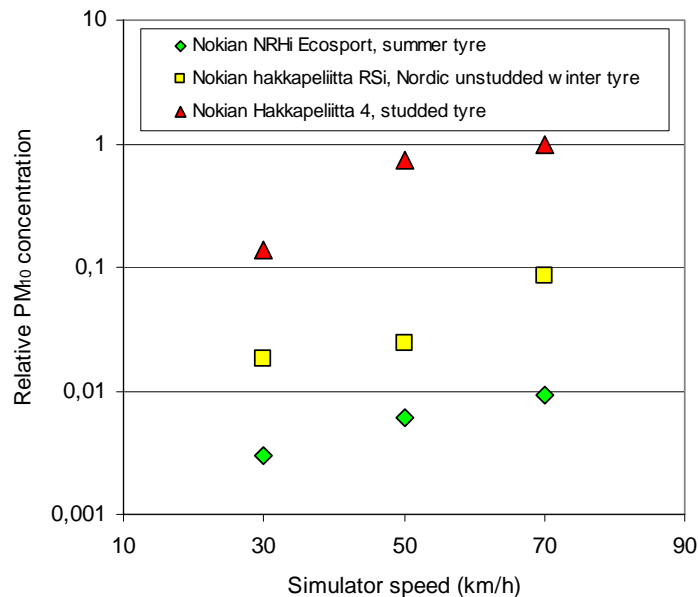


Figure 5.1.2 Relative PM_{10} concentration in relation to tyre type and simulator speed. The data are mean values from the grey shaded periods in Figure 5.1.1.

In Figure 5.1.3 the size distributions for the three types of tyres are shown for the three different speeds. The coarse fraction as measured by the APS instrument (shown to the right in the diagram) makes up most of the mass of PM₁₀. For the studded tyres, the size mode peaks at 3–4 µm and the concentration increases with increasing speed. For the Nordic unstudded winter tyres the peak of the PM concentration at 70 km/h is shifted to a coarser mode, but at lower speeds the size mode peaks at 2–4 µm. The summer tyres result in low concentrations of a finer particle mode, peaking just below 2 µm. Also in the case of summer tyres the concentration increases with speed, indicating a particle source.

The particle number distributions measured by the SMPS system are shown to the left in Figure 5.1.3. The only apparent particle mode generated in the experiments is observed for studded tyres, for which a particle mode peaking around 30 nm increases with increasing speed. The particle modes observed in the tests with the Nordic unstudded winter tyres and the summer tyres are unaffected or decrease with increasing speed, indicating that their source(s) are not the interaction between tyre and pavement, but are more likely aerosols already occurring in the background air.

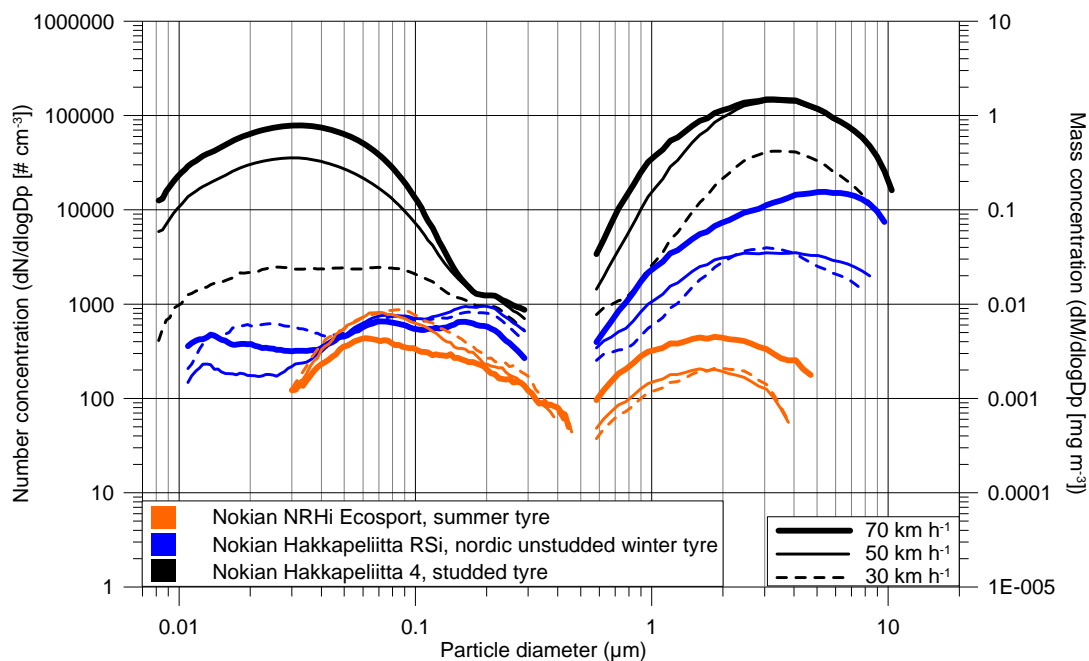


Figure 5.1.3 Particle size distributions for the three types of tyres investigated in the road simulator. Left: Number distributions of particles as measured by the SMPS system. Right: Mass distributions of particles measured by the APS instrument.

5.1.2 The influence of pavement

The pavement used in this project (SMA with quartzite (origin: Dalbo) <16 mm) has been compared to two pavements previously investigated in the road simulator (Gustafsson et al., 2008). These were a stone mastic asphalt (SMA) pavement with quartzite (origin: Kärri) <11 mm and a dense asphalt concrete (DAC) with granite (origin: Skärlanda) <16 mm. Since these two pavements were the first ever to be used in particle wear emission studies in the road simulator, they were not tested according to the previously described test cycle (see chapter 3.1.3). Figure 5.1.4 shows the results of measurements made during one hour at 70 km/h with the three different pavements.

Two comparisons can be made. Firstly, the difference between quartzite and granite pavements with the same maximum aggregate size is obvious (upper and middle lines). The granite pavement produces PM₁₀ concentrations that are almost 70 % higher in comparison to the quartzite pavement. The measured concentrations are, regardless of pavement, extremely high as a result of the confined hall.

Secondly, the two pavements with similar (but originating from different quarries) stone material (quartzite), but with different maximum aggregate size (11 and 16 mm respectively), also exhibit large differences in resulting PM₁₀ concentrations. The total wear of a pavement normally decreases with increasing aggregate size (Jacobson and Hornvall, 1999). However, it can be seen in this experiment that the properties of the different materials seem more important than aggregate size, since the pavement with the smaller aggregate size (quartzite <11 mm) leads to less PM₁₀ production than the coarser pavement (quartzite <16 mm).

These results indicate that by making proper choices regarding pavement material and maximum aggregate size, wear can be minimized. These results are in accordance with those from a study by Räsänen et al. (2003), who describes different materials' resistance to wear and states that mafic, volcanic rock is the most resistant, while granite is the least resistant to wear.

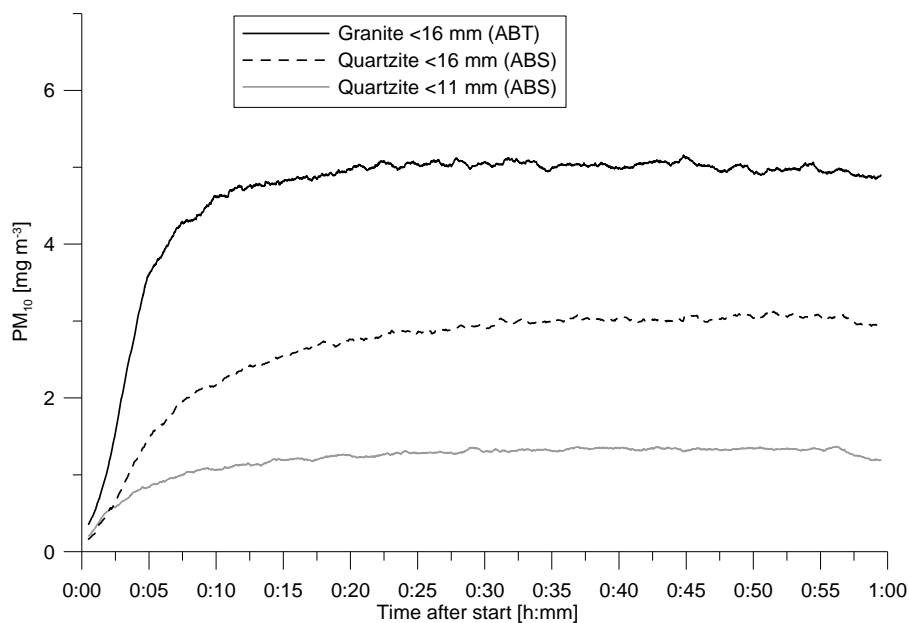


Figure 5.1.4 Measured concentrations of PM₁₀ in the road simulator hall with different pavements (granite <16 mm, quartzite <16 mm and quartzite <11 mm) under controlled ambient conditions. Results for studded winter tyres and road simulator speed set to 70 km/h (Gustafsson *et al.* 2009).

5.1.3 Morphology of wear particles

Characterizing the collected PM₁₀-particles with scanning electron microscopy (SEM) reveals the shape (morphology) of the particles generated under different combinations of pavement material in the road simulator, cf. Figure 5.1.5.

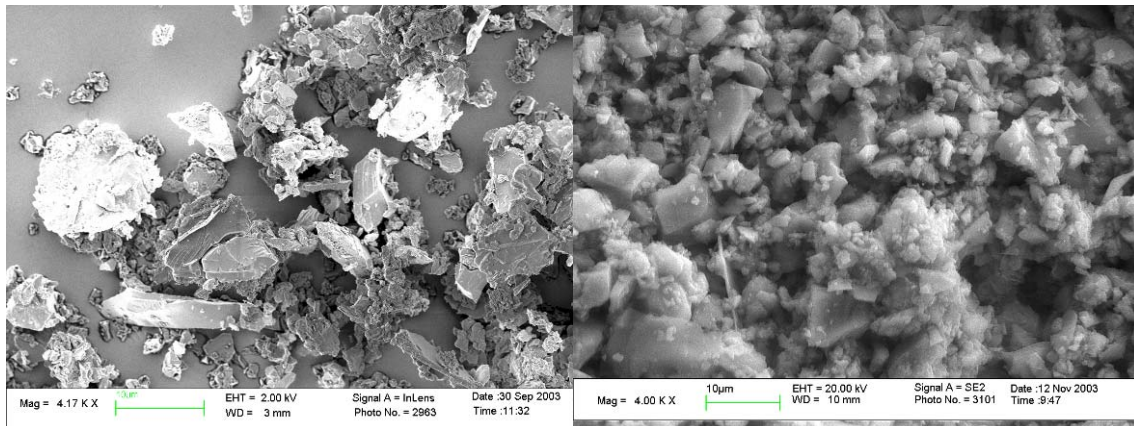


Figure 5.1.5 High volume filter samples of PM₁₀-particles collected in road simulator runs with studded tyres but with different pavements. Left: Dense asphalt concrete (DAC<16mm, granite from Skårlunda). Right: Stone mastic asphalt (SMA<11mm, quartzite from Kärr).

Note the large variation in particle morphology of the PM₁₀-fraction with granite origin. Both size and shape of different particles and aggregates reflect the fact that granite is a stone which is built up by a mix of several minerals, while quartzite is a more homogeneous stone. The PM₁₀ of quartzite origin (to the right) shows less variety of morphological shapes than PM₁₀ of granite origin. The morphology of the PM₁₀-particles will influence how they are measured and interpreted by different monitoring equipments, since it is often anticipated that the particles are of spherical shape.

5.1.4 The influence of ambient parameters

The data from the WEAREM-project in combination with data from the “sister project” NanoWear (Gustafsson et al., 2009) was used to study the influence of ambient parameters on wear particle emissions. In NanoWear ten tyres of the same types as used in the WEAREM-project were investigated.

Figure 5.1.6 shows the relation between the measured concentration of PM₁₀ and tyre temperature for all tyres included in the two projects. The tyres are divided into the three main groups: studded tyres (marked "D"), Nordic un-studded winter tyres (marked "F") and summer tyres (marked "S"). Black, blue and red dots represent the different speeds. Note that the PM₁₀ concentration has a logarithmic y-axis.

As already apparent from previous chapters, it can be seen also in Figure 5.1.6 studded tyres are generating the highest levels of PM₁₀. It can also be seen that the level of PM₁₀ decreases with increasing tyre temperature for all speeds for both studded tyres and Nordic un-studded tyres. On the contrary, for summer tyres the PM₁₀ concentration increases with increasing tyre temperature for all speeds. Tyre temperature is, of course, correlated to both pavement and room temperatures.

Figure 5.1.7 shows the results from the same experiments as those behind Figure 5.1.6, but with the specific humidity on the x-axis. The winter tyres (studded and Nordic un-studded) show a correlation to specific humidity with lower moisture content associated with higher levels of PM₁₀, while for summer tyres the PM₁₀ level tends to decrease with increasing specific humidity. This differs from the relationship with tyre temperature where summer tyres not followed the same

trend as the winter tyres. A simple analysis of the relationship between *relative* humidity and the concentration of PM₁₀ (not reported here) showed, in principle, the same pattern as for specific humidity. However, the pattern was not as consistent as for specific humidity.

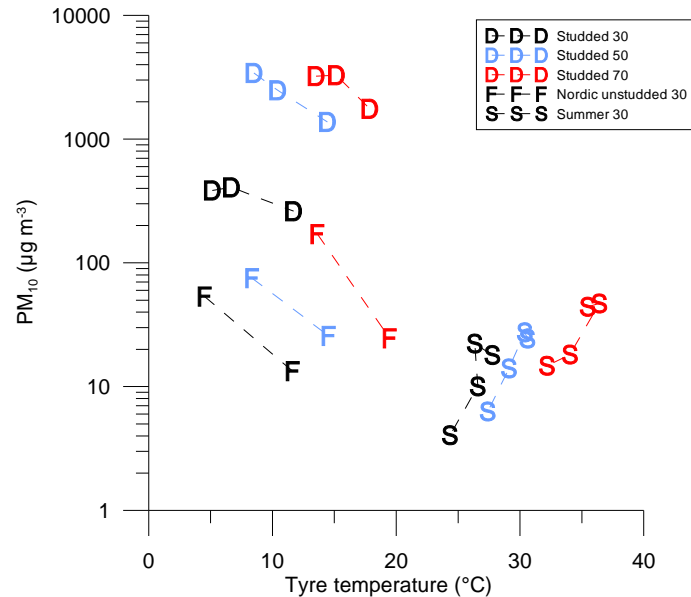


Figure 5.1.6 Relationship between the measured concentration of PM₁₀ and tyre temperature for various types of tyres and speeds. Note that scale of the PM₁₀ concentration is logarithmic. Data sorted by type of tyre (D = studded tyres, F = Nordic un-studded winter tyres, S = summer tyres) and speed (black = 30 km/h, blue = 50 km/h, red = 70 km/h).

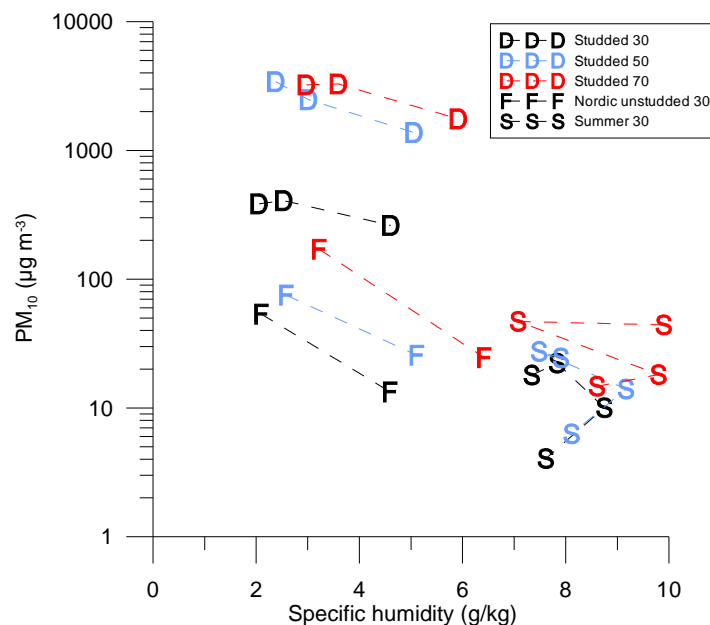


Figure 5.1.7 Relationship between the measured concentration of PM₁₀ and specific humidity (g/kg). Note that scale of the PM₁₀ concentration is logarithmic. Data sorted by type of tyre (D = studded tyres, F = Nordic un-studded winter tyres, S = summer tyres) and speed (black = 30 km/h, blue = 50 km/h, red = 70 km/h).

5.1.5 Emission factors

The APS data enabled estimations of k-values and emission factors, since the APS provides particle size selective measurements with a high time resolution (20 seconds). The time resolution of the TEOM was too poor (≈ 5 minutes) for the data to be used for emission factor calculations.

The k values for 30 and 70 km/h were calculated from the sequence of the test cycle, when the speed is reduced from 70 to 50 and 50 to 30 km/h, respectively. For 50 km/h it was possible to estimate the k-values from both the acceleration period (30 to 50 km/h) and deceleration period (70 to 50 km/h). In Figure 5.1.8 the estimated k-values are shown. The difference of the k-values for 50 km/h determined for the acceleration and reacceleration modes are less than 30 %

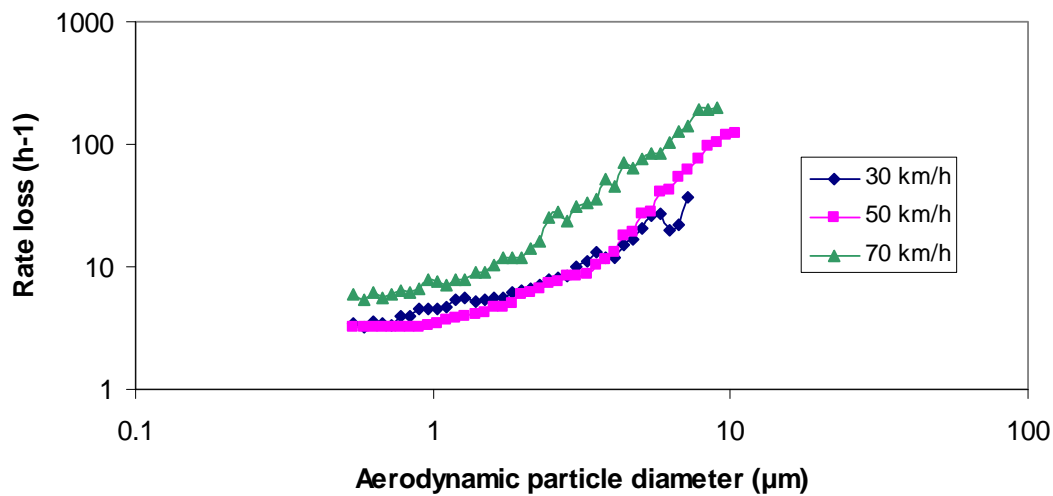


Figure 5.1.8 Estimated k-values of the road simulator hall at different speeds.

The $\text{EF}_{\text{PM}_{10}}$ was determined from the APS PM_{10} data and compared to the $\text{EF}_{\text{PM}_{10}}$ obtained by summing the emission values for each particle diameter. Figure 5.1.9 shows the PM_{10} concentration versus time. The PM_{10} concentration did not increase perfectly according to theory, and the estimated k-value depends on the fitting procedure. Estimated $\text{EF}_{\text{PM}_{10}}$ values are in the range 130 to 253 mg/vehkm (highest values obtained if only the first linear increase is used).

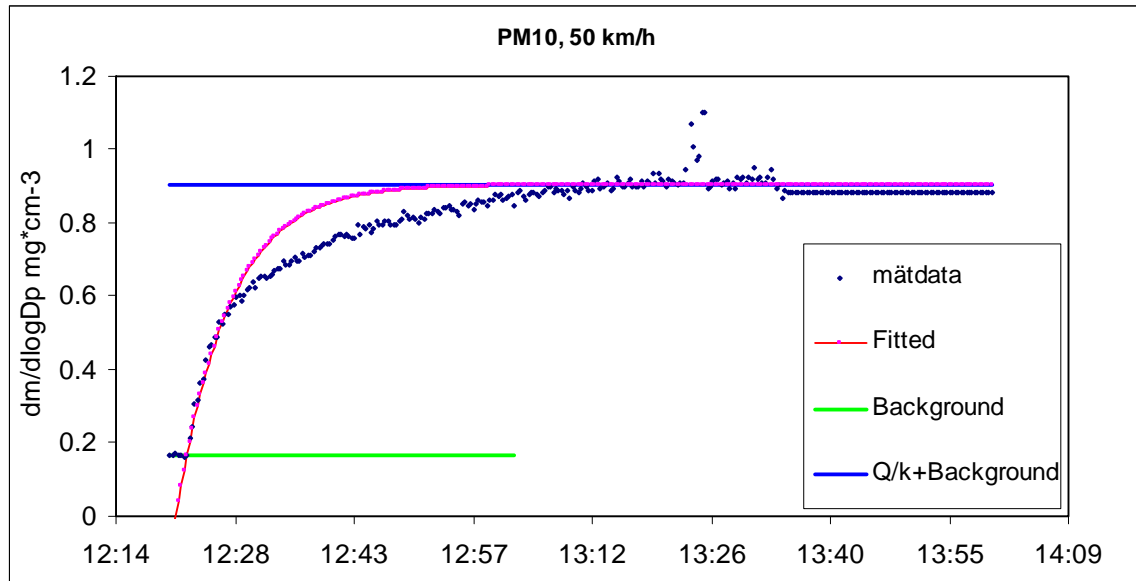


Figure 5.1.9 Fitting of PM_{10} data (black dots - “mätdata”) from the APS measurements according to Eq 4.1 in chapter 4.1.1.

Figure 5.1.10 shows the particle size dependant EF-values and summing all EF-values obtained for each particle diameter yields a value of 347 mg/vehkm. In summary, the most accurate determination of $EF_{PM_{10}}$ is obtained by determining EF as a function of particle diameter and then summarizing up to aerodynamic diameter 10 μm (this also means that the DustTrak data could not be used to estimate $EF_{PM_{10}}$). Figure 5.1.10 shows the increasing EF versus aerodynamic particle diameter. The peak and subsequent decrease at about 8 μm is caused by the increased sampling efficiency of the PM_{10} inlet.

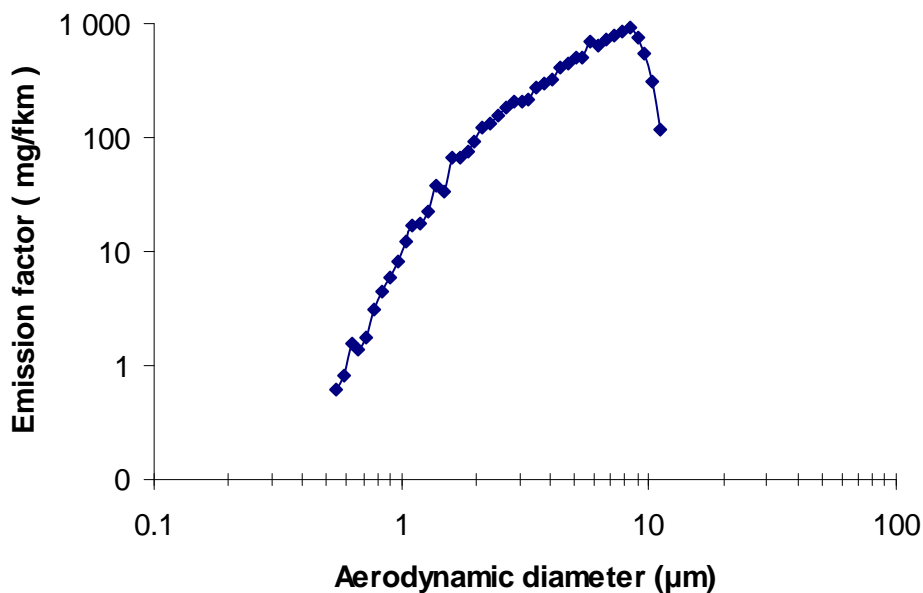


Figure 5.1.10 Estimated EF as a function of particle aerodynamic diameter for studded tyres in the road simulator experiments.

5.1.6 Source profiles

Figure 5.1.11 presents the results of the PIXE-analysis of the filters collected by the cascade impactor in the road simulator experiments. Note that these data only refers to samples collected at road simulator speed 70 km/h. All elements detected by PIXE are not presented - only those considered being relevant for the sources of current interest and that in most cases exceeded the detection limit.

Figure 5.1.11 shows for each type of tyre (from top to bottom):

- *the mass concentration* (in ng/m^3) for different elements and for the 12 different particle size ranges of the cascade impactor. Note the logarithmic y-scale for mass concentration.
- *the relative mass distribution including silicon* (Si). In this histogram (as well as the other histogram) are the results for the tyre, bitumen and filler in the bars to the far right.
- *the relative mass distribution excluding silicon* (Si). Since the silicon from the stones of the coating often dominates air concentrations, silicon has been excluded in order to the distribution of the other elements to appear more clearly.
- *the ratio between each element and silicon*. Note the logarithmic y-scale of the ratios. This figure illustrates the other elements which co-vary with silicon, i.e. if a constant ratio is obtained, the co-variation is large and one can assume that they have the same origin. Since silicon is mainly arising from the stones of the coating, a constant ratio shows that this element also arises from the stones of the coating. In all tyres there is more or less silicon, which must be taken into account in the dissemination of the graphs.

The graphs show that for winter tyres (especially studded tyres) the coarser fractions are dominated by mineral-related elements Si, Ca, K and Fe. Silicon - which in the relative mass distribution represents around 80% of the mass - arises from the main stone of the coating (quartzite), but the relatively large presence of other mineral-related elements indicate that also the filling stone of the coating ("ortens sten", which is granite in this case) contributes significantly to the PM_{10} generation. In particles $<0.25 \mu\text{m}$ other elements, primarily S and Cl, constitute a growing fraction. S occurs both in tyres and in bitumen, while the source of Cl remains unclear. An interesting observation is also that tungsten (W) appears in the coarse fraction of the particles emitted in the runs with studded tyres. Wolfram carbide is used in the studs and apparently also gives rise to some PM_{10} formation. The observation that the distribution of elements is very similar for the non-studded Nordic winter tyres and the studded tyres is remarkable, although another tyre of the former type yielded concentrations and distributions that were more similar to those of summer tyres (see Gustafsson et al., 2009). One possible explanation is that the runs with the non-studded Nordic winter tyres may have been contaminated by resuspension of dust due to failure in the cleaning of the road simulator track from a previous run. The particulate composition of summer tyres differs from that of winter tyres by Si being much less dominant. The concentrations are several orders of magnitude lower, but the relative distributions show significantly more Fe and Zn in the summer tyre runs. S and Cl also occur in the coarser fractions. Zn is usually a good indicator for tyre wear.

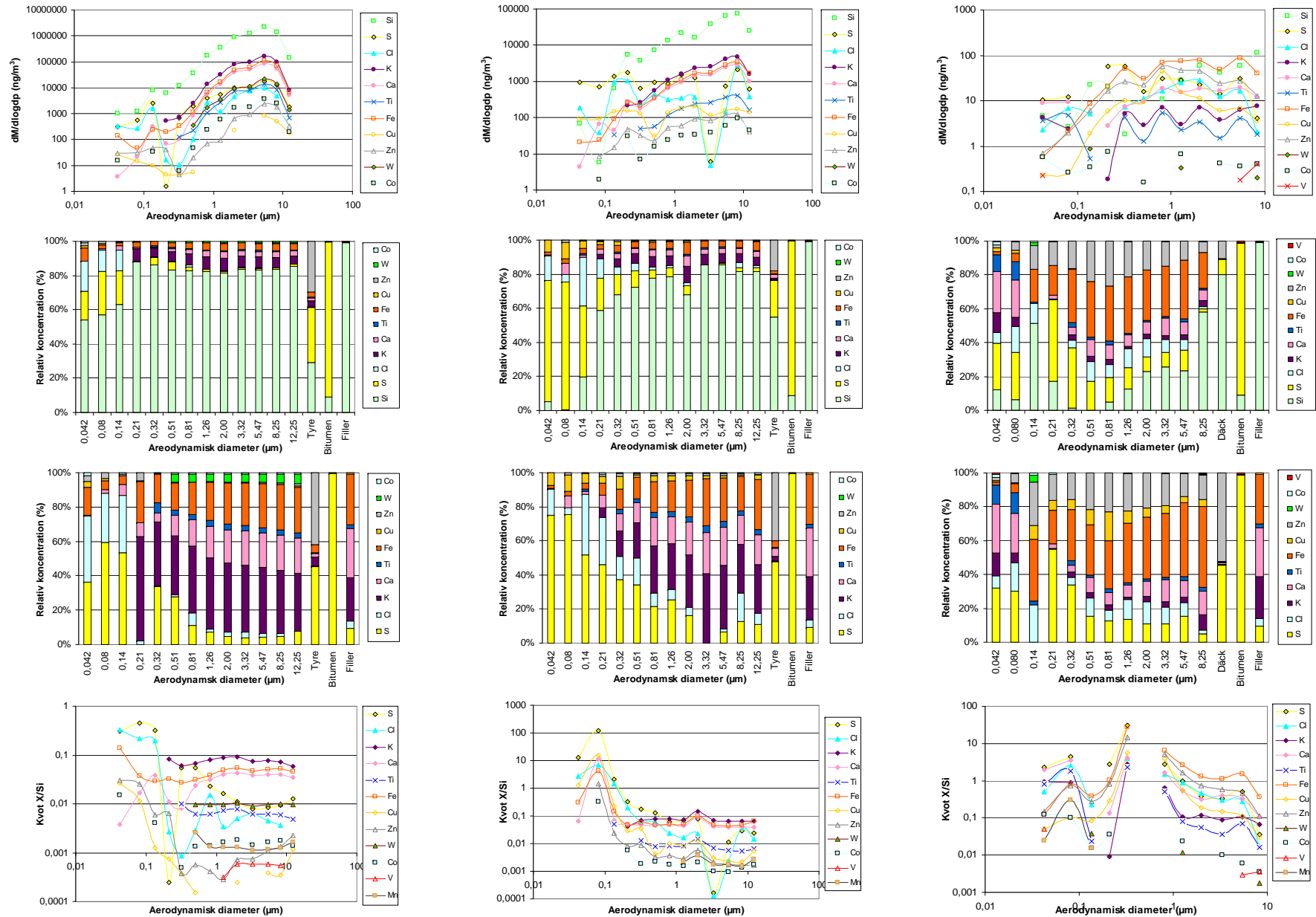


Figure 5.1.11 Elemental composition of various size fractions of PM in the road simulator runs. Left: studded tyres. Middle: friction tyres. Right: summer tyres.

5.1.7 PCA models

Principal Component analysis (PCA) is a good tool when comparing data sets with many variables. PCA analysis was done on the measured metal and PAH concentrations on particle fractions sampled in the road simulator runs with different types and brands of tyres. In Figures 5.1.12 and 5.1.13 the score and loadings plot, respectively, are shown for the metals.

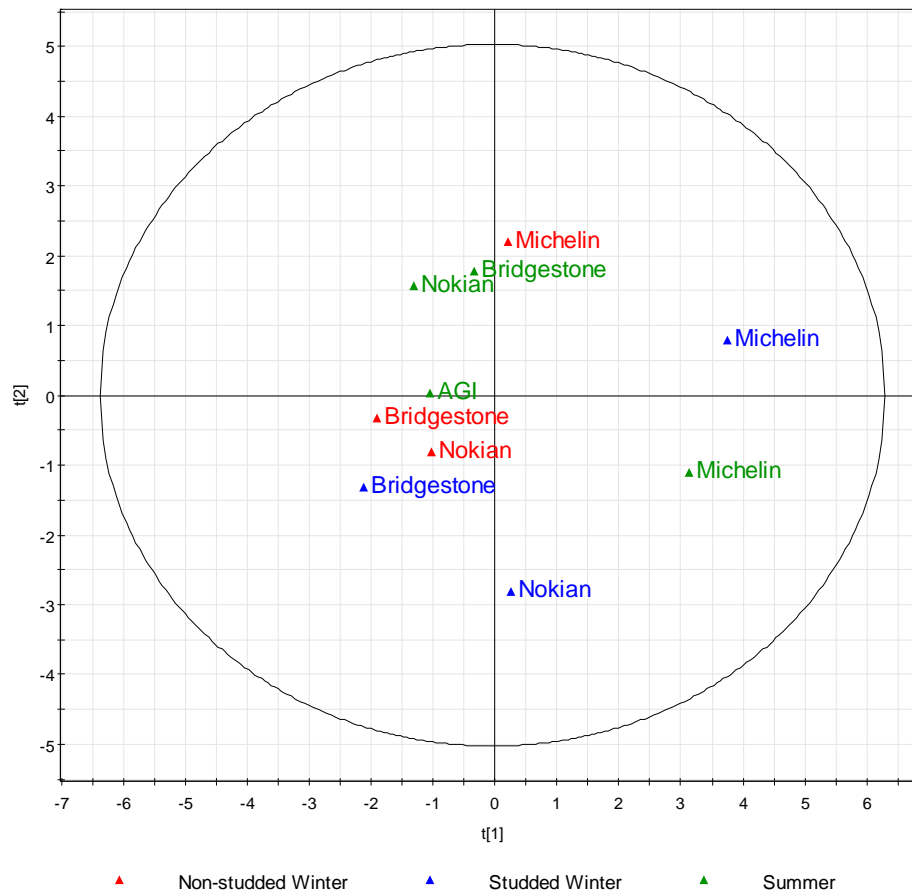


Figure 5.1.12 Score plot based on PCA modeling of measured metal concentrations in particle samples taken in the road simulator runs for different types and brands of tyres.

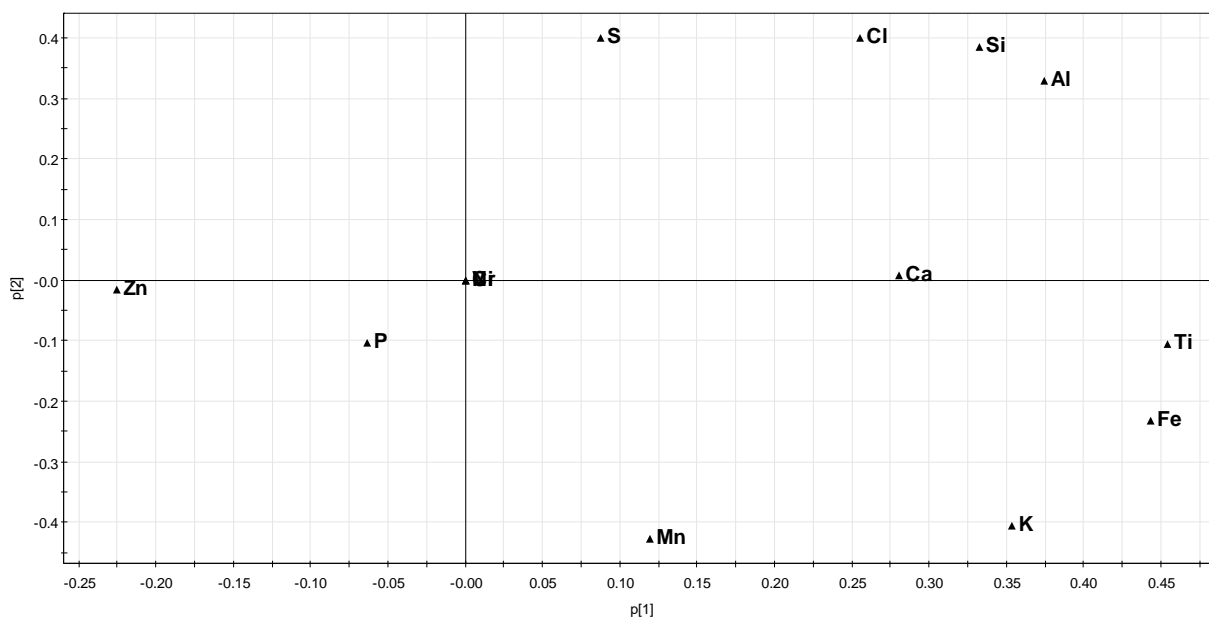


Figure 5.1.13 Loading plot based on PCA modeling of measured metal concentrations in particle samples taken in the road simulator runs.

The different types and brands of tyres are not forming any obvious groups in the score plot. Two remarks can however be done. The first is that the summer and studded tyre from Michelin are the ones most to the left in the score plot, implying that they have a higher concentration of the elements to the most left in the loading plot, i.e. Ca, Ti, Fe, K, Al, Si, Cl and lower concentration of Zn than the other tyres in the study. The elements Cr, Ni and V are all located at origo and thus not influencing the results. The reason for this is the high number of missing values in the analysis for these metals.

All PAH data, both from the analysis of tyre material and from the PM₁₀ samples, was evaluated in the same PCA ($R^2=0.98$, $Q^2=0.88$). In Figure 5.1.14 the observations have been coloured by the origin of the samples. The observations in red are from PAH-analysis of PM₁₀ samples and the blue from PAH-analysis of tyre material. It is clear that the PAH composition of the PM₁₀ samples do not correspond with the PAH composition in the tyre material, except in the case of one tyre. In these results also data from analysis of bitumen is included.

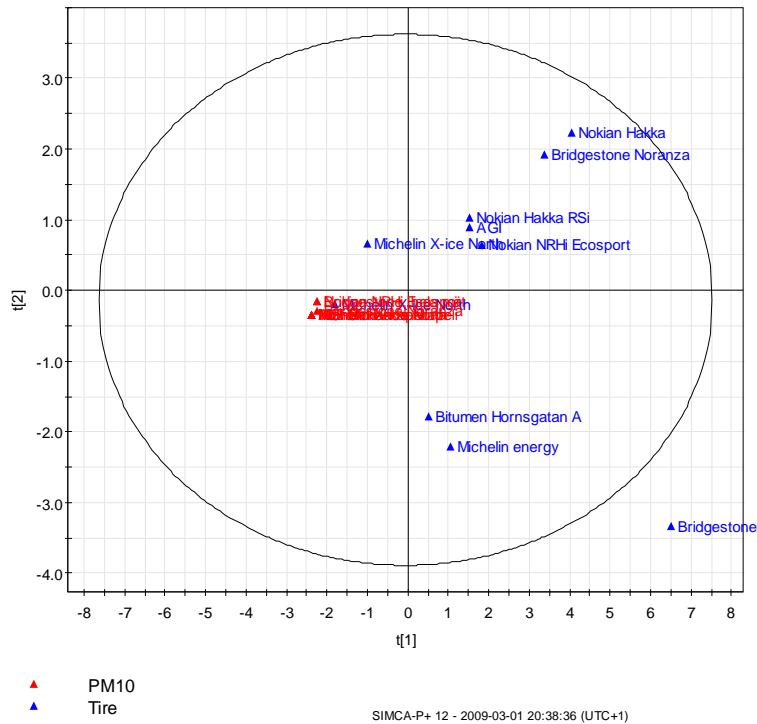


Figure 5.1.14 Score plot for PCA on PAH analysis of PM₁₀ samples and tyre material.

The score plot in Figure 5.1.15 is the same the score plot in Figure 5.1.14, just differently coloured by type of tyre. Grouping of the observations are not distinct. The different types are not close to each other, but rather scattered throughout the plot. This indicate that it is hard, based on the PAH analysis, to class the type of tyre. In Figure 5.1.16 the loadings plot for the PCA is shown.

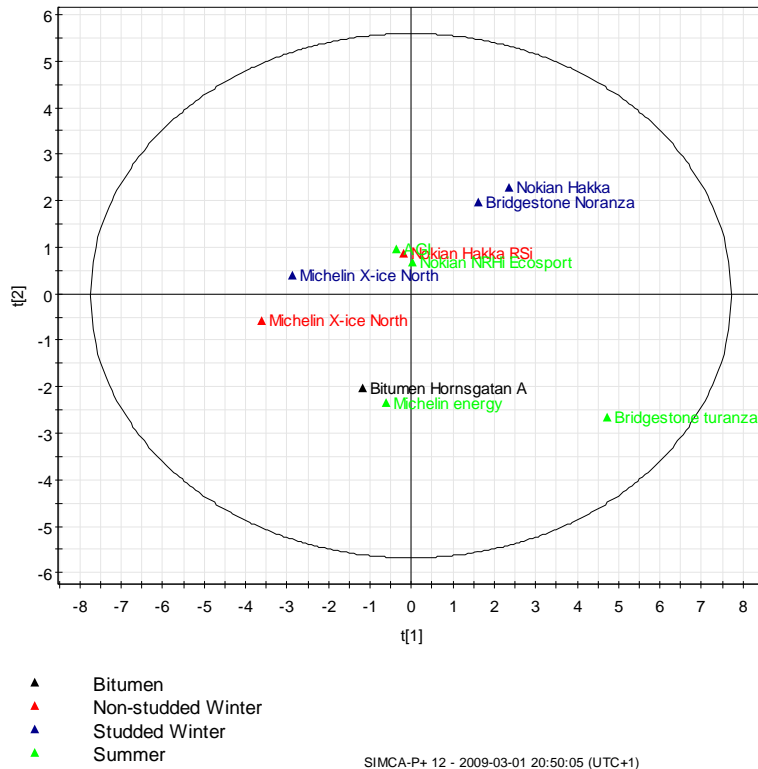


Figure 5.1.15 Score plot for PCA on PAH analysis on PM10 and tyre.

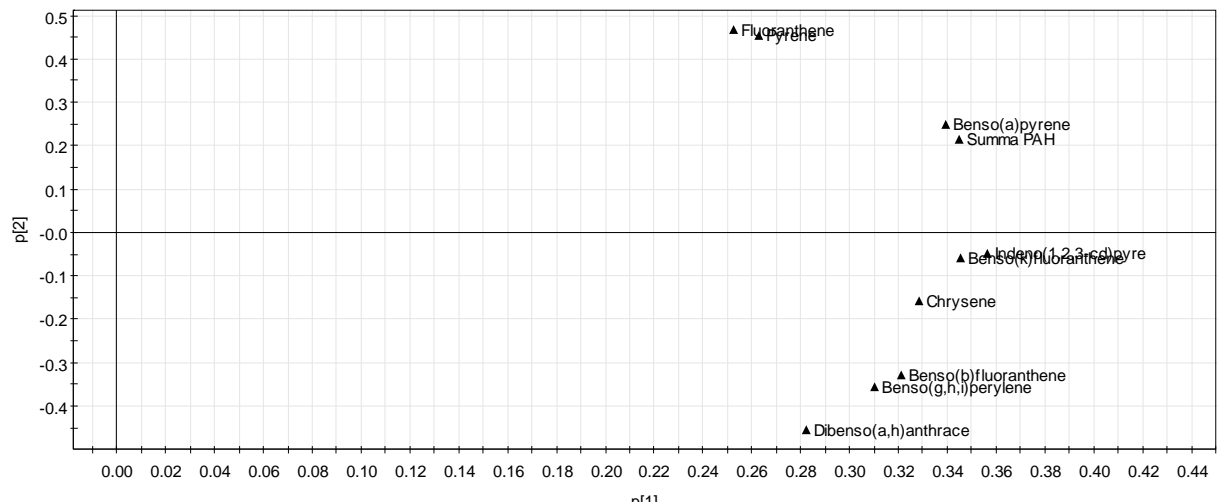


Figure 5.1.16 Loading plot for PCA on PAH analysis on PM10 and tyre.

PCA was also performed on the PIXE results for the different tyres. In the score plot in Figure 5.1.17, two tyres are sticking out from the rest of the tyres. These are the studded winter tyres from Michelin and Nokian. The Michelin studded winter tyre has generated higher concentrations of As, Br and V compared to studded winter tyre from Nokian and the other tyres. The Nokian studded

winter tyre has generated more P in the particles than the others, which can also be seen in the loading plot in Figure 5.1.18.

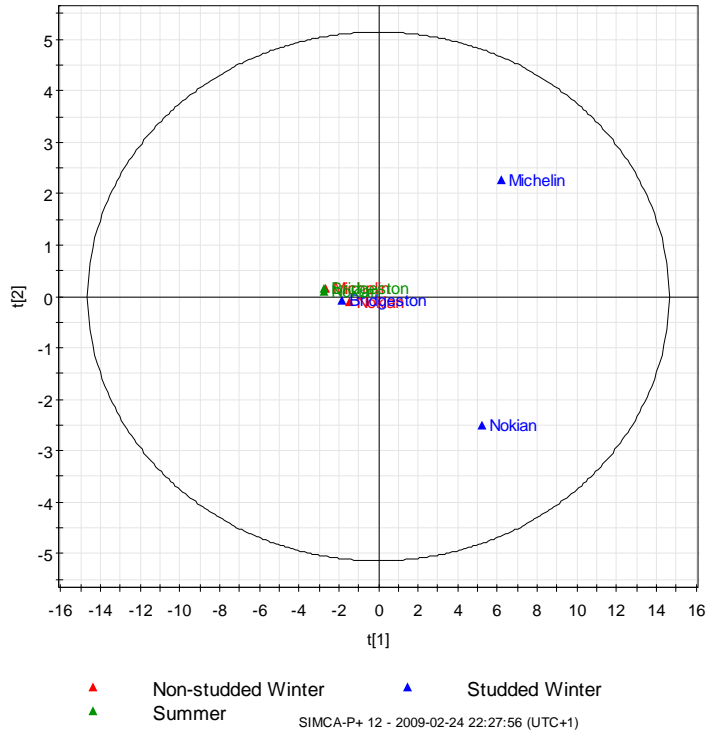


Figure 5.1.17 Score plot for the PIXE results from the road simulator runs with different tyres.

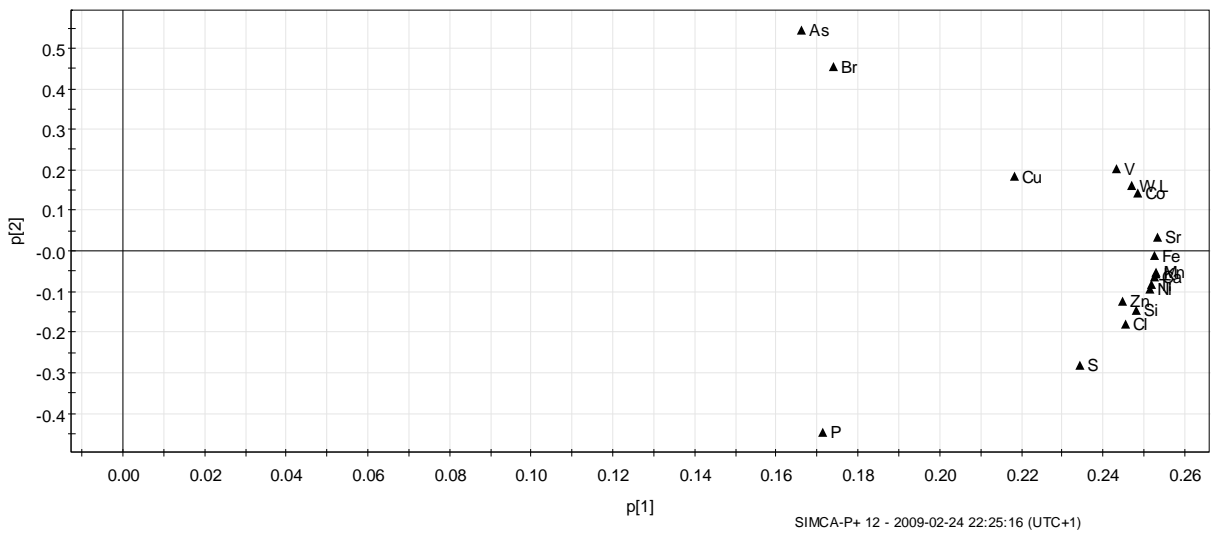


Figure 5.1.18 Loading plot for the PIXE results from the simulator runs with different tyres.

5.2 Mass closure/mass balance of measured data

5.2.1 Stockholm

ICP-MS versus IC analysis

In ICP-MS the total amount of the element is analysed, while in IC only free ions are analysed. Calcium salts are used for ice melting and as dust-binding agent as in CaCl_2 and CMA. Calcium is also common in rocks used as building material or in paved roads. It is then bound in a water insoluble form. The ICP-MS analyses should therefore give a higher concentration than IC. For this reason the concentrations obtained with ICP-MS should also exceed the concentrations obtained by IC for magnesium, sodium and potassium.

The correlation coefficients of the concentration obtained by IC as a function of the concentration obtained by ICP-MS are given in Table 5.2.1. The correlation usually gets poorer when smaller particle sizes are investigated due to approaching of the detection limit.

Table 5.2.1 Correlation coefficient r^2 , for concentrations ($\mu\text{g m}^{-3}$) obtained by IC versus those obtained by ICP-MS.

Site		PM _x	Ca	K	Mg	Na
Hornsgatan	PM ₁₀	0.88	0.59	0.13	0.33	0.49
Hornsgatan	PM _{2.5}	0.86	0.56	0.00	0.29	0.42
Hornsgatan	PM ₁	0.93	0.02	0.21	0.02	0.61
Torkel Knutssonsgatan	PM ₁₀	0.60	0.32	0.06	0.34	0.76
Torkel Knutssonsgatan	PM _{2.5}	0.77	0.46	0.00	0.91	0.89
Both	all	0.92	0.75	0.25	0.56	0.70

In Table 5.2.2 the ratio between the average concentrations are shown. The ion/element ratio is usually lower at Hornsgatan than at Torkel Knutssonsgatan and lowest for PM₁₀, indicating the presence of rock material from the street.

Table 5.2.2 Ratio between concentrations ($\mu\text{g m}^{-3}$) obtained by ICP-MS and IC.

Site		PM _x	Ca	K	Mg	Na
Hornsgatan	PM ₁₀	1.11	0.57	0.08	0.18	0.64
Hornsgatan	PM _{2.5}	1.04	0.76	0.17	0.22	0.75
Hornsgatan	PM ₁	0.94	5.41	0.56	0.51	1.25
Torkel Knutssonsgatan	PM ₁₀	1.11	1.00	0.27	0.42	0.87
Torkel Knutssonsgatan	PM _{2.5}	1.04	1.41	0.40	0.50	0.82
Both	all	1.09	0.68	0.11	0.24	0.74

Mass balances

The dominating elements obtained by ICP-MS analyses of the PM samples were; Na, Mg, Al, Si, K, Ca and Fe. In rocks they are present as oxides. The particle mass was estimated from these seven elements using the factors presented in Table 5.2.3.

Table 5.2.3 Factors for mass balance for dominating elements of the analysed filters.

Element	Compound	Factor
Na	Na ₂ O	1.35
Mg	MgO	1.66
Al	Al ₂ O ₃	1.89
Si	SiO ₂	2.14
K	K ₂ O	1.21
Ca	CaO	1.40
Fe	Fe ₂ O ₃	1.43

The correlation between the calculated mass using the factors in Table 5.2.3 with that obtained from weighing the filters are shown for Hornsgatan in Figure 5.2.1. Sometimes the calculated mass exceeds the weighed, but on average the agreement is good for PM₁₀ (99±53 %), but doesn't leave anything for the organic fraction. For PM_{2.5} a smaller fraction is calculated (54±21 %) and for PM₁ even smaller (45±23 %).

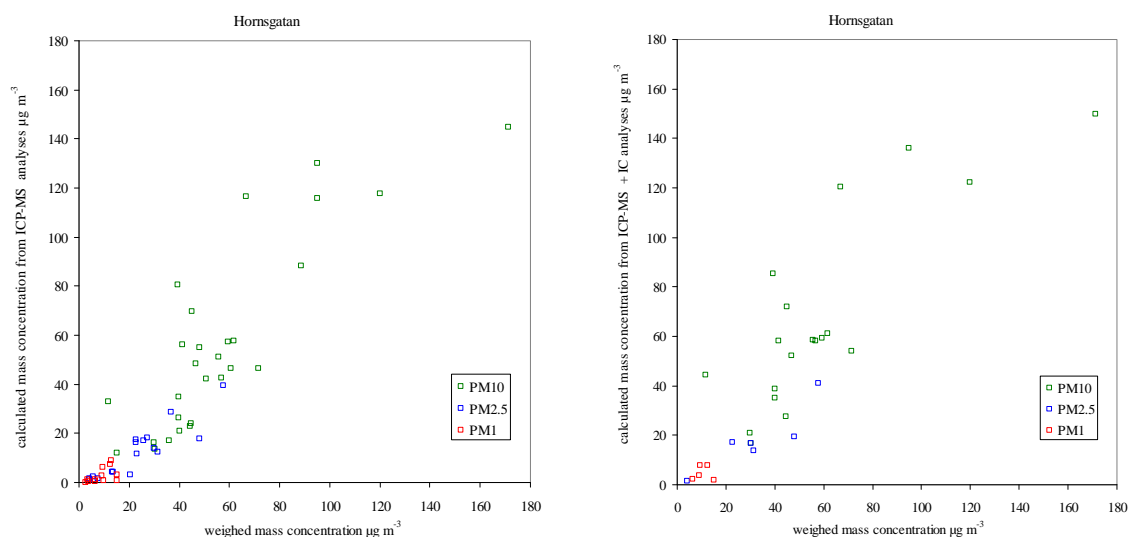


Figure 5.2.1 Correlation between the calculated mass using the factors in Table 5.2.3 with that obtained from weighing the filters for Hornsgatan. Left = ICP-MS-data only. Right = ICP-MS + IC-data.

In some PM_{2.5} samples from Torkel Knutssonsgatan the calculated mass was very small compared to the weighed mass, see Figure 5.2.2. This was always the case at Aspvreten, even for PM₁₀.

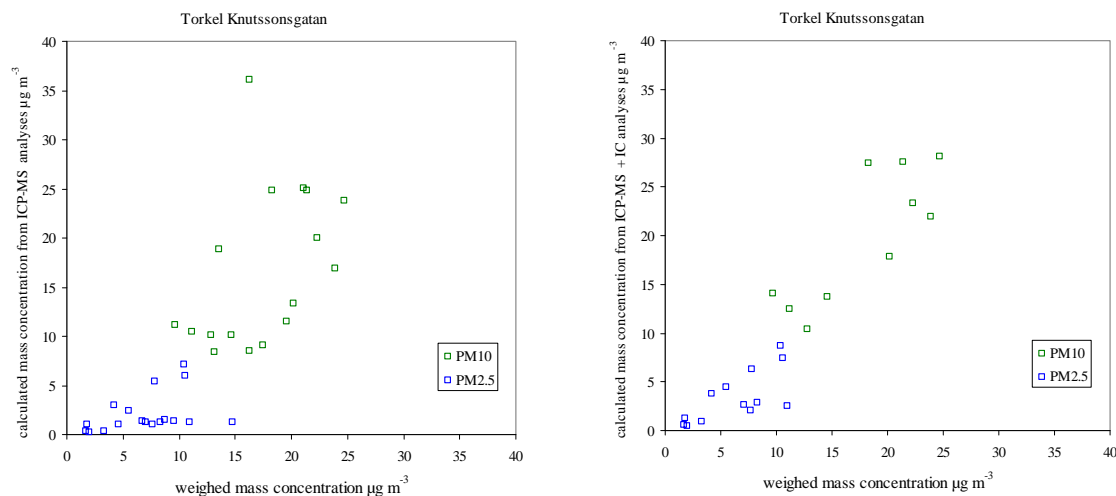


Figure 5.2.2 Correlation between the calculated mass using the factors in Table 5.2.3 with that obtained from weighing the filters for Torkel Knutssonsgatan. Left = ICP-MS-data only. Right = ICP-MS + IC-data.

Comparing street, urban and regional background concentrations of PM₁₀ and PM_{2.5}

A few daily PM₁₀ and PM_{2.5} samples from the regional background site Aspvreten south of Stockholm were analysed for metals by ICP-MS. These samples were not synchronous with analysed samples from Hornsgatan and Torkel Knutssonsgatan. The results are shown in Figure 5.2.3. The concentrations of PM_{2.5} at Torkel Knutssonsgatan were unusually low for these days. The concentrations of PM₁₀ and PM_{2.5} at Aspvreten were lower than the annual average during these periods. PM₁₀, PM_{2.5} and PM₁ were measured at Aspvreten during the whole year 2006. The yearly average concentrations were 11.8, 9.4 and 4.9 $\mu\text{g m}^{-3}$, respectively (Ferm et al., 2008).

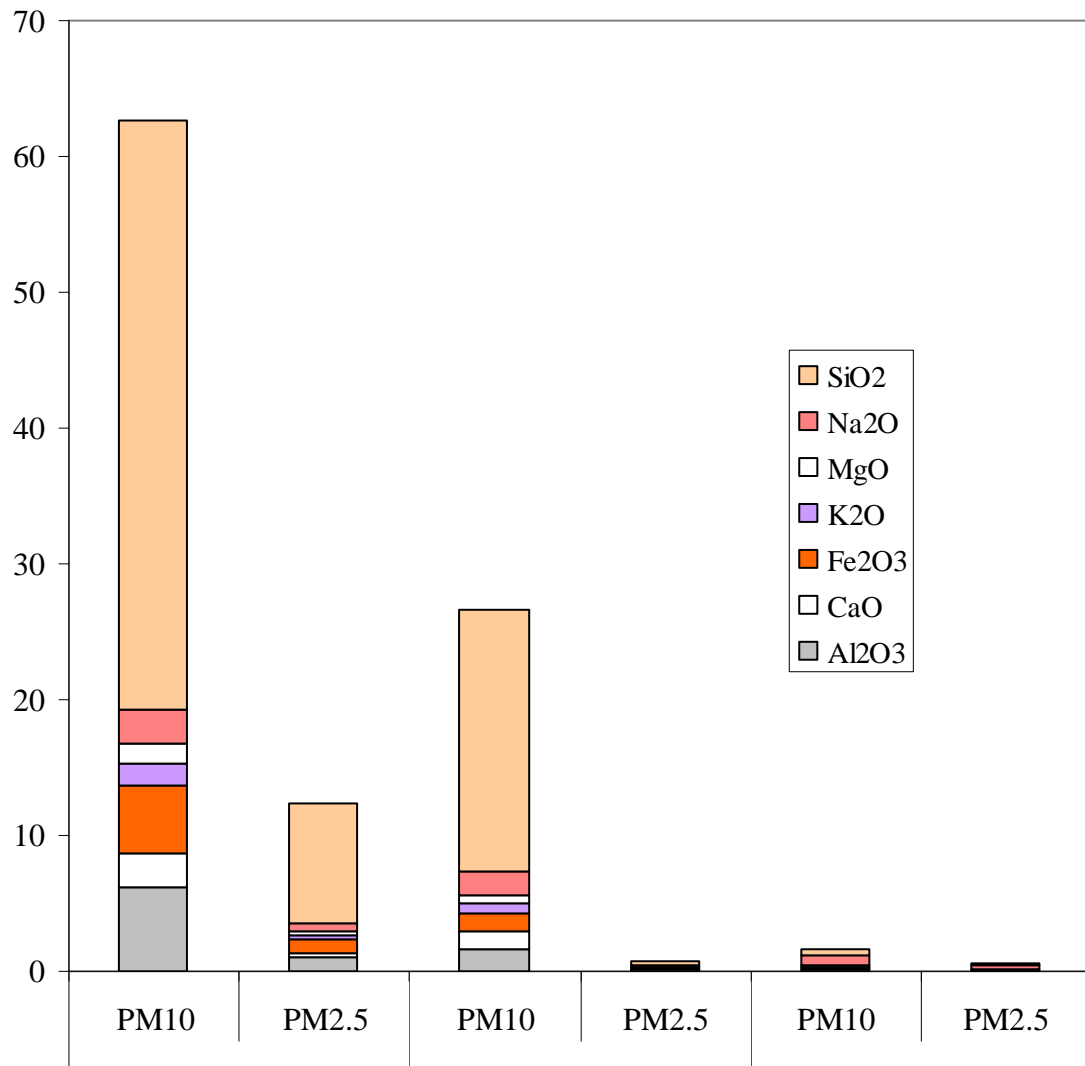


Figure 5.2.3 PM10 and PM2.5 concentrations and corresponding composition of element for the regional background site Aspvreten south of Stockholm compared with Hornsgatan and Torkel Knutssongatan.

5.2.3 Road simulator

From the measurements in the road simulator there were only a few samples analysed by ICP-MS, so the basis for the mass balance was rather poor. Nevertheless, a fairly good correlation was found, cf. Figure 5.2.4.

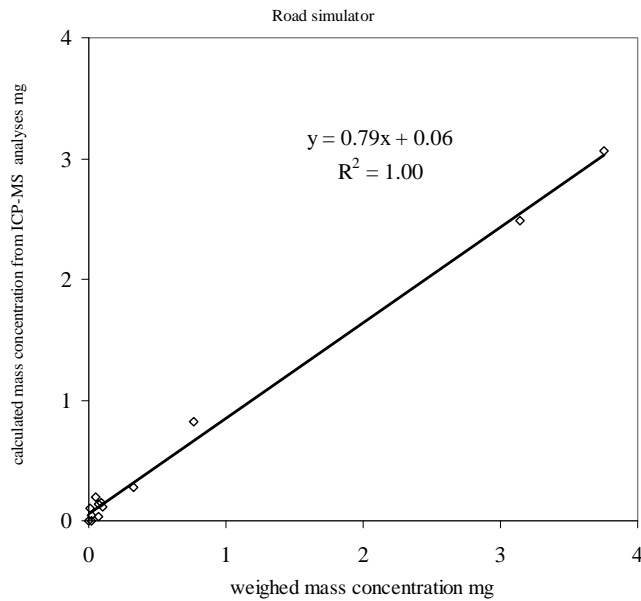


Figure 5.2.4 Correlation between the calculated mass using the factors in Table 5.2.3 with that obtained from weighing the filters for PM samples from the road simulator runs.

5.2.4 Swedish Urban Air Quality Network

With one exception (Kävlinge, a small city in southern Sweden), a generally good correlation between calculated mass (from elemental analysis) and weighed mass was found for PM₁₀ measured in a number of cities within the Swedish Urban Air Quality Network (Figure 5.2.6).

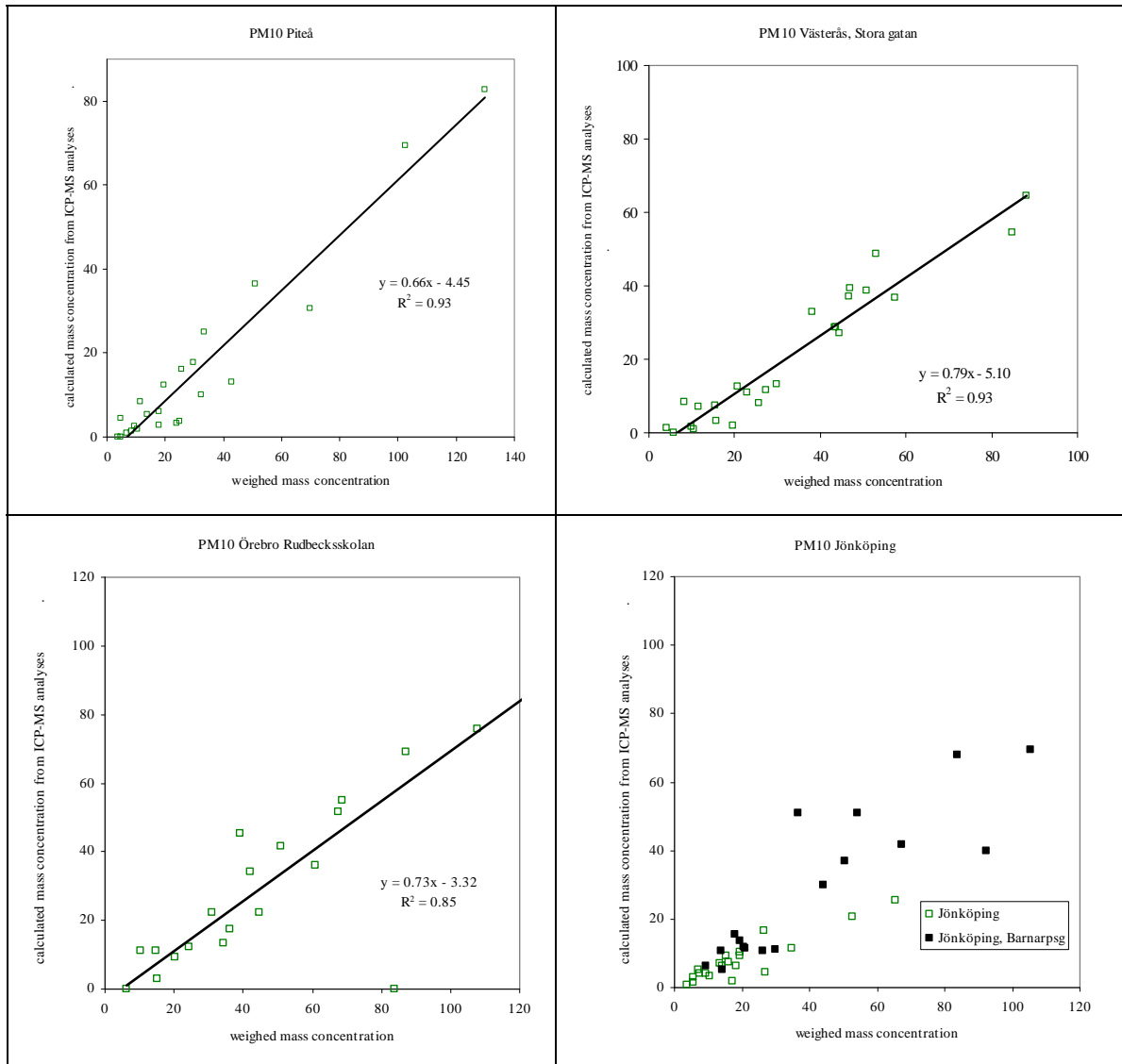


Figure 5.2.6 Correlation between calculated mass and weighed mass of PM₁₀ samples (roof level) collected in the cities of Piteå (northern Sweden), Västerås and Örebro (middle Sweden), and Jönköping (southern Sweden). All data refer to roof level (urban background) measurements, except for Jönköping Barnarpsgatan, which represents street level measurements.

5.3 Receptor modeling of field data

5.3.1 Source profiles

For COPREM input source profiles are needed. Default values are given in Table 5.3.1 and illustrated in Figure 5.3.1. For exhaust the main marker is NO_x. Emissions of typical crustal elements are also fixed to give negligible contributions. For brake lining wear copper and antimony are tracers and there is no NO_x emission.

For the tyre wear the profile is based on the analyses reported in this project. Studded tyres are weighted to contribute with 70% and non-studded winter tyres give contribution of 30%. This is not representative for the all samples since some should have much less studded tyre contributions, but as can be seen in Figure 5.3.2, the relative composition of the different types of tyres is quite similar. Somewhat surprisingly, the relative composition of the tyres is similar to the road wear profile (see Figure 5.3.1), with similar Al, Si and Fe composition. In this case the default road wear profile is taken from a filter sampled in a road simulator experiment, with studded tyres and Hornsgatan as pavement. This profile is assumed representative for Hornsgatan road wear.

For the rural background contribution (long-range transport) five filter samples (PM₁₀) from Aspvreten were analysed and considered to be representative. The samples were from March, April and November.

In addition to the default profiles, some alternative profiles were used in order to assess the uncertainty in the resulting contributions. The alternative profiles were:

1. No constraints: The same source profiles as in the base case, but there were no constraints in the model calculations; all substances will adapt to the best fit, but the source profiles are initial values for the solution.
2. Quartzite: The measured source profile for road wear was represented by “pure” quartzite instead of the filter sample from the road simulator. Constraints were the same as in the base case. This stone is the hard material in the pavement. The other source profiles and constraints were the same as in the base case.
3. Local stone material: The measured source profile for road wear was represented by local stone material (the filler stone used at Hornsgatan) instead of the filter sample from the road simulator. Constraints were the same as in the base case. This stone material is much softer than the quartzite. The other source profiles and constraints were the same as in the base case.
4. Tyre of Hjortenkrans et al., 2007: The source profile for tyre wear was represented by the tyre analyses and sales estimates according to Hjortenkrans et al. (2007) instead of the tyre material analysed within this project. The analyses did not include the same elements, so they cannot be compared. The other source profiles and constraints were the same as in the base case.

Table 5.3.1 Default source profiles. Values in bold are fixed and those in italics are free in the COPREM simulations.

	Exhaust	Brake wear	Tyre wear	Road wear	Long-range tr.
PM _x	<i>0.0250</i>		1	1	1
Ag	<i>0</i>		<i>0</i>	<i>0</i>	5.5E-06
Al	0		<i>0</i>	0.0623	0.0690
As	<i>0</i>		<i>0</i>	<i>0</i>	4.9E-05
Ba	<i>0</i>		<i>0</i>	<i>0</i>	0.0002
Bi	<i>0</i>		<i>0</i>	<i>0</i>	5.0E-06
Ca	0		<i>0</i>	0.0029	0.0114
Cd	<i>0</i>	<i>1.1E-06</i>	<i>0</i>	<i>0</i>	1.3E-05
Co	<i>0</i>	<i>0</i>	<i>0</i>	<i>0</i>	9.6E-06
Cr	<i>3.8E-06</i>	<i>0</i>	<i>0</i>	<i>0</i>	6.6E-05
Cu	<i>0</i>	0.0499	0	8.0E-05	0.0001
Fe	<i>0</i>	<i>0</i>	<i>0.0035</i>	<i>0.0145</i>	0.0126
K	<i>0</i>	0	<i>0.0032</i>	<i>0.0223</i>	0.0186
Li	<i>0</i>	<i>0</i>	<i>0</i>	<i>0</i>	1.3E-05
Mg	<i>0</i>	0	<i>0</i>	<i>0</i>	0.0117
Mn	<i>0</i>	<i>0</i>	0.0001	0.0004	0.0004
Mo	<i>0</i>	<i>0</i>	<i>0</i>	<i>0</i>	4.1E-05
Na	<i>0</i>	0	<i>0</i>	<i>0</i>	0.064145
Ni	<i>5.3E-06</i>	<i>0</i>	<i>0</i>	<i>0.0001</i>	0.0003
Pb	<i>0.0001</i>	<i>0.0005</i>	<i>0</i>	<i>0</i>	0.0005
Rb	<i>0</i>	<i>0</i>	<i>0</i>	<i>0</i>	5E-05
Sb	<i>0</i>	0.0071	0	0	3.6E-05
Si	0	<i>0</i>	0.2757	0.2891	0.0617
Sr	<i>0</i>	<i>0</i>	<i>0</i>	<i>0</i>	8.1E-05
Th	<i>0</i>	<i>0</i>	<i>0</i>	<i>0</i>	2.8E-06
Ti	<i>0</i>	0	0.0004	0.0019	0.0005
Tl	<i>0</i>	<i>0</i>	<i>0</i>	<i>0</i>	1.3E-06
U	<i>0</i>	<i>0</i>	<i>0</i>	<i>0</i>	7.7E-07
V	<i>0</i>	0	<i>0</i>	<i>0</i>	0.0006
Zn	<i>0.0001</i>	<i>0.0144</i>	0.0348	0.0003	0.0023
NO _x	0.8	0	0	0	<i>0.2727</i>

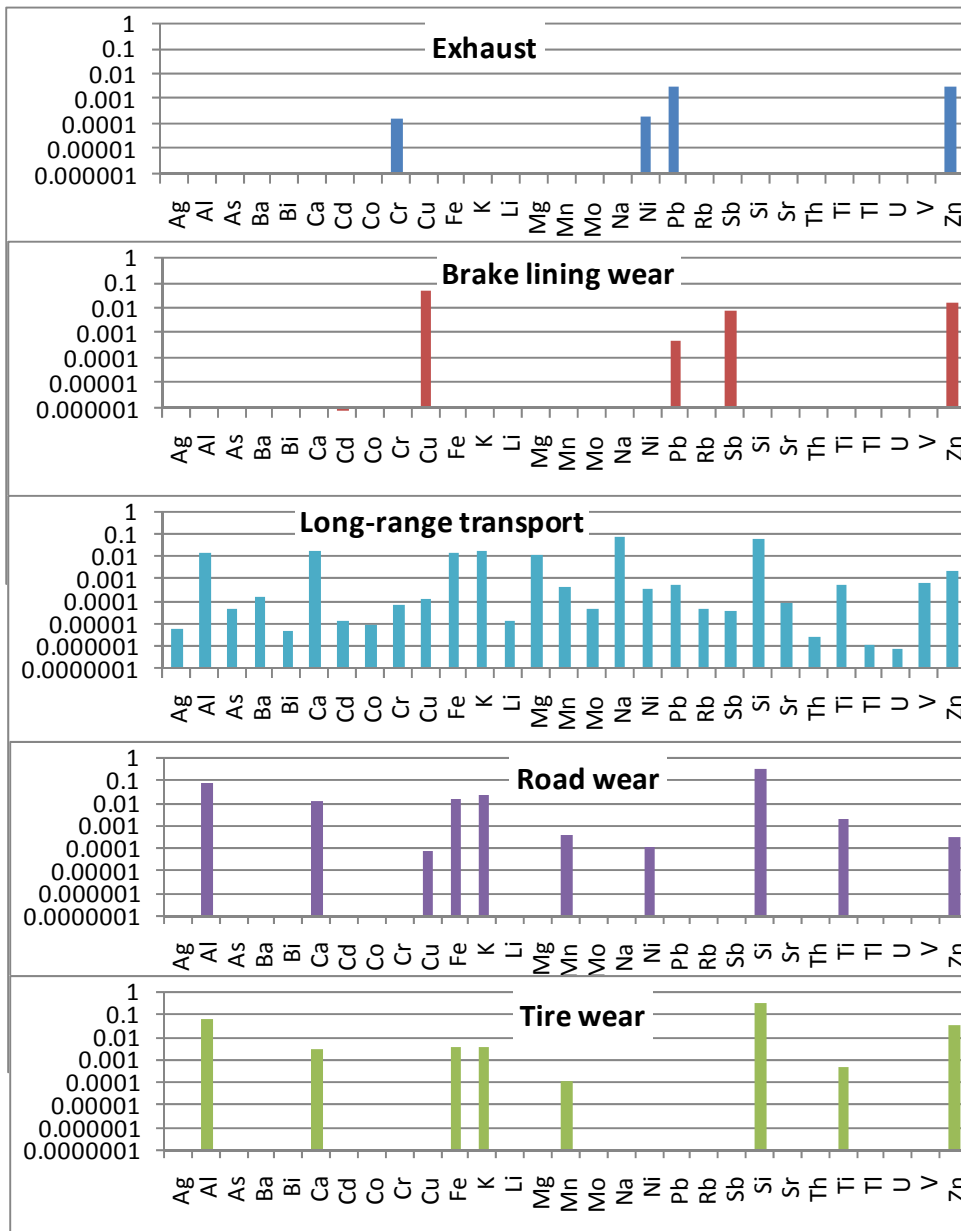


Figure 5.3.1 Default profiles used for COPREM. Relative composition with total particle mass being 1.

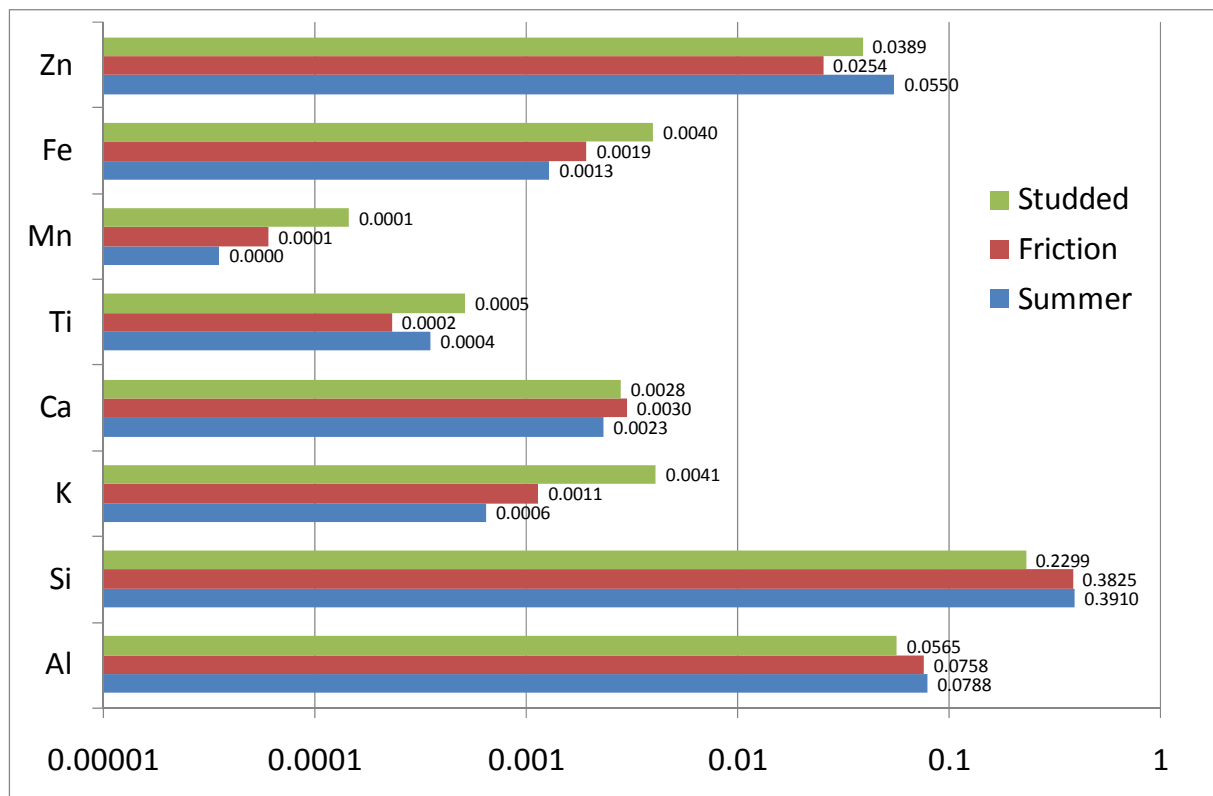


Figure 5.3.2 Relative composition of different types of tyres analysed in this project.

5.3.2 COPREM - Base results for PM₁₀, Hornsgatan

The total PM₁₀ contributions for all samples taken at Hornsgatan are shown in Figure 5.3.3. As can be seen the R² value is very high (0.85), but the total mass is somewhat overestimated (by almost 30%). This result is quite acceptable since it should be kept in mind that the measured total PM₁₀ concentrations are quite uncertain. A comparison between the gravimetric PM₁₀ (filter weighed) and TEOM data of PM₁₀ shows an R²-value of 0.77 and that the TEOM instrument (corrected for losses by multiplying the values by 1.2) yields about 20% higher values than the gravimetrically derived PM₁₀.

Resulting mean source contributions to the mean concentrations for all compounds are presented in Table 5.3.2. As can be seen the residual values (calculated minus measured total concentrations) are generally very small. Based on these source contributions it is possible to estimate emission factors for the different sources by using the total emission factors determined from the street minus roof concentrations as described earlier, see Table 5.3.3.

For PM₁₀ the emission factors for exhaust, brake, tyre and road wear derived to 39, 7.4, 2.2 and 227 mg/vehicle km, respectively. These values are in good agreement with earlier estimates for Hornsgatan (e.g. Johansson et al., 2004). The most robust value obtained is for road wear, since there are several typical crustal road elements analysed that make a large contribution to the total mass. The emission factor for exhaust particles for Hornsgatan in 2007 according to the ARTEMIS Road Model is 32.3 mg/vehicle km, which is close to the value obtained from the COPREM

calculations. The least accurate estimate is the tyre wear contribution, since there are no unique tracers included in the analyses and since the profile of the elements used is very similar to the road wear profile.

The accuracy of the emission factors of individual elements is more difficult to assess. For copper the emission factor for brake lining wear dominates (87 %), as expected from the source profiles. Vehicle exhaust contributes with 12 %. This is consistent with estimates by Johansson et al. (2009). Important tyre wear contributions are for vanadium, lead, nickel and zink, but these contributions need to be confirmed with more studies. For lead Johansson et al. (2009) estimated a large contribution (90%) from exhaust, whereas in the present calculations exhaust make a minor contribution (16%).

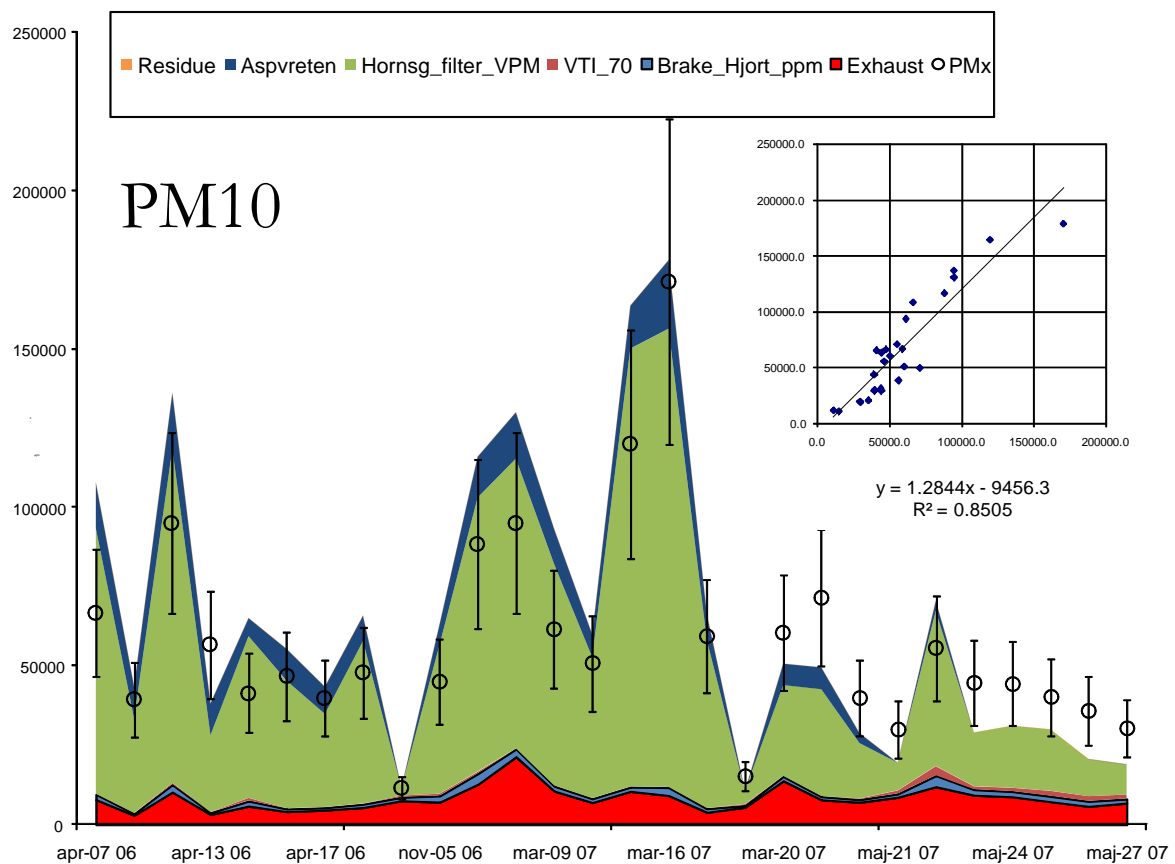


Figure 5.3.3 Contributions to total PM_{10} by different sources (colored areas) calculated by the COPREM model, and measured concentrations with error bars. In the scatter plot calculated total concentrations are plotted against measured concentrations.

Table 5.3.2 Calculated (based on COPREM) source contributions to the measured concentrations in PM₁₀ samples from Hornsgatan. Units: ng/m³.

	Exhaust	Brake wear	Tyre wear	Asphalt wear	Long-range transport	Residue
PM ₁₀	8134	1528	461	46917	7168	5.0E-07
Ag	0	0	0.012	0	0.039	0.14
Al	0	0	28.7	3236	92.8	2.8E-05
As	0	0	0.21	0	0.35	0.0048
Ba	5.40	25.8	0.83	13.2	1.12	-9.0E-05
Bi	0.172	0.351	0.142	0	0.0358	0.0044
Ca	0	767	1.32	537	134	-7.8E-06
Cd	0	0	0.0142	0	0.0956	0.072
Co	0.198	0.0447	0.0190	1.133	0.0686	7.5E-05
Cr	0	3.30	0.659	1.62	0.476	8.7E-05
Cu	10.6	76.3	0	0	0.986	0.00136
Fe	325	1858	48.4	1072	90.4	-7.9E-07
K	544	0	0	0	133	-0.00033
Li	0	0.0790	0	1.13	0.0961	0.000927
Mg	0	0	72.9	578	83.9	8.2E-06
Mn	0	31.7	0.0553	0	2.95	-0.00447
Mo	1.29	3.01	0.734	0	0.295	0.00241
Na	814	0	0	257	459	3.7E-06
Ni	0.466	0	1.561	0	2.358	0.00166
Pb	1.045	0	1.922	0	3.44	0.010199
Rb	0.363	0	0.0536	4.88	0.358	-0.00120
Sb	2.46	10.9	0	0	0.257	0.00330
Si	0	1037	127	13564	442.0	-1.7E-07
Sr	0.648	0	0.426	5.87	0.581	0.00025
Th	0	0	0.0385	0.640	0.0198	-0.0026
Ti	45.3	0	0.198	87.0	3.857	-0.0012
Tl	0.00428	0	0.00161	0.0137	0.00911	-0.0015
U	0	0.013	0.00296	0.147	0.00550	-0.012
V	0	0	1.58	0	4.42	-0.0035
Zn	7.50	10.7	16.1	13.6	16.7	0.00017
NO _x	132891	0	0	0	0	1.4E-06

Table 5.3.3 Calculated mean emission factors based on the derived default COPREM source contributions and the total emission factors estimated (independently) using NO_x as tracer and the street increment as presented earlier. Unit is µg/vkm except for PM₁₀ which is mg/vkm.

Emission factor	Total emission factor	Exhaust	Brake wear	Tyre wear	Asphalt wear
PM ₁₀	310.5	39.3	7.4	2.2	226.9
Ag	0.38	0.0	0.0	0.1	0.0
Al	18094	0.0	0.0	154.8	17439
As	2.01	0.0	0.0	0.7	0.0
Ba	231.6	27.0	129.0	4.2	65.8
Bi	3.66	0.9	1.8	0.7	0.0
Ca	7240	0.0	3859	6.6	2701
Cd	0.06	0.0	0.0	0.0	0.0
Co	8.46	1.1	0.3	0.1	6.5
Cr	41.73	0.0	22.8	4.5	11.1
Cu	454.7	54.7	394.9	0.0	0.0
Fe	17309	1658	9478	247.0	5465
K	7163	5754	0.0	0.0	0.0
Li	7.17	0.0	0.4	0.0	6.2
Mg	4060	0.0	0.0	402.6	3194
Mn	188.4	0.0	172.1	0.3	0.0
Mo	24.76	6.0	14.0	3.4	0.0
Na	7291	3879	0.0	0.0	1224
Ni	15.61	1.7	0.0	5.6	0.0
Pb	22.27	3.6	0.0	6.7	0.0
Rb	33.58	2.2	0.0	0.3	29.0
Sb	64.73	11.7	51.8	0.0	0.0
Si	140059	0.0	9578	1174	125226
Sr	39.72	3.4	0.0	2.2	31.0
Th	4.30	0.0	0.0	0.2	3.9
Ti	1063	353.3	0.0	1.5	678.1
Tl	0.10	0.0	0.0	0.0	0.0
U	1.03	0.0	0.1	0.0	0.9
V	32.26	0.0	0.0	8.5	0.0
Zn	276.2	32.1	45.9	68.7	58.1

5.3.3 COPREM-results for PM_{2.5}

For PM_{2.5} there were 17 samples analysed for Hornsgatan. Based on these, COPREM was used to estimate source contributions for exhaust brake and road wear and long-range transport. The emission factors are presented in Table 5.3.4. The profile and form settings were the same as for the base case for PM₁₀. The total emission factors for PM_{2.5} and the elements in the PM_{2.5} fraction were estimated from simultaneous measurements at street and urban background (Hornsgatan and Torkel Knutssongatan).

As can be seen in Table 5.3.4 the PM_{2.5} emission factors for exhaust, brake and road wear are lower than PM₁₀. Exhaust emission factor would be expected to be the same for PM₁₀ and PM_{2.5}, but the difference might be due to uncertainties in the model. Road wear largely exceeds (a factor 3) exhaust. The ratio of brake to road wear for PM_{2.5} is about the same as for PM₁₀.

Table 5.3.4 Emission factors for PM_{2.5} based on COPREM. Unit: µg/vkm (except for PM_{2.5}).

Emission factor	Total emission factor	Exhaust	Brake wear	Road wear
PM2.5 (mg/vkm)	75.79	17.2	2.2	56.4
Al	3305	0.0	0.0	3305
Ba	40.68	0.8	21.6	18.2
Bi	0.30	0.1	0.2	0.0
Ca	1334	0.0	868.6	465.8
Co	1.83	0.3	0.8	0.7
Cr	48.01	9.4	38.6	0.0
Cu	65.96	0.0	66.0	0.0
Fe	2816	0.0	2105	711.1
K	1426	105.6	101.8	1219
Li	0.44	0.4	0.1	0.0
Mg	786.6	0.0	94.7	691.9
Mn	35.64	0.0	20.2	15.4
Mo	7.60	0.0	7.6	0.0
Na	1810	186.5	0.0	1624
Ni	27.66	11.0	16.7	0.0
Pb	2.95	0.1	2.8	0.0
Rb	6.61	0.0	0.0	6.6
Sb	9.13	0.0	9.1	0.0
Si	20894	0.0	0.0	20894
Sr	9.31	1.0	0.0	8.3
Th	0.43	0.2	0.2	0.1
Ti	229.0	0.0	0.0	229.0
U	0.12	0.1	0.0	0.0
V	5.66	0.0	5.7	0.0
Zn	48.24	27.4	11.6	9.3

5.3.4 COPREM-results for PM₁

Source contributions to PM₁ based on COPREM are shown in Table 5.3.5. Source profiles and form values were the same as for PM₁₀ base scenario. There were only 12 samples. According to the COPREM model runs the occurrence of PM₁ at Hornsgatan is due to exhaust (38%), brake (37%), road wear (35%) and long range transport (27%).

For copper 75% is due to brake wear and 17% due to exhaust, and for lead exhaust contributes with 8%, whereas brake lining wear contributes with 56% of the concentrations in PM₁.

Emission factors for PM₁ have not been calculated since there were no data of urban background concentrations and hence the road increment could not be derived.

Table 5.3.5 Estimated source contributions to PM₁ concentrations at Hornsgatan according to the COPREM model runs. Unit ngm⁻³.

	Exhaust	Brake wear	Road wear	Background
PM ₁	3060 (38%)	36.6 (0%)	2765 (35%)	2121 (27%)
Al	0.00 (0%)	0.00 (0%)	132.5 (91%)	13.47 (9%)
Ba	0.32 (19%)	0.40 (23%)	0.91 (53%)	0.09 (5%)
Cu	0.41 (17%)	1.83 (75%)	0.00 (0%)	0.20 (8%)
Fe	0.00 (0%)	122.4 (100%)	0.00 (0%)	0.60 (0%)
K	1.67 (3%)	0.00 (0%)	51.93 (85%)	7.17 (12%)
Mg	0.00 (0%)	0.00 (0%)	27.54 (95%)	1.39 (5%)
Mn	0.00 (0%)	0.63 (37%)	0.87 (50%)	0.22 (13%)
Mo	0.08 (35%)	0.02 (8%)	0.10 (46%)	0.02 (11%)
Na	0.00 (0%)	79.92 (100%)	0.00 (0%)	0.00 (0%)
Ni	0.00 (0%)	0.06 (7%)	0.05 (6%)	0.80 (87%)
Pb	0.07 (8%)	0.50 (56%)	0.00 (0%)	0.32 (36%)
Rb	0.00 (0%)	0.00 (0%)	0.25 (100%)	0.00 (0%)
Sb	0.00 (0%)	0.26 (87%)	0.00 (0%)	0.04 (13%)
Si	47.58 (7%)	0.00 (0%)	554.2 (77%)	114.1 (16%)
Ti	4.06 (100%)	0.00 (0%)	0.00 (0%)	0.00 (0%)
V	0.02 (2%)	0.00 (0%)	0.24 (22%)	0.84 (76%)
Zn	2.25 (34%)	0.73 (11%)	2.27 (34%)	1.33 (20%)

5.3.5 COPREM – Variation of contribution due to source profiles

Table 5.3.6 shows a comparison of emission factors for some compounds depending on the source profile used in the COPREM runs. For total PM₁₀ the emission factors are within a factor 2 or 3 in all cases except for tyre wear when no constraints are used. In some cases changes compared to the base case are drastic, especially when no constraints are used. For aluminum tyre wear exceeds road wear if no constraints are set with the base profiles and exhaust emission become 10% of road wear emissions, which is unrealistic. For copper exhaust emission factors varies from 0 to 139 µg/vkm depending on the profile used, but the brake wear emission factor is relatively constant, which is consistent with the fact that most copper is due to brake wear. Lead is more variable for all source profiles. For iron the contribution from brake wear is very important in all cases. Also for zinc brake wear is estimated to be a very important source.

Table 5.3.6 Comparison of calculated emission factors for different source profiles in COPREM.

		<i>Exhaust</i>	<i>Brake wear</i>	<i>Tyre wear</i>	<i>Road wear</i>
Base case	PM_x mg/fkm	39.3	7.4	2.2	226.9
No constraints	PM _x	20.7	25.2	122.3	78.0
Local stone material	PM _x	29.5	9.3	1.8	259.7
Quartzite stone	PM _x	98.1	9.8	1.7	184.5
Tyre Hjortenkrans et al.	PM _x	73.6	9.2	5.2	197.6
Base case	Al	0.0	0.0	154.9	17439.2
No constraints	Al	259.1	370.1	13383.6	2343.9
Local stone material	Al	0.0	1197.9	133.0	16602.2
Quartzite stone	Al	0.0	2167.5	116.2	15577.4
Tyre Hjortenkrans et al.	Al	0.0	650.3	6088.3	11092.8
Base case	Cu	55.4	394.2	0.0	0.0
No constraints	Cu	91.4	271.8	4.4	50.0
Local stone material	Cu	0.0	453.3	0.0	0.0
Quartzite stone	Cu	1.2	451.5	0.0	0.0
Tyre Hjortenkrans et al.	Cu	138.6	313.7	0.0	0.0
Base case	Fe	1666	9471	248	5463
No constraints	Fe	1962	5588	6065	2159
Local stone material	Fe	569	8988	1656	5965
Quartzite stone	Fe	368	10029	719	5997
Tyre Hjortenkrans et al.	Fe	2902	6092	5906	2185
Base case	Pb	3.6	0.0	6.7	0.0
No constraints	Pb	2.7	9.1	3.1	2.5
Local stone material	Pb	0.4	11.6	0.0	6.9
Quartzite stone	Pb	0.0	15.0	1.6	0.6
Tyre Hjortenkrans et al.	Pb	5.2	7.8	0.0	3.4
Base case	Zn	32.2	45.8	68.7	58.1
No constraints	Zn	32.3	125.3	52.7	27.2
Local stone material	Zn	0.0	178.5	52.4	24.9
Quartzite stone	Zn	0.0	198.0	47.5	0.0
Tyre Hjortenkrans et al.	Zn	53.5	122.3	31.4	34.2
Base case	NO_x	772.0	0.0	0.0	0.0
No constraints	NO _x	772.0	0.0	0.0	0.0
Local stone material	NO _x	772.0	0.0	0.0	0.0
Quartzite stone	NO _x	772.0	0.0	0.0	0.0
Tyre Hjortenkrans et al.	NO _x	772.0	0.0	0.0	0.0

5.3.6 PMF modelling results

A decision was made to use the same number of sources in the comparisons between PMF and COPREM. It was also decided to remove cadmium from the PMF analysis since it had too many values below the detection limit.

The decision was:

PM₁₀ 5 sources

PM_{2.5} 4 sources

PM₁ 4 sources

However, we built PMF-models for each fraction with a span of a number of factors, not only with 5 and 4 factors, respectively. Figure 5.3.4 shows the explained variance for the different fractions PM₁₀, PM_{2.5} and PM₁. For comparison we have also added pooled absolute errors for the elements. From Figure 5.3.4 (PM₁₀) it can be seen that it seems reasonable to obtain more than 5 statistical factors, i.e. more likely 7 factors. For PM_{2.5} it is likely that 5-7 statistical factors could have been used instead of 4. Likewise for PM₁ probably 5 factors could have been used. However, there are a low number of samples for PM_{2.5} and PM₁ and in that perspective 4 factors is likely a correct decision. In addition, the interpretation may become more difficult for each added factor. This is due to possible mix-up in the resolved sources.

$$\mathbf{X} = \mathbf{FG} + \mathbf{E}$$

F Source matrix

G Sample matrix

E Error matrix

PMF was from start built with summation normalization for the source-matrix (for the F-matrix), but this was changed to summation normalization of the sample-matrix (for the G-matrix) in order to be able to compare PMF with COPREM. In addition to this we also estimated models where NO_x was locked towards zero in two factors for the PM₁₀, PM_{2.5} and PM₁ models. This was to ensure that we did not get any exhaust contributions in more than three (PM₁₀) or two (PM_{2.5} and PM₁) factors.

In this chapter the calculated contributions to PM_x (PM₁₀, PM_{2.5} and PM₁) from different sources using the two variants of PMF models are shown in graphs. Calculated source contributions and estimated emission factors for different sources to the PM₁₀ fraction according to the two PMF models for PM₁₀, and calculated source contributions for the PM_{2.5} and PM₁ fractions from the two variants of PMF-models are presented in a series of tables in Appendix 1.

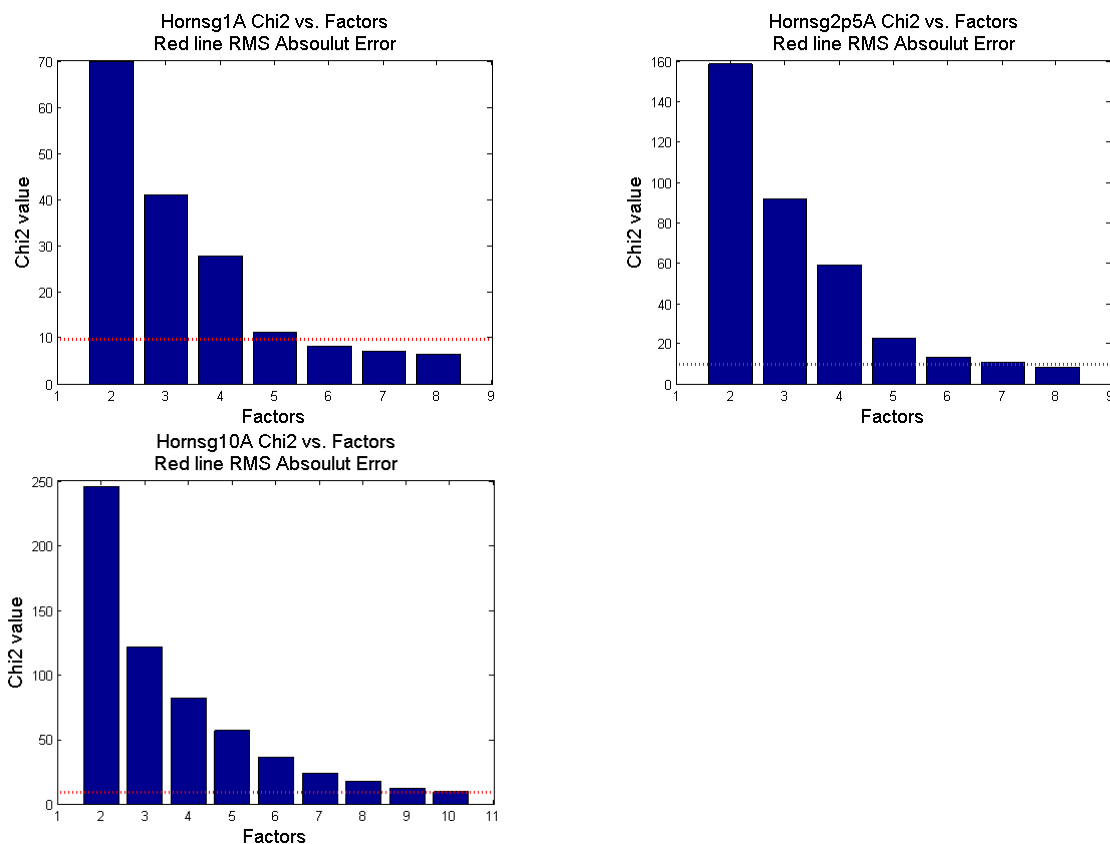


Figure 5.3.4 Chi2 vs. factors for PM₁, PM_{2.5} and PM₁₀ for the PMF models. The red line is the root mean square sum of the absolute errors of the measurements. Values from PMF models with F sum normalized.

We have manually assigned the factor labels for the PMF-models based on source profiles from the literature and the knowledge from source profiles used in COPREM. Here we show the overall results in order not to overcrowd with information. The results from the PMF models for PM₁₀ with and without NO_x locked (both with G-matrix sum normalized) are presented in Figure 5.3.5 and 5.3.6. It seems that the contribution from long-range transport is larger for the NO_x-locked model than for the non-locked model. The opposite applies to contribution from road wear, in which case the non-locked model shows a larger contribution, which is partially explained by the fact that the NO_x-locked model transfers most of the contribution to a factor entitled “winter”.

The results from the PMF models for PM_{2.5} without and with NO_x locked (both with G-matrix sum normalized) are presented in Figure 5.3.7 and 5.3.8. A more distinct division is achieved using the NO_x-locked model, in which the winter, brakes/long-range transport, road wear and exhaust source seem more physically/chemically likely than the non-locked models results.

The results from the PMF models for PM₁ with and without NO_x locked (both with G-matrix sum normalized) are presented in Figure 5.3.9 and 5.3.10. Here the main difference is that the contribution from long-range transport is increased with the NO_x-locked model compared to the non-locked model, and also gives more likely uniformity of the exhaust contribution (e.g. it is not likely to have higher exhaust contribution in May 2007 than in March, cf. Figure 5.3.9).

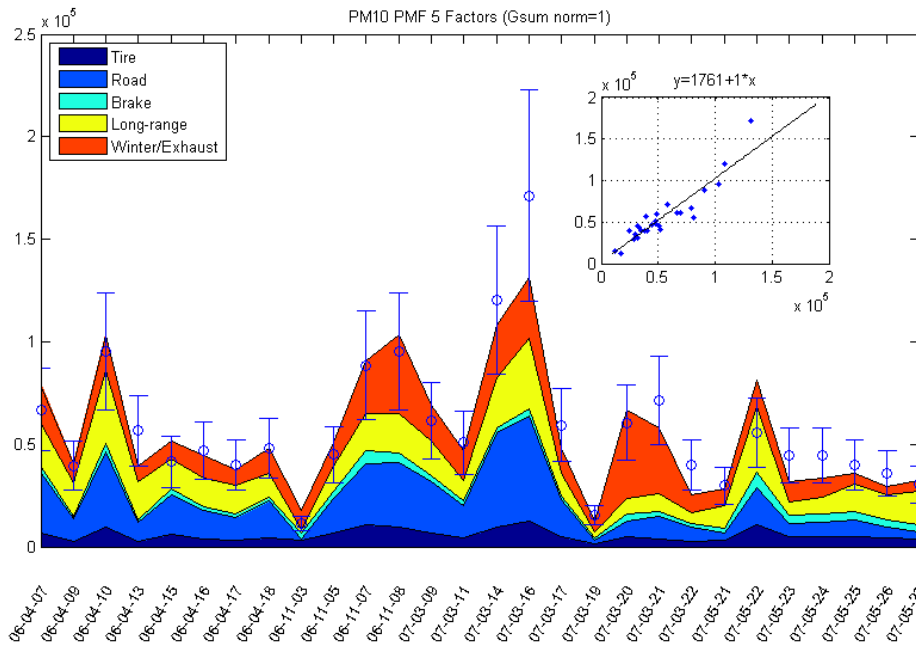


Figure 5.3.5 Results from a five factor non-locked PMF model for the PM₁₀ samples at Hornsgatan analysed for metals (G sum-normalized).

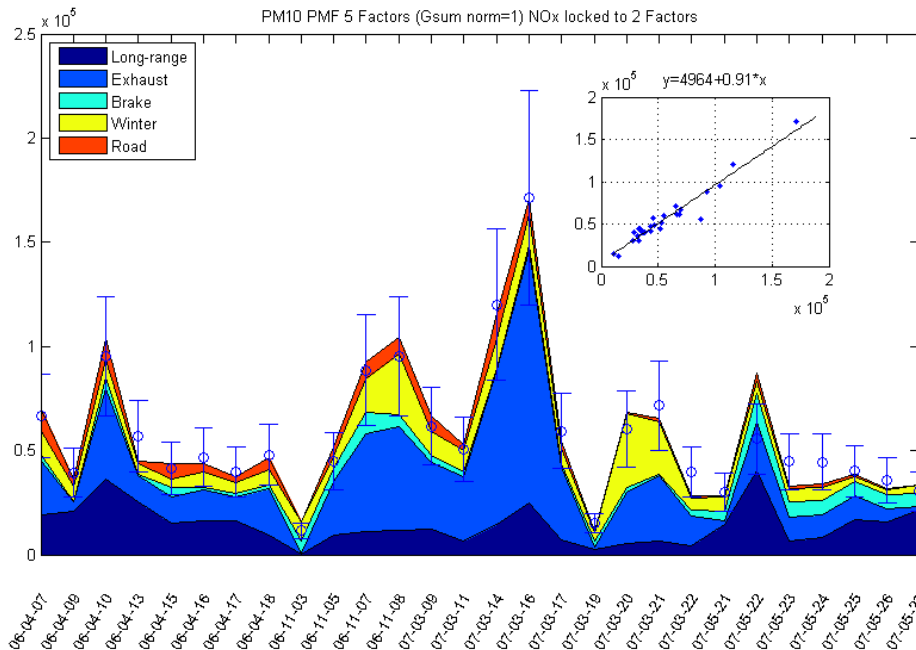


Figure 5.3.6 Results from a five factor NO_x-locked PMF model for the PM₁₀ samples at Hornsgatan analysed for metals (G sum-normalized).

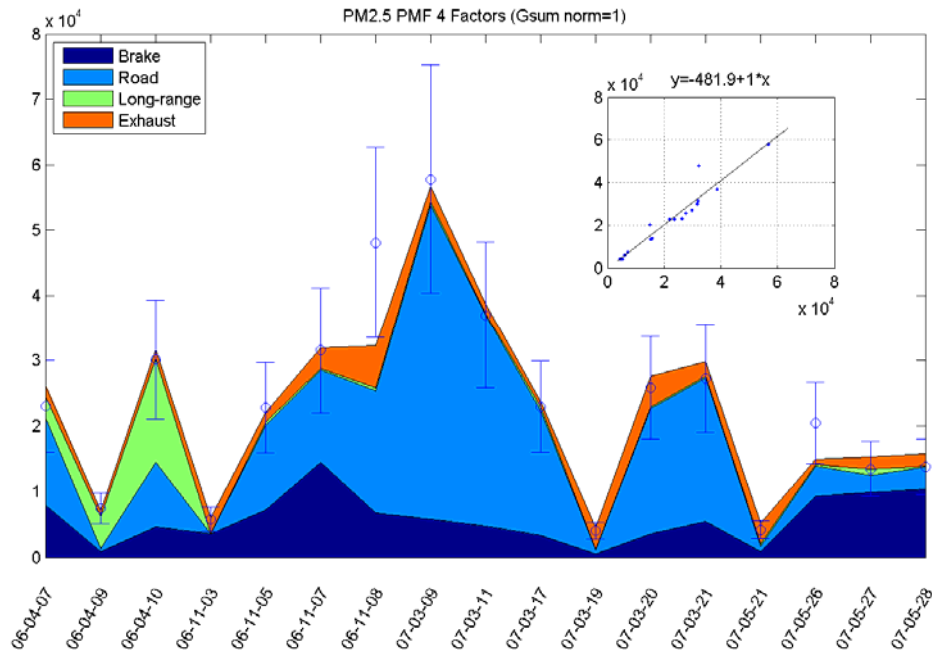


Figure 5.3.7 Results from a four factor non-locked PMF model for the PM_{2.5} samples at Hornsgatan analysed for metals (G sum-normalized).

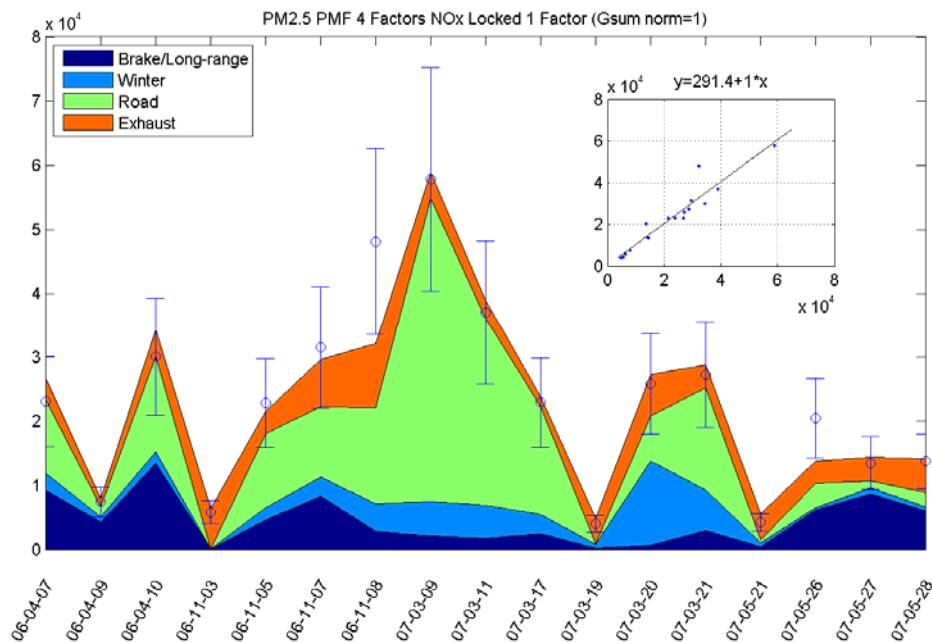


Figure 5.3.8 Results from a four factor NO_x-locked PMF model for the PM_{2.5} samples at Hornsgatan analysed for metals (G sum-normalized).

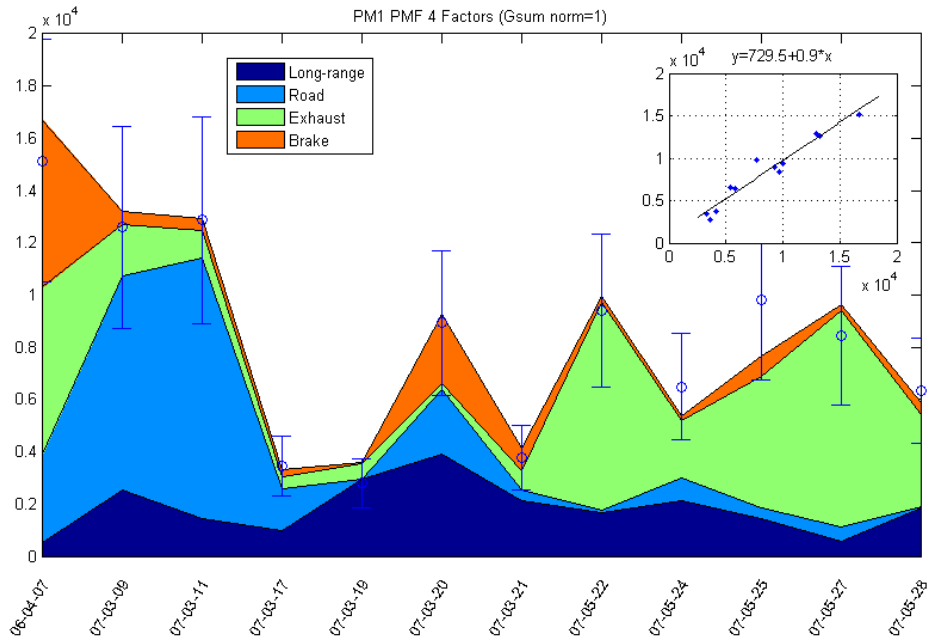


Figure 5.3.9 Results from a four factor non-locked PMF model for the PM₁ samples at Hornsgatan analysed for metals (G sum-normalized).

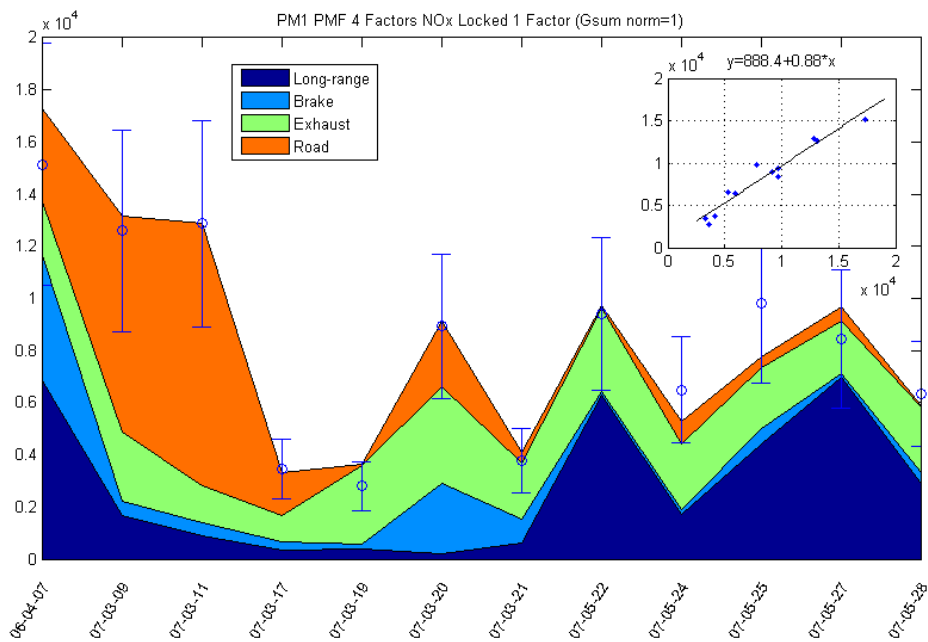


Figure 5.3.10 Results from a four factor NO_x-locked PMF model for the PM₁ samples at Hornsgatan analysed for metals (G sum-normalized).

5.3.8 Swedish Urban Air Quality Network

The COPREM model was also applied to the data from the selected PM samples from the Swedish Urban Air Quality Network. The same default source profiles as those used in the COPREM modeling for the Hornsgatan PM samples was used, with one exception. Because of the lack of data on NO_x from the Swedish Urban Air Quality Network sites, the NO_x profile was omitted from the source profile. In Figure 5.3.11 the calculated source contributions to PM₁₀ for the different urban sites including the results from Hornsgatan are presented. This is a relative contribution for the different sources at the sites. The detailed results for all sources and elements for the four cities in Figure 5.3.11 are presented in Appendix 2. The dominating contribution from road wear to the PM₁₀ concentrations in urban areas in Sweden is obvious.

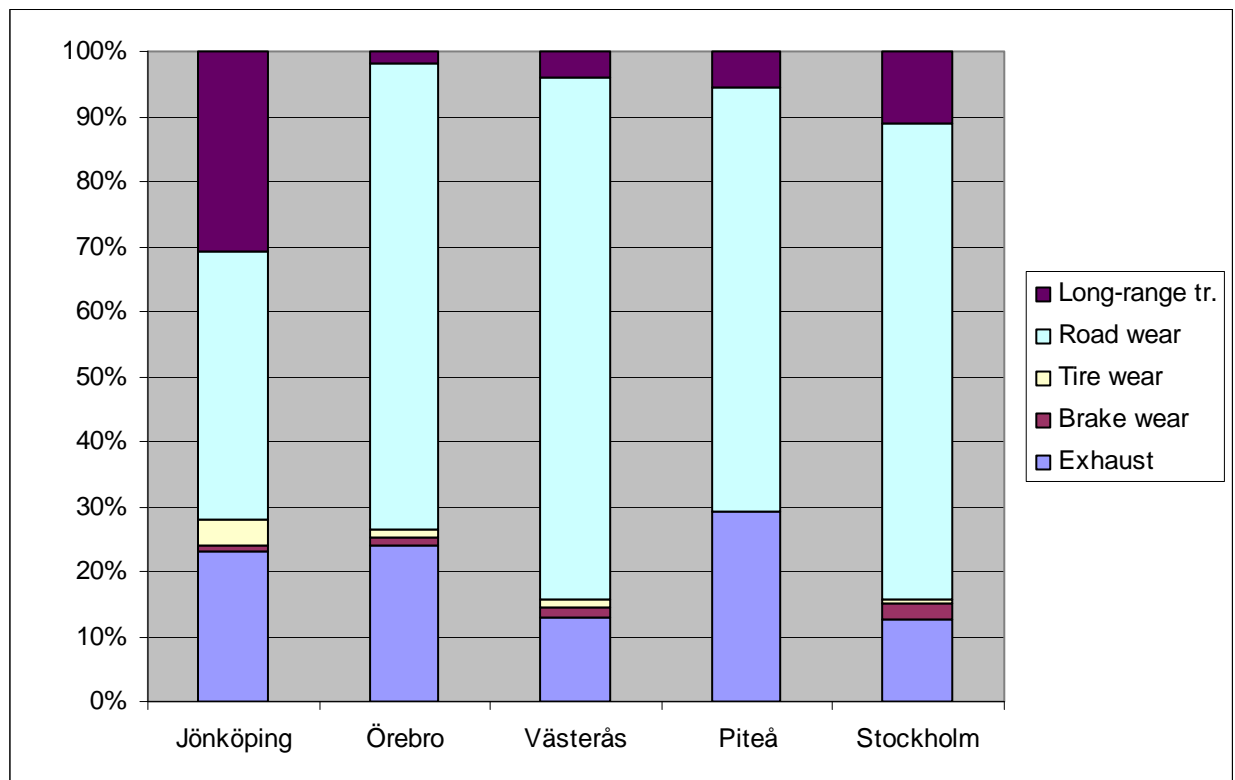


Figure 5.3.11 Relative contribution from sources to urban and Stockholm sites. All contributions for one measurement place are summed and divided by the sum to yield relative contribution of that measurement place.

5.3.9 Comparison of results from different receptor models

First the total emission factor was calculated for Hornsgatan with NO_x as tracer. Then the source profiles from PMF and COPREM was normalized element by element to sum one, for all factors except for the factor identified as long-range transport. Thereafter each normalized source profile was multiplied by the total emission factor. Finally source emission factors according to the PMF and COPREM modeling, respectively, were plotted in log-log diagrams to visualize the differences

and similarities between the source emission factors obtained by the two methods, cf. Figure 5.3.12. There were only three factors out of the five that have distinct interpretable common sources, i.e. tyre, brake and road wear, cf. Figure 5.3.12.

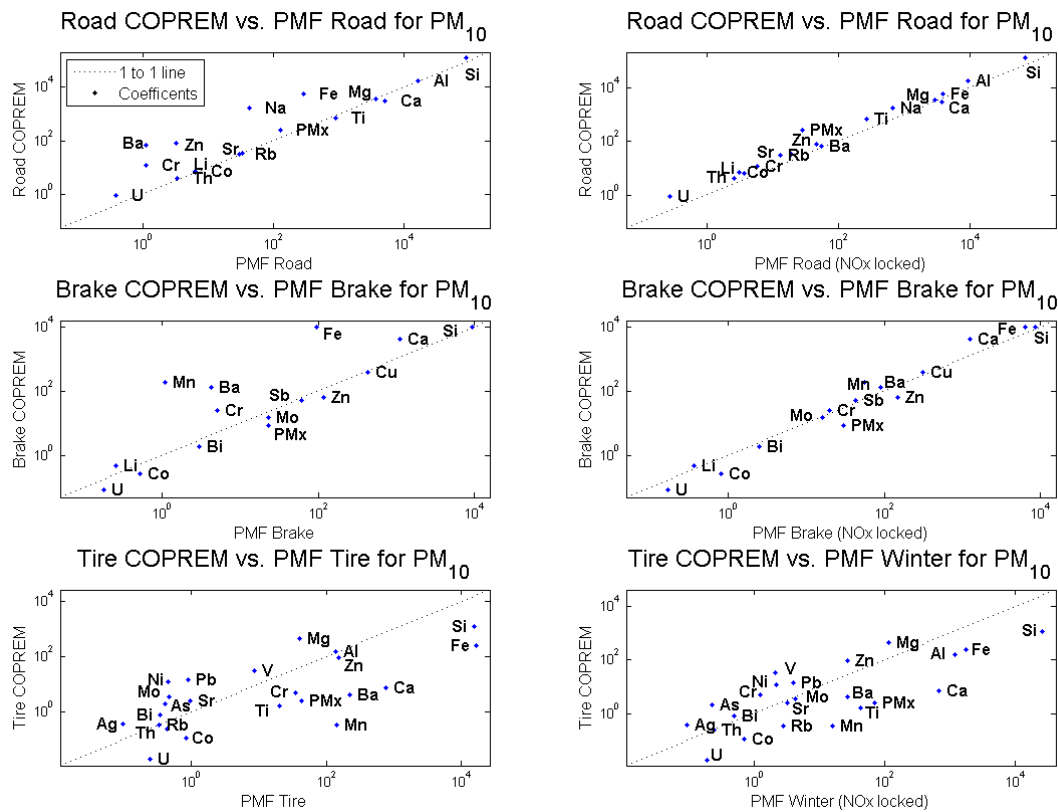


Figure 5.3.12 Comparison of source (from top to bottom: road, brakes and tyres, respectively) emission factors obtained from COPREM and PMF modeling, respectively, with NO_x unlocked (diagrams to the left) and with NO_x locked (diagrams to the right).

In Figure 5.3.12 the results for the NO_x non-locked mode are displayed to the left, whereas the results for NO_x-locked mode are displayed to the right. For the road wear fraction of PM₁₀ (“Road”) there is a good agreement between the two models, although the COPREM model yields slightly higher values than the PMF model. For the brake fraction there is a good agreement for most elements - in particular for the NO_x-locked mode, although the PMF model yields slightly higher values than the COPREM model - except for Mn, Ba and Fe. Regarding the tyre wear fraction the COPREM model yields generally lower values for Si and Fe, but higher values for As, Ni, and Pb than the PMF model, and the agreement between the two models is in general poorer than for the other two PM₁₀ sources. Also, in general the NO_x-locked mode yields a slightly better agreement between the models than the non-locked mode.

One thing worth mentioning further is that in some cases we found a “winter” source in the PMF modeling, other than road wear. This raises the issue if there are other significant yet unknown sources than road wear that increase ambient PM concentrations during winter. Obtaining source profiles for e.g. cold brakes, cold tyres, exhaust during cold start/warm-up of the engine and catalyst, and fuels, would increase the possibility to resolve and investigate such yet unknown phenomena.

The use of pre-separators or not for the sampling of PM₁ and PM_{2.5} may have introduced variations in the base data that possibly affect the quality of the results obtained in the receptor modeling.

5.4 PM and trace element emission factors

5.4.1 Stockholm

Road traffic emission factors (g/vehicle kilometres; g veh⁻¹ km⁻¹) were estimated using NO_x as tracer for traffic emissions as described in Johansson et al. (2009):

$$Ef^{PM} = Ef^{NO_x} \cdot \frac{C_{Street}^{PM} - C_{UB}^{PM}}{C_{Street}^{NO_x} - C_{UB}^{NO_x}}$$

where Ef^{PM} and Ef^{NO_x} are the emission factor for PM (or metal) and NO_x, respectively. C_{street} and C_{UB} are the measured concentrations at street (Hornsgatan) and urban background, respectively. This method has been successfully used in several earlier studies (Ketzler et al., 2003; Gidhagen et al., 2004; Gidhagen et al., 2005; Omstedt et al. 2005). Emission factors for NO_x for Hornsgatan were estimated based on the regional emission data base for Stockholm, hosted by local and regional authorities.

The mean impact of different contributions to fine and coarse PM concentrations at Hornsgatan and the urban background site in central Stockholm is illustrated in Figure 5.4.1 (Johansson & Eneroth, 2007). It can be seen that for coarse particles the contribution from the local traffic at Hornsgatan dominates, whereas for fine particles non-local sources make the largest contribution even at Hornsgatan.

At the urban background site fine particles are mainly from non-local sources and about half of the coarse particle concentrations are due to non-local sources.

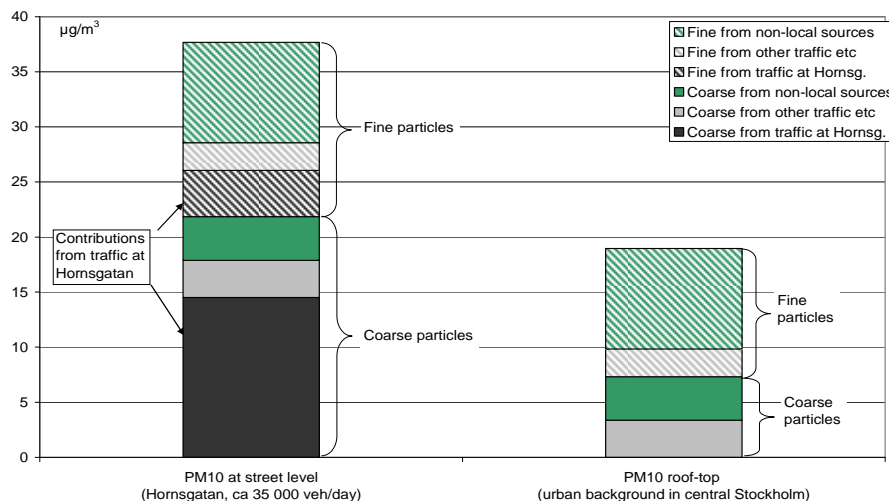


Figure 5.4.1 The relationship between the contribution from local traffic and other sources to the PM₁₀ concentration at Hornsgatan and at Torkel Knutssonsgatan (urban background) in central Stockholm (annual mean contributions). “Fine” particles refer to PM_{2.5} and “Coarse” particles to PM₁₀-PM_{2.5}.

Road wetness has been shown earlier to be very important for the PM emissions from roads (e.g. Norman & Johansson, 2006; Johansson et al., 2008). Since end of 2005 road wetness sensors record the road surface wetness at Hornsgatan. Figure 5.4.2 shows calculated emission factors for PM₁₀ for Hornsgatan for wet and dry periods. Hourly mean road wetness is obtained based on electrical resistance at the road surface. This is a qualitative measurement and in this case wet periods were defined as signals below 2 volts and dry above 2 volts. The emission factor was calculated based on incremental NO_x and PM₁₀ measurements for a three-year period (2006-2008). The emission factors are a factor 4-6 higher for dry compared to wet periods during November to April. For May to October the difference is less than a factor 3. The mean emission factor for dry and wet periods during this period is 281 and 84 mg/vehicle km, respectively. Since road wetness is not easily quantified, other criteria for road wetness may yield different values.

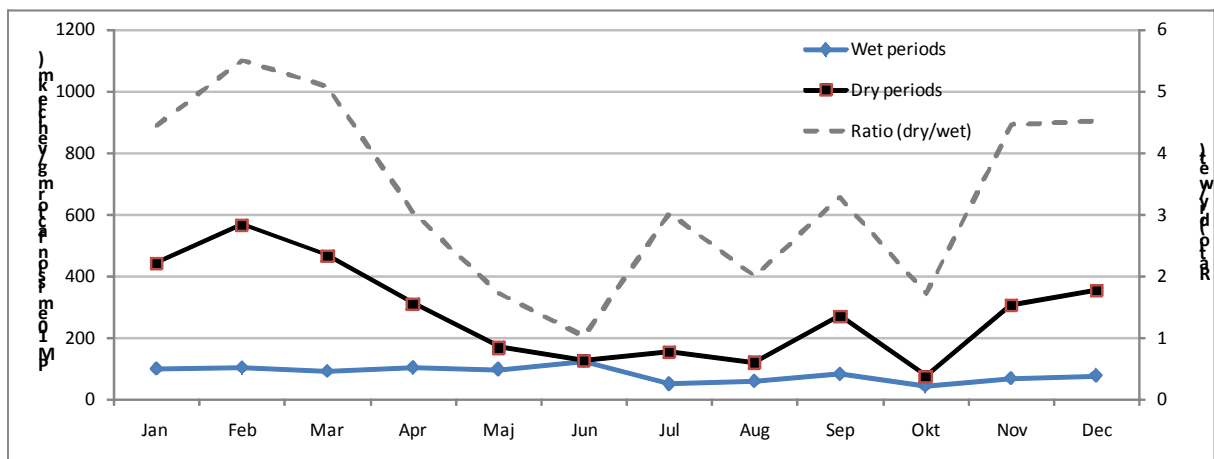


Figure 5.4.2 Influence of road wetness on the derived emission factor for PM₁₀ at Hornsgatan, Stockholm. The data are mean monthly values for 3 years 2006 – 2008, based on hourly measurements of PM₁₀ and NO_x at street and urban background.

Table 5.4.1 shows calculated emission factors for PM, BC and elements based on the daily mean concentrations at Hornsgatan and urban background.

Table 5.4.1 Emission factors for PM₁₀ and PM_{2.5} for Hornsgatan calculated from simultaneous measurements of daily mean concentrations during 2006 and 2007 at the street and at urban background (roof).

	Emission factor PM _{2.5}		Emission factor PM ₁₀		Emission factor PM ₁₀ -PM _{2.5} *=difference not significant	% PM _{2.5} of PM ₁₀ *=difference not significant
	mean ± 95p conf	N	mean ± 95p conf	N		
NO _x (mg/vkm)	775.6 ± 29.9	10	771.6 ± 24.3	14		
PM _x filter (mg/vkm)	75.8 ± 56.2	10	310.5 ± 105.5	13	234.7	0.244
TEOM x1.2 (mg/vkm)	42.0 ± 15.3	6	361.1 ± 144.4	13	319.2	0.12
Sot (<2.5 um) (mg/vkm)	17.7 ± 3.07	6				
Ag (µg/vkm)	0.010 ± 0.007	7	0.38 ± 0.35	9	0.367	0.028
Al (µg/vkm)	3305 ± 2671	9	18094 ± 6909	13	14789	0.183
As (µg/vkm)	0.11 ± 0.07	8	2.01 ± 1.06	9	1.898	0.056
Ba (µg/vkm)	40.7 ± 25.9	10	231.6 ± 55.8	14	190.9	0.176
Bi (µg/vkm)	0.30 ± 0.14	9	3.66 ± 0.97	14	3.36	0.082
Ca (µg/vkm)	1334 ± 1286	6	7240 ± 2369	13	5905	0.184
Cd (µg/vkm)	0.03 ± 0.02	8	0.06 ± 0.06	10	0.03 *	*
Co (µg/vkm)	1.83 ± 1.29	9	8.46 ± 3.44	13	6.63	0.217
Cr (µg/vkm)	48.0 ± 75.9	3	41.7 ± 10.9	5	-6.28 *	*
Cu (µg/vkm)	66.0 ± 24.8	9	454.7 ± 98.4	14	388.8	0.145
Fe (µg/vkm)	2816 ± 1710	9	17309 ± 4618	14	14492	0.163
K (µg/vkm)	1426 ± 1098	9	7163 ± 2728	13	5737	0.199
Li (µg/vkm)	0.44 ± 0.67	8	7.17 ± 3.10	12	6.73	0.062
Mg (µg/vkm)	786.6 ± 567.9	8	4060 ± 1544	13	3273	0.194
Mn (µg/vkm)	35.6 ± 23.8	9	188.4 ± 57.7	14	152.8	0.189
Mo (µg/vkm)	7.60 ± 6.65	10	24.8 ± 5.50	14	17.2	0.307
Na (µg/vkm)	1810 ± 1503	9	7291 ± 3896	12	5481	0.248
Ni (µg/vkm)	27.7 ± 46.1	9	15.6 ± 3.50	13	-12.1 *	*
Pb (µg/vkm)	2.95 ± 1.99	9	22.3 ± 5.54	13	19.3	0.132
Rb (µg/vkm)	6.61 ± 6.28	7	33.6 ± 13.1	13	27.0	0.197
Sb (µg/vkm)	9.13 ± 3.58	9	64.7 ± 15.3	14	55.6	0.141
Si (µg/vkm)	20894 ± 15020	9	140059 ± 82158	13	119165	0.14918
Sr (µg/vkm)	9.31 ± 7.34	8	39.7 ± 14.2	13	30.4	0.234
Th (µg/vkm)	0.43 ± 0.37	9	4.30 ± 1.70	13	3.87	0.100
Ti (µg/vkm)	229.0 ± 202.9	6	1063 ± 425	13	833.9	0.215
Tl (µg/vkm)	0.01 ± 0.01	8	0.10 ± 0.11	10	0.09 *	*
U (µg/vkm)	0.12 ± 0.09	8	1.03 ± 0.49	13	0.905	0.117
V (µg/vkm)	5.66 ± 4.08	8	32.3 ± 11.0	12	26.6	0.176
Zn (µg/vkm)	48.2 ± 21.9	9	276.2 ± 70.1	14	228.0	0.175

For Hornsgatan it can be seen that most of the PM₁₀ emission is due to emissions of coarse particles for all elements. This is expected for crustal elements, like e. g. Al, Si, Ti and Fe. For the crustal elements the fine particle emissions are around 10%-20%. But it is interesting that also elements like Pb (87%) and Zn (83%) are mainly due to emissions in the coarse fraction, indicating that these elements are mainly due to mechanical processes, not associated with combustion. When comparing PM₁₀ and PM_{2.5} concentrations at Hornsgatan, Cu and Sb are mainly coarse (82% and 85%, respectively, was in the coarse fraction). This is somewhat unexpected since laboratory studies have shown most brake wear PM to be in the fine fraction (e. g. Garg et al., 2000). Wåhlin et al. (2006) found that roughly 50% of the brake wear was in the coarse fraction in traffic emissions from streets in Copenhagen.

In 2003/2004 heavy metals were sampled at street and roof level in a similar way as has been done now (Johansson et al., 2009). A comparison with emission factors for some metals obtained from earlier studies in Stockholm (Johansson et al., 2009) is given in Table 5.4.2. It should be noted that the measurements in 2003/2004 was for a full year. In general the emission factors for Hornsgatan obtained based on the 2003/2004 sampling campaign is similar to the sampling made within the present study (2006/2007). For lead the emission factor 2006/2007 (this study) is significantly lower, indicating that the emissions are decreasing, which is consistent with the decrease noted by Johansson et al. (2009) when comparing measurements 2003/2004 with measurements in 1999.

Table 5.4.2 Comparison of emission factors for different metals for Hornsgatan in Stockholm based on measurements 2003/2004 and 2006/2007 (this study) (PM₁₀). Some other studies are also included ($\mu\text{g veh}^{-1} \text{ km}^{-1}$).

Metal	Emission factor (this study) Mean \pm 95 % confidence limit	Emission factor Hornsgatan 2003/2004 (Johansson et al., 2009)	Kaisermühlen-tunnel (Austria, 2002) ¹⁾	Tingstad and Lundby tunnels (Gothenburg, Sweden, 1999/2000) ²⁾	Gelezinis Vilkas tunnel (Vilnius, Estonia, 2000) ³⁾	Söderleden road tunnel (Stockholm, Sweden, 1999) ⁴⁾
Cobalt (Co)	8.5 \pm 3.4	3.5				
Chromium (Cr)	42 \pm 11	41				
Copper (Cu)	455 \pm 98	542	30	Tingstad: 172 Lundby: 147	159	214
Manganese (Mn)	188 \pm 58	110				
Nickel (Ni)	16 \pm 3.5	6.5	1.8			0.14
Lead (Pb)	22.2 \pm 5.5	41	9.5	Tingstad: 36.9 Lundby: 35.1	54	4.8
Zinc (Zn)	276 \pm 70	260	34	Tingstad: 205 Lundby: 239	206	24
Molybdenum (Mo)	24.8 \pm 5.5	22				
Wolfram (W)	-	15				
Tin (Sn)		126				
Antimony (Sb)	64.7 \pm 15.3	144				

¹⁾ Laschober et al. (2004). ²⁾ Sternbeck et al. (2002). ³⁾ Valiulis et al. (2002). ⁴⁾ Kristensson et al. (2004).

5.4.2 Malmö

The emission factors for PM₁₀ and PM_{2.5} were calculated from equation 5.1.

$$EF_{PMx} = EF_{NOx} \frac{(PM_{X,street} - PM_{X,roof})}{([NO_{X,street}] - [NO_{X,roof}])} \quad \text{Eq. (5.1)}$$

The NO_x emission was calculated from actual traffic intensity measurements and emission factors according to Swedish official data provided by the National Road Administration. For light-duty vehicles a factor of 0.6 g NO_x (as NO₂) per vehicle and km was used, and for heavy-duty vehicles 4 g vehicle⁻¹ km⁻¹.

As expected most of the nitric oxide concentration came from local traffic on Amiralsgatan, see Figure 5.4.3. Figure 5.4.4 shows the origin of fine (PM_{2.5}) and coarse (PM₁₀ - PM_{2.5}) particles. Only a small portion of PM_{2.5} comes from Amiralsgatan.

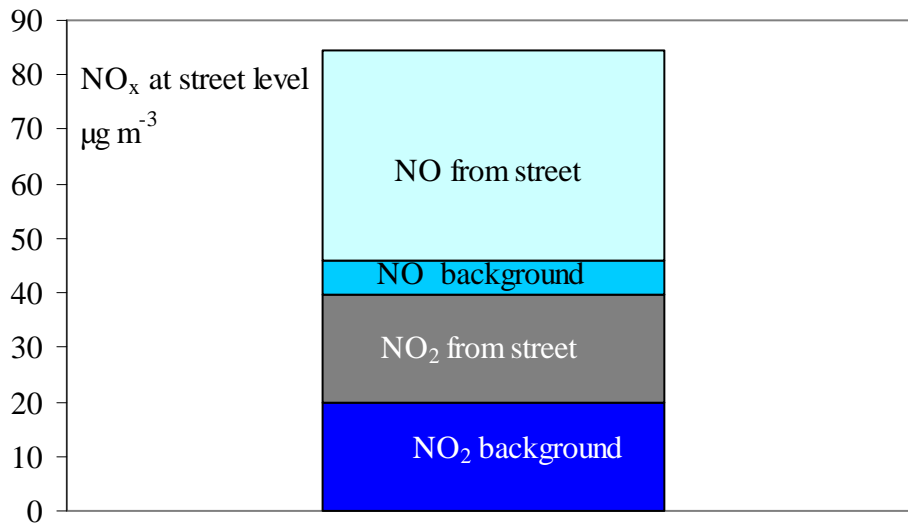


Figure 5.4.3 Origin of ambient air concentrations of NO_x at Amiralsgatan in Malmö.

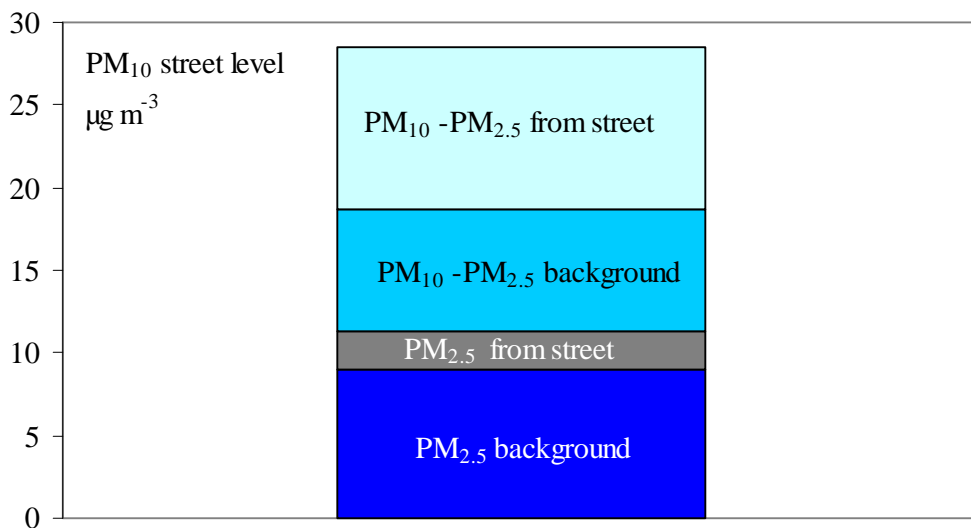


Figure 5.4.4 Origin of fine (PM_{2.5}) and coarse (PM₁₀ - PM_{2.5}) particles at Amiralsgatan.

The calculated average emission factors for PM₁₀ during March to June 2005 are shown in Figure 5.4.5 as hourly means. The average emission factors were calculated as an arithmetic mean value (Eq. 5.2) for data when both NO_x and PM_x concentrations were at least 30 % higher at street level than in the urban background.

$$\overline{EF}_{PM_x} = \frac{1}{n} \sum_1^n EF_{PM_x} \quad \text{Eq. (5.2)}$$

The calculated emission factor for PM₁₀ when the road was wet (it rained the hour before the measurement) is also shown in the same figure. As can be seen from the figure water on the pavement has a drastic effect on the emission of PM₁₀ particles, in accordance with the results for Hornsgatan in Stockholm presented in chapter 5.4.1.

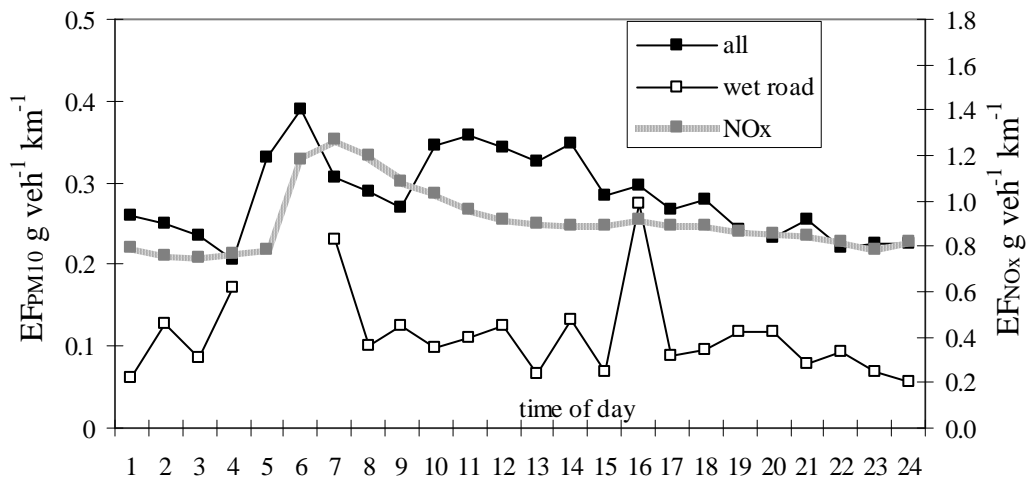


Figure 5.4.5 Hourly average emission factor of PM₁₀ and NO_x as a function of stop time ("wet road" means occasions with rain during the hour before the measurement).

The calculated emission factors for PM_{2.5} during March to June 2005 are shown in Figure 5.4.6 as hourly means. The factors are much lower than for PM₁₀. Heavy traffic consists most of diesel vehicles. The emission factor for NO_x is almost seven times higher for heavy-duty vehicles than for light-duty vehicles. The highest emission factors are found during the morning hours when there is a peak in the fraction of heavy-duty vehicles. This implies that EF_{PM2.5} must be at least seven times higher for heavy-duty vehicles than for light-duty vehicles. The emission factor is not affected so much by wet roads as it is for PM₁₀, indicating that most of the PM_{2.5} arises from exhaust.

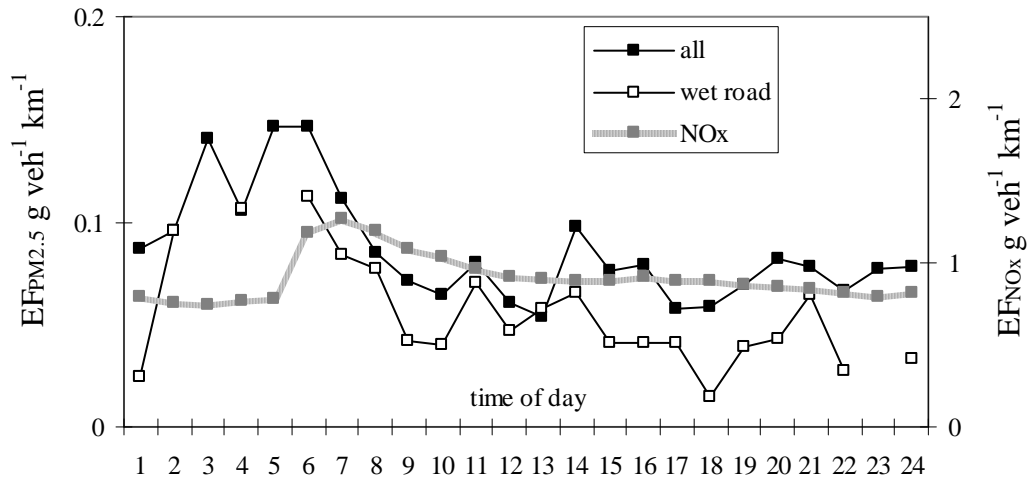


Figure 5.4.6 Hourly average emission factor of PM_{2.5} and NO_x as a function of stop time. ("wet road" means occasions with rain during the hour before the measurement).

In Table 5.4.3 the average emission factors have been calculated in another way (Eq. 5.3) in order to get use of all data. In this way long-term averages of PM_x concentrations can also be estimated from long-term averages of NO_x concentrations.

$$\overline{EF}_{PM_x} = \overline{EF}_{NO_x} \frac{(\overline{PM_{x,street}} - \overline{PM_{x,roof}})}{(\overline{NO_{x,street}} - \overline{NO_{x,roof}})} \quad \text{Eq. (5.3)}$$

Table 5.4.3 Average emission factors for the different months 2005 in g veh⁻¹ km⁻¹.

	March	April	May	June
$\overline{EF}_{PM_{10}} \cdot \text{all}$	0.33	0.22	0.19	0.09
$\overline{EF}_{PM_{10}} \cdot \text{wet road}$	0.10	0.11	0.11	0.03
$\overline{EF}_{PM_{2.5}} \cdot \text{all}$	0.05	0.05	0.03	0.03
$\overline{EF}_{PM_{2.5}} \cdot \text{wet road}$	0.04	0.06	0.04	0.01

The emission factor from traffic of an element x in course mode (index c, PM₁₀ – PM_{2.5}) EF_{x,c} was estimated in the following way. Index "m" indicates the particle mass which was averaged from TEOM measurements. Index "street" is measurements from Amiralsgatan and index "roof" is measurements at the roof of the town hall.

$$EF_{x,c} = PM_{x,c,street} \frac{EF_{NO_x}}{(\overline{NO_{x,street}} - \overline{NO_{x,roof}})} \cdot \frac{(PM_{m,c,street} - PM_{m,c,roof})}{PM_{m,c,street}} \quad (1)$$

Only measurements when $(PM_{m,c,street} - PM_{m,c,roof})/PM_{m,c,street}$ was > 0.7 was used. Only 21 out of 115 measurements fulfilled this criteria and when all other parameters in eq. 1 was available. Most of these measurements represented the month March. Table 5.4.4 summarises the emission factors.

Table 5.4.4 Emission factors for different elements in the course mode.
The total mass was taken from TEOM measurements.

element	EF _{x,c}	S.D.
	mg/km	mg/km
Si	1.93	1.32
K	0.16	0.12
Ca	0.49	0.35
Ti	0.04	0.04
Mn	0.02	0.02
Fe	2.82	1.89
Ni	0.0002	0.0041
Cu	0.14	0.10
Zn	0.03	0.04
Mo	0.75	0.68
mass	409	213

In order to see if any of the elements was emitted from the same source a correlation analysis was made, see Table 5.4.5. Only data that fulfilled the criteria for Table 5.4.4 was used. No element was well correlated to the particle mass. K, Ca and Ti were well correlated with one another, as were Mn, Fe and Cu.

Table 5.4.5 Correlation coefficients r^2 between the air concentration of the elements and the mass of particles in course mode at Amiralsgatan.

	Si	K	Ca	Ti	Mn	Fe	Ni	Cu	Zn	Mo	mass
Si											
K	0.23										
Ca	0.13	0.88									
Ti	0.22	0.83	0.88								
Mn	0.03	0.61	0.56	0.53							
Fe	0.01	0.56	0.55	0.58	0.88						
Ni	0.05	0.28	0.31	0.40	0.60	0.65					
Cu	0.00	0.47	0.48	0.49	0.87	0.99	0.64				
Zn	0.01	0.50	0.54	0.44	0.76	0.73	0.28	0.75			
Mo	0.03	0.15	0.15	0.12	0.02	0.06	0.04	0.06	0.19		
mass	0.28	0.03	0.04	0.04	0.01	0.00	0.05	0.00	0.07	0.27	

5.5 Methods comparison

5.5.1 PM mass measurements

At several sites within this study, several different methods for airborne PM mass determination were used in parallel. This allowed for some methods comparison. In Figure 5.5.1 the TEOM-instrument is compared with the IVL sampler and DustTrak, respectively, for PM₁₀ in the road simulator experiments. Typically, there is a considerable scatter in the comparisons, but the general trend shows a fairly good agreement.

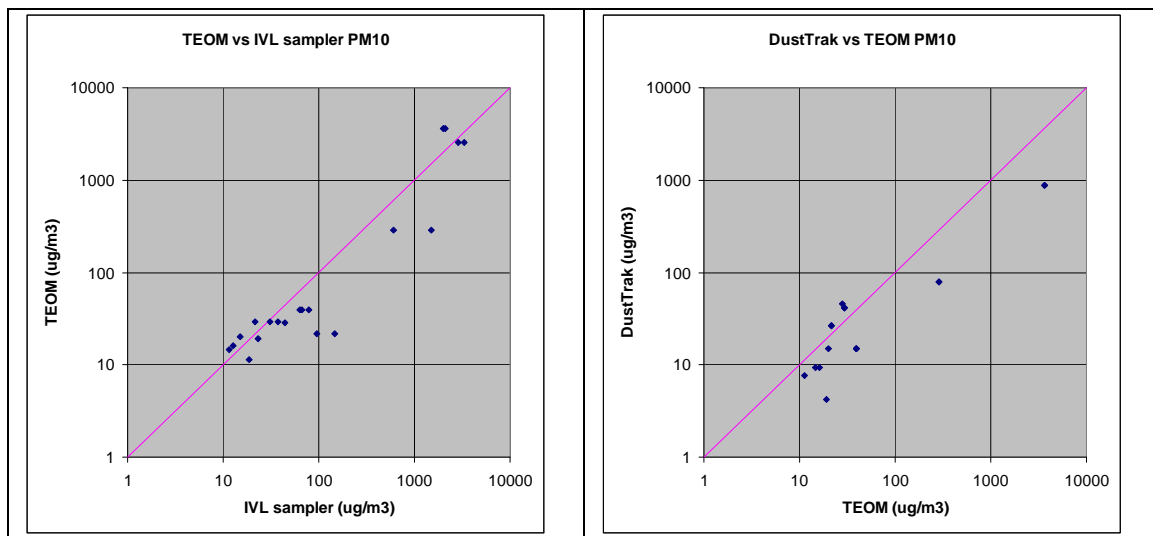


Figure 5.5.1 Comparison between TEOM, the IVL sampler and DustTrak for PM₁₀ in the road simulator experiments.

5.5.2 Elemental and chemical speciation

In some of the road simulator experiments parallel filter samples with the cascade impactor and the IVL sampler were analysed by PIXE and ICP-MS, respectively. A fairly good agreement between the two methods was observed for studded tyres and PM₁₀, whereas for smaller PM fractions, i.e. PM₁, and for summer tyres in general, the agreement was poor cf. Figure 5.5.3. It was believed that the main reason for this was the much lower particle mass encountered for the PM₁ fraction and in the summer tyre runs, thus noise and detection limits of the two analytical methods had much larger influence on the results.

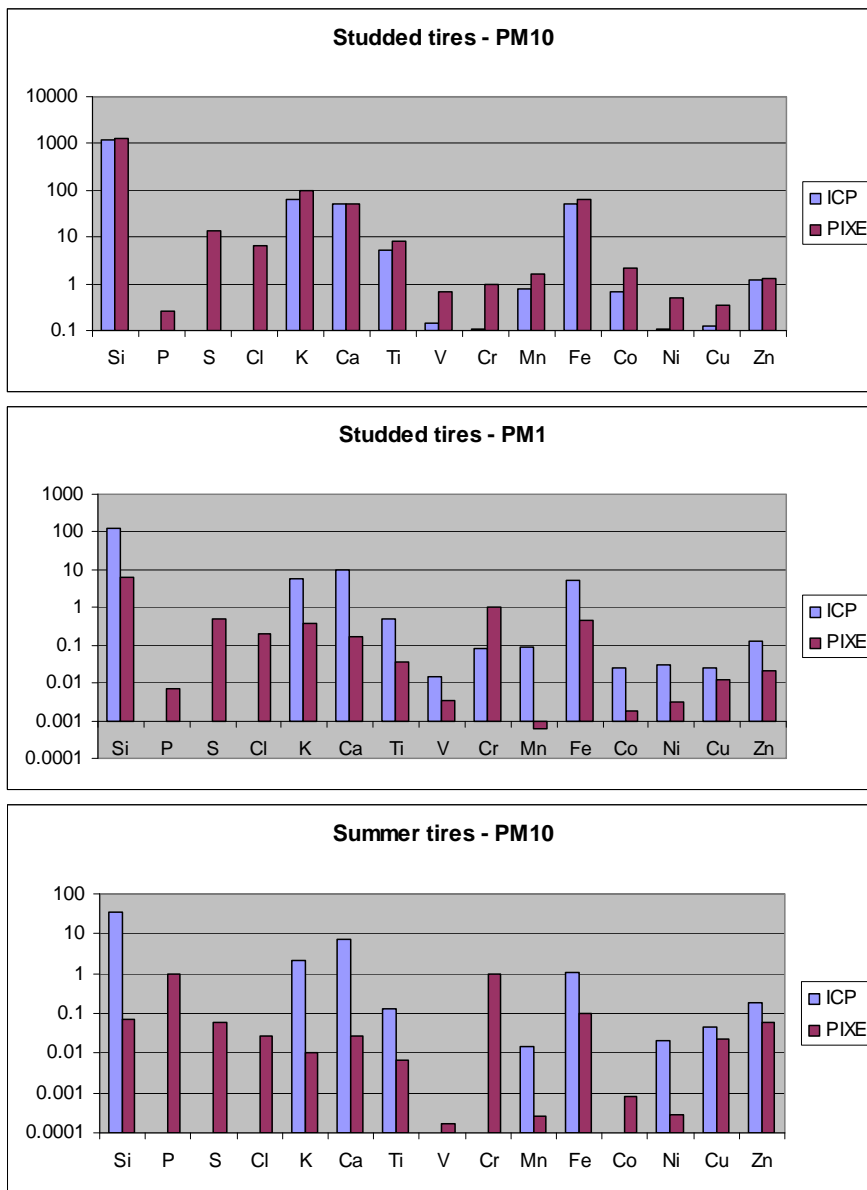


Figure 5.5.3 Comparison of PIXE and ICP-MS analytical results for elements in the road simulator runs for PM₁₀ and PM₁ and studded and summer tyres, respectively.

5.6 Sites comparison

5.6.1 ICP-MS

In Table 5.6.1 the relative concentrations of the elements analysed by ICP-MS (concentration in air in ng m^{-3} divided by PM_X concentration in $\mu\text{g m}^{-3}$) are compared between the road simulator and Hornsgatan. In PM_1 there is a remarkably lower concentration of the stone materials (Si, Al, Ca, K) at Hornsgatan compared to the road simulator. These compounds are more common in PM_{10} than in PM_1 at Hornsgatan. A possible more severe overload of particles on the PM_1 impactor in the road simulator measurements could be one explanation. The combustion compounds (Ni, Pb, Sb, V and Zn) and copper (brakes) are as expected more common in the PM_1 fraction in the Hornsgatan samples than in the road simulator samples.

Regarding PM_{10} , the elemental composition of the stone material is very similar for the Hornsgatan samples and the road simulator samples. The elements Sb, Mo and As are almost non-existing in the road simulator samples.

Table 5.6.1 Elemental concentrations in particulate matter and calculated total mass of oxides.

mg/g	road simulator		Hornsgatan	
	PM_1	PM_{10}	PM_1	PM_{10}
Ag		0.0043		0.0010
Al	45	50	17	53
As		0.0008	0.0039	0.0094
Ba	0.33	0.45	0.21	0.81
Ca	12	24	4	27
Cd		0.0225		0.0005
Co	0.071	0.327	0.009	0.026
Cr	0.026	0.015	0.026	0.106
Cu	0.18	0.32	0.41	1.59
Fe	14	15	17	59
K	14	20	6	22
Li	0.015	0.032	0.006	0.023
Mg	4.7	8.5	3.4	13.5
Mn	0.24	0.23	0.21	0.67
Mo	0.000	0.002	0.045	0.096
Na	11	12	11	31
Ni	0.043	0.080	0.156	0.080
Pb	0.032	0.027	0.122	0.111
Rb	0.058	0.074	0.027	0.099
Sb	0.000	0.001	0.034	0.247
Si	300	304	112	315
Sr	0.098	0.154	0.027	0.131
Th	0.003	0.008	0.001	0.013
Ti	1.2	1.4	1.0	3.2
Tl		0.00016		0.00044
V	0.04	0.04	0.15	0.11
Zn	0.3	1.2	1.0	1.1
Total mass	0.80	0.86	0.33	0.99

The results in Table 5.6.1 are presented graphically for the PM_{10} fraction in Figure 5.6.1. As can be seen the PM_{10} mass is dominated by silicon.

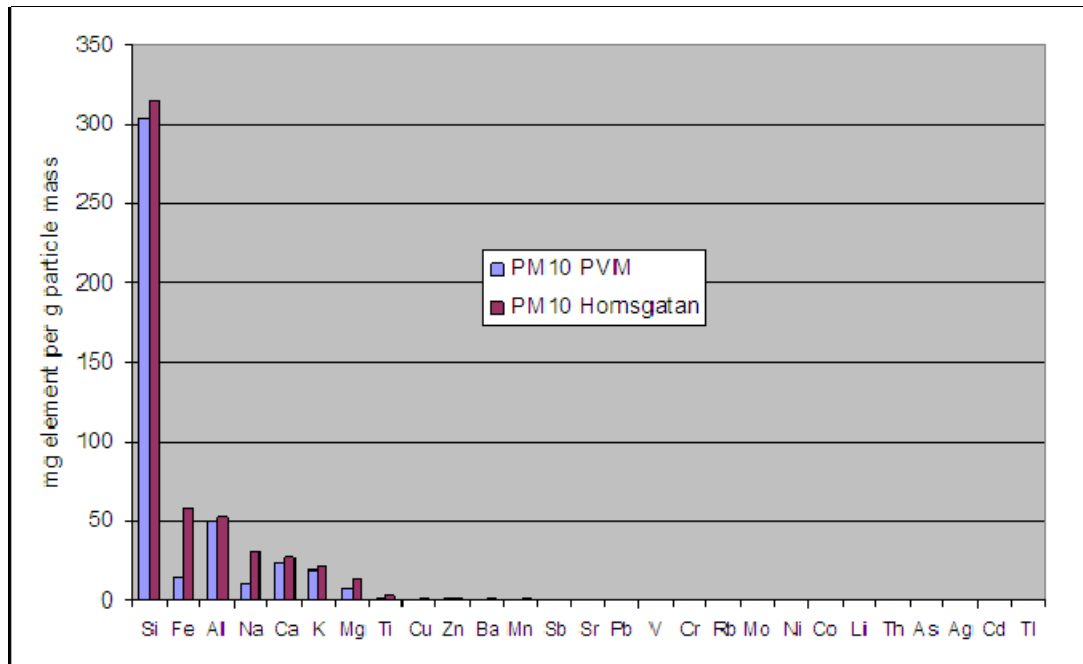


Figure 5.6.1 Average elemental composition of PM₁₀ samples from the road simulator and Hornsgatan, respectively, as analysed by ICP-MS.

5.6.2 PM emission factor determination

For PM₁₀, the following emissions factors were derived for three different sites:

- **Road simulator:** 350 mg/vehkm for studded tyres and speed 70 km/h.
- **Hornsgatan:** 100-600 mg/vehkm during wintertime, the lower range representing wet conditions, the higher range representing dry conditions.
- **Amiralsgatan:** 100-300 g/vehkm during wintertime, the lower range representing wet conditions, the higher range representing dry conditions.

Thus, there was a reasonable agreement in the PM₁₀ emission factor between the three sites.

6 Discussion

The particle size distribution at Hornsgatan is very different from the size distribution at urban background stations. There are much more particles in the coarse mode near the source compared to an urban background site, where most measurements are performed. A large amount of coarse particles therefore has to be removed on the greased impactor plate of the sampler. The smaller size fraction that is selected the more particulate matter has to be removed. Because all three size fractions (PM₁₀, PM_{2.5} and PM₁) are sampled using the same air flow rate, a smaller cut-off is obtained by decreasing the diameter of the jet in front of the impactor plate. This implies that the area of the spot with particles on the impactor plate will approximately be proportional to the aerodynamic cut-off diameter. More particulate matter on a smaller spot will eventually lead to a surface consisting of particles instead of grease. The particles will then bounce-off and be deposited on the filter instead, leading to overestimated concentrations. A photo showing impactors overloaded with particles after sampling of PM_{2.5} is shown in Figure 6.1.

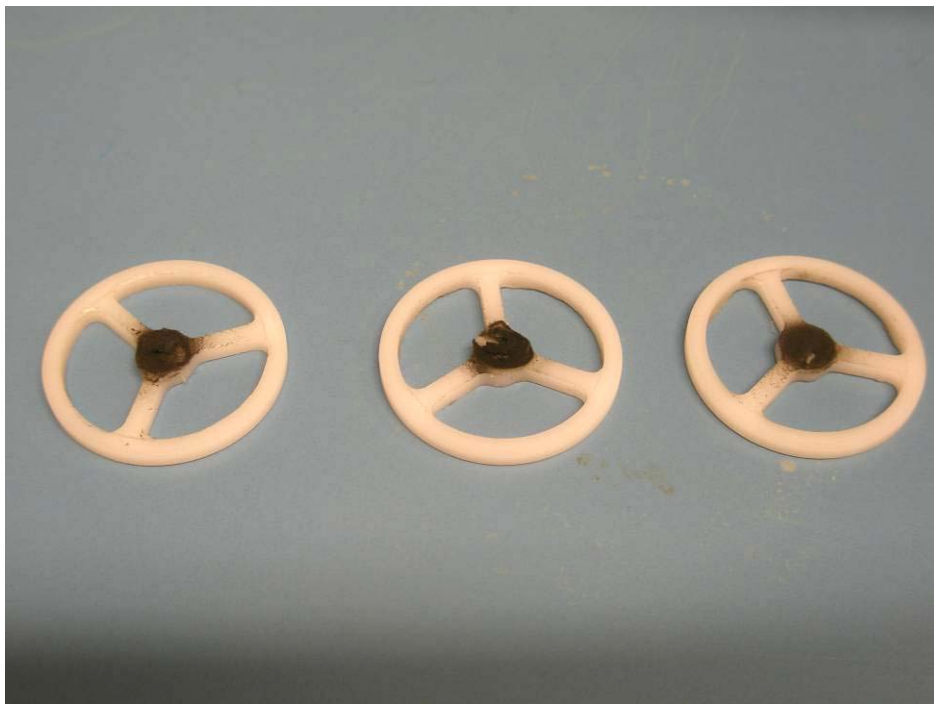


Figure 6.1 Visual evidence of overload of particles on the PM_{2.5} impactor plates.

To eliminate the impactor plate particle overload problem, a pre-separator that fits directly to the inlet of the PM_{2.5}/PM₁ heads and has a cut-off of 10 µm was constructed. The pre-separator was used during the last measurement campaign at Hornsgatan as well as in some experiments in the road simulator.

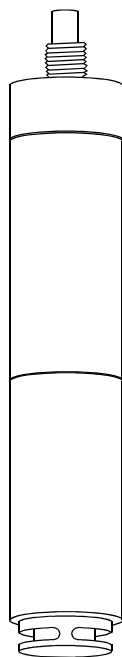


Figure 6.2 PM_{2.5} or PM₁ head with a PM₁₀ pre-separator in front.

The pre-separator was used for PM_{2.5} and PM₁ in the last campaign. Only a few separators were made and the use of a pre-separator was not simultaneously compared to a sampler without pre-separator. The percentage of each element compared to the total mass was compared without pre-separator and with pre-separator. The first and third campaigns were compared to the fourth. The patterns were in most cases, but not always, similar for PM_{2.5} and PM₁. When the pre-separator was used there was less aluminium, calcium, potassium, magnesium, sodium and titanium. The percentages of arsenic, lead and vanadium were rather similar with and without pre-separator.

Furthermore, to log air flow-rate, humidity, temperature and possibly some indicator on traffic density each minute during sampling with above mentioned samplers would be suitable. This could give further information regarding the sampling issues and provide a means of screening out samples that could be less suitable for analysis. That even before any laboratory measurements has been done and if remotely accessible may provide possibility for corrective actions.

In addition the laboratory methods for ICP-MS and PIXE analysis should be scrutinized so that correction factor between methods could be established. For instance silicon for ICP-MS needs more attention.

The sampling procedure using applied grease to catch oversize particles should be further evaluated regarding characterization of elements in the grease used, a sample should be taken and analysed for each batch of grease.

7 Conclusions

From the road simulator study it can be concluded that:

- PM₁₀ emissions for studded tyres in the road simulator are roughly 100 times higher than for summer tyres.
- Use of studded tyres in the road simulator emits ultrafine particles. Other tyre types do not (see Gustafsson et al., 2009 NanoWear).
- PM₁₀ emissions increase with speed for all three tyre types.
- PM₁₀ emissions decrease with increasing tyre temperature and specific humidity for studded and Nordic unstudded tyres, but increase with temperature for summer tyres.
- The coarser part of PM₁₀ when using winter tyres is dominated by mineral particles from the pavement, mainly Si, but also Ca, K and Fe. For summer tyres, the relative contribution of Fe and Zn becomes equally important.
- In the finest size fractions measured using the SDI, the relative concentration of S increases, originating in tyres and/or bitumen.
- For summer tyres and Nordic friction tyres, Zn appears in most size modes, originating in tyres.
- For studded tyres W appears, originating in the tyre studs.

The road simulator can be used to study differences in particle emissions and characteristics and to study how different factors affect these. This project also shows that emission factors can be calculated using the increase and decrease phases after acceleration and deceleration in the road simulator. The emission factors thus calculated seem realistic in comparison with emission factors calculated from measurements in the field. Nevertheless, some uncertainties remain on how to compare the conditions in the road simulator with reality. The effects of the simulator's accelerated road surface wear and constant speed needs to be evaluated and related to real-world conditions. By comparison with emission factors calculated for roads with more similar traffic (constant speeds) and combine these data with relations between road and simulator road wear, it should be possible to calculate PM emission factors representative for real-world conditions.

A good agreement has been observed in the derived PM₁₀ emission factor between the road simulator, Hornsgatan in Stockholm and Amiralsgatan in Malmö. For dry weather conditions in the wintertime (with frequent use of studded tyres) an overall PM₁₀ emission factor of 350-600 mg/vehkm was derived. Wet weather conditions lower the PM₁₀ emission factor significantly, to around 100 mg/vehkm.

Road wear was found to be the dominating source to PM₁₀ in particularly busy streets but also in the urban background in all cities (from southern to northern Sweden) explored in the present study, whereas long-range transport dominates PM₁ at street level and PM_{2.5} at roof level. Our conclusion is that the most cost-effective method to reduce PM₁₀ levels and the exceedances of air quality limits for PM₁₀ in traffic and urban environments is to reduce the number and use of studded tyres.

A possible "winter source", related to low ambient temperatures has been identified as a potentially important source to both PM₁₀ and PM_{2.5}, which needs further investigation.

To improve our understanding of the contribution of various sources to occurring PM concentrations in street and urban environments, above all there is a need of improved knowledge regarding source profiles, in particular tyre wear including studs wear, and elemental composition of the airborne particulate matter.

In the PCA of analysis of PAH from both tyres/bitumen and from air samples from the road simulator, it could be observed that the difference was not as large between different tyres and bitumen. It is therefore recommended that in addition to measure PAH, to measure also other organics with relative low volatility, in order to facilitate separation of different tyre types, e.g. for screening out winter vs. summer tyres. Also a better knowledge of the elemental content of tyres, in particular rubber blends used by trucks and buses, is also vital to facilitate better estimates of the various source contributions to particulate matter in urban environments.

Finally, combined use of different receptor models, such as COPREM and PMF, is encouraged since it may provide complementary information that cannot be obtained by one model only.

8 References

- Cahill, T. A., Eldred, R. A., Barone, J. B., and Ashbaugh, L. L. (1979). Ambient Aerosol Sampling with Stacked Filter Units, Report No. FHWA-RD-78-178, U.S. Department of Transportation, Washington D.C., 73 pp.
- Ferm M., Areskoug H., Makkonen U., Wählin P. and Yttri K. E. (2008). Measurements of PM₁, PM_{2.5} and PM₁₀ in air at Nordic background stations using low-cost equipment. IVL report B1791
- Ferm M., Gudmundsson A. and Persson K. (2001) Measurements of PM₁₀ and PM_{2.5} within the Swedish urban network. Proc. from NOSA Aerosol Symposium Lund, Sweden 8-9 Nov. 2001.
- Garg, B.D., Cadle, S.H., Mulawa, P.A., Groblicki, P.J. (2000). Brake wear particulate matter emissions. *Environmental Science & Technology* 34, 4463–4469.
- Gidhagen, L., C. Johansson, J. Langner and G. Olivares (2004). Simulation of NO_x and ultrafine particles in a street canyon in Stockholm, Sweden, *Atmospheric Environment* 38, 2029-2044.
- Gidhagen, L., C. Johansson, J. Langner and V. Foltescu (2005) Urban scale modeling of particle number concentration in Stockholm. *Atmospheric Environment*, 39, 1711-1725.
- Gidhagen, L., Johansson, C., Langner, J. & Olivares, G. (2003) Simulation of NO_x and Ultrafine Particles in a Street Canyon in Stockholm, Sweden. *Atmospheric Environment, Atmospheric Environment*, 38, 2029-2044.
- Gustafsson, M., Blomqvist, G., Gudmundsson, A., Dahl, A., Jonsson, P. & Swietlicki, E. (2009) Factors influencing PM₁₀ emissions from road pavement wear, *Atmospheric Environment*, In press. (doi:10.1016/j.atmosenv.2008.04.028)
- Gustafsson, M., G. Blomqvist, A. Gudmundsson, A. Dahl, E. Swietlicki, M. Bohgard, J. Lindbom, and A. Ljungman (2008) Properties and toxicological effects of particles from the interaction between tyres, road pavement and winter traction material. *Science of the Total Environment*, 393, 226-240.
- Gustafsson, M., G. Blomqvist, E. Brorström-Lundén, A. Dahl, A. Gudmundsson, C. Johansson, P. Jonsson, and E. Swietlicki (2009) NanoWear - nanopartiklar från däck- och vägbaneslitage? VTI Rapport R660.
- Hansson, H.-C. and Nyman, S. (1985). Microcomputer-controlled two size fractionating aerosol sampler for outdoor environments, *Env. Sci. Technol.* 19, 1110-1115.
- Hjortenkrans, D.T., Bergbäck, B., Häggerud, A.V. (2007) Metal Emissions from Brake Linings and Tires: Case Studies of Stockholm, Sweden 1995, 1998 and 2005. *Env. Sci. Technol.*, 41, 5224-5230.
- Hopke P K, Raunema T, Biegalski S, Landsberger S, Maenhaut W, Artaxo P, Cohen D. (1997) Characterization of the Gent Stacked Filter Unit PM₁₀ sampler. *Aerosol Sci. & Technol.* 27, 726-735
- Jacobson, T., Hornvall, F. (1999) Beläggningsslitage från dubbade fordon, VTI notat 44 (in Swedish). Swedish National Road and Transport Research Institute (VTI), Linköping, Sweden.
- Johansson, C. (2003) TEOM – IVL's filtermetod. En metodjämförelse. SLB Analys rapport SLB 1:2003. http://slb.nu/slb/rapporter/pdf8/slb2003_001.pdf

- Johansson, C., Norman, M. and Burman, L. (2009) Road traffic emission factors for heavy metals. *Atmospheric Environment*, 43, 4681-4688.
- Johansson, C., Norman, M., Gustafsson, M., Lövenheim, B. (2008) Genomsnittliga emissionsfaktorer för PM₁₀ i Stockholmsregionen som funktion av dubbdäcksandel och fordonshastighet. 2008 Stockholm Environment & Health Protection Administration (Miljöförvaltningen) SLB report, 2:2008.
- Johansson, C. & Eneroth, K. (2007) TESS - Traffic Emissions, Socioeconomic valuation and Socioeconomic measures. PART 1. Emissions and exposure of particles and NO_x. Luftvårdsförbundet i Stockholms Uppsala län, 2007:2. SLB-rapport. Miljöförvaltningen, Stockholm. http://www.slb.nu/slb/rapporter/pdf/lvf2007_2.pdf
- Johansson, C., Norman, M., Omstedt, G., Swietlicki, E. (2004) Partiklar i stadsmiljö – källor, halter och olika åtgärders effekt på halterna mätt som PM₁₀. SLB analys rapport nr. 4:2004. Miljöförvaltningen, Box 38 024, 10064 Stockholm. http://www.slb.nu/slb/rapporter/pdf/pm10_4_2004_050117.pdf.
- Johansson, C., Omstedt, G. & Gidhagen, L. (2004) Traffic related source contributions to PM₁₀ near a highway. Presented at the European Aerosol Conference, Budapest, Sep., 6 - 9, 2004.
- Kaye, G. W. C. and Laby, T. H. (1959) Tables of physical and chemical constants and some mathematical functions, Longmans, Green (London and New York), 12th Edition, 231 p.
- Ketzel, M., Omstedt, G., Johansson, C., Düring, I., Pohojola, M., Oettl, D., Gidhagen, L., Wählin, P., Lohmeyer, A., Haakana, M., Berkowicz, R (2007) Estimation and validation of PM_{2.5}/PM₁₀ exhaust and non-exhaust emissionfactors for practical street pollution modelling. *Atmos. Environ.* 41, 9370-9385.
- Ketzel, M., Wählin, P., Berkowicz, R., Palmgren, F. (2003). Particle and trace gas emission factors under urban driving conditions in Copenhagen based on street and roof-level observations. *Atmospheric Environment* 37, 2735–2749.
- Kristensson, A., Johansson, C., Westerholm, R., Swietlicki, E., Gidhagen, L.,
- Laschober, C., Limbeck, A., Rendl, J., Puxbaum, H. (2004) Particulate emissions from on-roadvehicles in the Kaisermuhlen-tunnel (Vienna, Austria). *Atm. Env.* 38, 2187–2195.
- Maenhaut, W., Salma, I., Cafmeyer, J., Annegarn, H. J., and Andreae, M. O. (1996) Regional atmospheric aerosol composition and sources in the eastern Transvaal, South Africa, and impact of biomass burning. *J. Geophys. Res.*, 101, 631-650-
- Marsteen L. and Schaug J. (2007) A PM₁₀ intercomparison exercise in Norway. Norwegian Institute for Air Research. Report No 41/2007.
- Martens, H. and Naes, T., *Multivariate calibration*, John Wiley and Sons, Chichester 1989.
- Norman, M. & Johansson, C. (2006) Studies of some measures to reduce road dust emissions from paved roads in Scandinavia. *Atmospheric Environment*, 40, 6154-6164.
- Olivares, G., Johansson, C., Ström, J. Hansson, H.C. (2007) The role of ambient temperature for particle number concentrations in a street canyon. *Atmospheric Environment*, 41, 2145-2155.
- Omstedt, G. & Johansson, C. (2004). Uppskattning av emissionsfaktor för bensen. SLB analys rapport nr. 2:2004. Miljöförvaltningen, Box 38 024, 100 6 Stockholm.
- Omstedt, G., Johansson, C., & Bringfelt, B. (2005). A Model for vehicle Induced Non-tailpipe Emissions of Particles Along Swedish Roads. *Atmospheric Environment*, 39, 6088-6097.

- Paatero P., Tapper U. (1994) Positive Matrix Factorization: a non-negative factor model with optimal utilization of error estimates of data values *Environmetrics*, 5, 111-126.
- Paatero, P. (1997) Least squares formulation of robust non-negative factor analysis studies *Chemom. Intell. Lab. Syst.*, 37, 23-35.
- Paatero, P., Hopke, P. K. (2003) Discarding or downweighting high-noise variables in factor analytic models. *Analytica Chimica Acta*, 490, 277–289. Swietlicki, E., Nilsson, T., Kristensson, A.,
- Räsänen, M., Kupiainen, K., Tervahattu, H. (2003) The effect of mineralogy, texture and mechanical properties of anti-skid and asphalt aggregates on urban dust. *Bulletin of Engineering Geology and the Environment* 62, 359-368.
- Shariff A, Bulow K, Elfman M, Kristiansson P, Malmqvist K, Pallon J. (2003) Calibration of a new chamber using GUPIX software package for PIXE analysis. *Nucl. Instr. & Meth. Phys. Res. B* 189, 131-137.
- Sternbeck, J., Sjödin, A. (2002) Metal emissions from road traffic and the influence of resuspension - results from two tunnel studies. *Atmospheric Environment* 36 (30), 4735–4744.
- Valiulis, D., Cerburnis, D., Sakalys, J., Kvietkus, K. (2002) Estimation of atmospheric trace metal emissions in Vilnius City, Lithuania, using vertical concentration gradient and road tunnel measurement data. *Atmospheric Environment* 36, 6001–6014.
- Wählin, P., Berkowicz, R., Palmgren, F. (2006) Characterisation of traffic-generated particulate matter in Copenhagen, *Atmospheric Environment*, 12, 2151-2159.
- Wold, S., Esbensen, K. och Geladi, P. (1987) Principal Component Analysis, *Chemom. Intell. Lab. Syst.* 2, 37-52.
- Wågberg, L.-G. (2003) Bära eller Brista, Handbok i tillståndsbedömning av belagda gator och vägar - ny omarbetad upplaga. Svenska Kommunförbundet, Stockholm. Wählin, P., 2003. COPREM – A multivariate receptor model with a physical approach. *Atmospheric Environment* 37 , 4861-4867.

Appendix 1.

**Calculated source contributions for the PM₁₀, PM_{2.5}
and PM₁ fractions at Hornsgatan according to PMF**

Table A1.1 Calculated PMF (G sum normalized) source contributions to the measured concentrations in PM10 samples at Hornsgatan. Units: ng/m³.

	Tyre	Road	Brake	Winter/Exhaust	Long-range
PM ₁₀	5646	16537	3028	15032	14904
Ag	0.02	0.02	0.03	0.02	0.02
Al	23.20	2749	11.19	263.5	8.93
As	0.10	0.05	0.30	0.04	0.09
Ba	44.90	0.22	0.85	0.27	0.20
Bi	0.06	0.03	0.55	0.04	0.05
Ca	153.7	1015	222.9	65.26	58.07
Co	0.14	1.07	0.09	0.14	0.07
Cr	4.87	0.15	0.72	0.07	0.07
Cu	1.17	1.65	87.45	0.53	0.37
Fe	3270	56.75	18.61	24.95	23.57
K	29.48	1027	23.28	132.0	22.97
Li	0.07	1.12	0.05	0.06	0.06
Mg	6.75	613.4	64.03	1.07	77.58
Mn	29.44	7.93	0.22	0.68	0.31
Mo	0.10	0.12	5.09	0.09	0.06
Na	10.63	10.56	8.07	1772	7.56
Ni	0.07	0.04	2.27	0.03	2.00
Pb	0.16	0.16	3.66	0.13	2.15
Rb	0.06	4.93	0.04	0.59	0.05
Sb	0.15	0.31	13.42	0.15	0.15
Si	1717	9858	1028	2725	1884
Sr	0.18	6.09	0.83	0.32	0.08
Th	0.07	0.55	0.05	0.04	0.06
Ti	3.32	144.8	7.49	19.26	6.61
U	0.04	0.07	0.03	0.04	0.04
V	0.03	0.04	0.02	0.03	6.25
Zn	31.92	0.65	24.36	0.23	6.41
NO _x	1059	616.7	81963	43839	593.8

Table A1.2 Calculated mean emission factors based on the derived default PMF (G sum normalized) source contributions and the total emission factors estimated (independently) using NOx as tracer and the street increment as presented earlier. Unit is $\mu\text{g}/\text{vkm}$ except for PM₁₀ which is mg/vkm.

Emission factor	Total emission factor	Tyre	Road	Brake	Winter/Exhaust
PM ₁₀					
mg/fkm	310.5	43.56	127.6	23.37	116.0
Ag	0.38	0.10	0.09	0.10	0.09
Al	18094	137.8	16325	66.43	1564
As	2.01	0.40	0.22	1.25	0.15
Ba	231.60	224.94	1.09	4.24	1.33
Bi	3.66	0.33	0.18	2.95	0.19
Ca	7240	763.7	5044	1107	324.3
Co	8.46	0.82	6.28	0.53	0.84
Cr	41.73	34.99	1.10	5.14	0.50
Cu	454.7	5.84	8.29	438.0	2.64
Fe	17309	16793	291.5	95.60	128.1
K	7163	174.32	6071	137.6	780.4
Li	7.17	0.39	6.19	0.25	0.34
Mg	4060	40.00	3634	379.3	6.32
Mn	188.4	144.9	39.04	1.09	3.35
Mo	24.76	0.46	0.53	23.34	0.43
Na	7291	43.03	42.73	32.68	7173
Ni	15.61	0.44	0.24	14.75	0.18
Pb	22.27	0.89	0.86	19.79	0.72
Rb	33.58	0.33	29.50	0.23	3.52
Sb	64.73	0.71	1.44	61.87	0.71
Si	140059	15685	90083	9391	24899
Sr	39.72	0.94	32.59	4.47	1.73
Th	4.30	0.43	3.35	0.31	0.21
Ti	1063	20.15	880.2	45.51	117.1
U	1.03	0.24	0.38	0.18	0.23
V	32.26	8.49	9.82	6.02	7.94
Zn	276.2	154.2	3.15	117.7	1.11

Table A1.3 Calculated (based on PMF, G sum normalized and NO_x locked towards zero for two factors) source contributions to the measured concentrations in PM₁₀ samples at Hornsgatan. Units: ng/m³.

	<i>Exhaust</i>	<i>Brake</i>	<i>Winter</i>	<i>Road</i>	<i>Long-range</i>
PM ₁₀	25091	4162	9979	4030	14302
Ag	0.02	0.03	0.02	0.02	0.03
Al	1102	41.55	188.1	1443	279.6
As	0.05	0.26	0.05	0.09	0.11
Ba	10.67	16.70	4.98	10.28	3.71
Bi	0.07	0.43	0.09	0.05	0.09
Ca	291.5	244.3	134.6	747.4	115.3
Co	0.63	0.14	0.12	0.52	0.12
Cr	2.11	2.74	0.17	0.82	0.11
Cu	10.11	58.03	12.20	3.75	7.19
Fe	940.2	1128	318.9	698.1	311.6
K	465.1	21.38	138.5	463.7	153.6
Li	0.47	0.06	0.07	0.64	0.11
Mg	98.80	54.54	19.15	484.2	114.6
Mn	12.53	10.39	2.95	9.17	3.67
Mo	0.31	3.33	0.90	0.55	0.37
Na	291.1	78.99	1227	162.2	36.22
Ni	0.13	1.68	0.38	0.49	1.83
Pb	0.65	2.43	0.83	0.66	1.77
Rb	2.60	0.05	0.43	2.00	0.61
Sb	1.22	8.58	2.13	0.85	1.36
Si	3789	968.3	2989	8074	1956
Sr	2.28	0.69	0.56	3.28	0.72
Th	0.17	0.07	0.04	0.42	0.07
Ti	105.3	7.92	6.51	40.54	23.83
U	0.07	0.03	0.03	0.05	0.04
V	1.51	0.18	0.17	0.67	3.81
Zn	10.17	28.30	5.29	8.90	11.57
NO _x	0.00	59465	59142	11973	0.00

Table A1.4 Calculated mean emission factors based on the derived default PMF (G sum normalized and NOx locked towards zero for three factors) source contributions and the total emission factors estimated (independently) using NOx as tracer and the street increment as presented earlier. Unit is $\mu\text{g}/\text{vkm}$ except for PM_{10} which is mg/vkm .

	Total emission factor	Winter	Road	Brake	Exhaust
PM_{10}					
mg/fkm	310.5	71.62	28.92	29.87	180.1
Ag	0.38	0.09	0.10	0.11	0.08
Al	18094	1227	9411	271.0	7186
As	2.01	0.23	0.40	1.14	0.24
Ba	231.6	27.07	55.84	90.70	57.99
Bi	3.66	0.51	0.30	2.47	0.38
Ca	7240	687.2	3816	1248	1489
Co	8.46	0.71	3.12	0.82	3.81
Cr	41.73	1.24	5.84	19.60	15.05
Cu	454.7	65.97	20.26	313.8	54.68
Fe	17309	1789	3916	6328	5275
K	7163	911.4	3051	140.7	3060
Li	7.17	0.38	3.71	0.37	2.72
Mg	4060	118.4	2993	337.2	610.8
Mn	188.4	15.85	49.29	55.86	67.39
Mo	24.76	4.37	2.67	16.23	1.49
Na	7291	5085	672.2	327.4	1207
Ni	15.61	2.20	2.88	9.78	0.75
Pb	22.27	4.05	3.22	11.84	3.15
Rb	33.58	2.84	13.24	0.32	17.18
Sb	64.73	10.80	4.30	43.44	6.19
Si	140059	26466	71479	8573	33541
Sr	39.72	3.26	19.12	4.03	13.31
Th	4.30	0.24	2.59	0.42	1.05
Ti	1063	43.16	268.8	52.51	698.4
U	1.03	0.19	0.27	0.17	0.39
V	32.26	2.15	8.55	2.30	19.27
Zn	276.2	27.73	46.69	148.4	53.35

Table A1.5 Calculated (based on PMF, 4 factors, G sum normalized) source contributions to the measured concentrations in PM_{2.5} samples at Hornsgatan. Units: ng/m³.

	<i>Brake</i>	<i>Road</i>	<i>Exhaust</i>	<i>Long-range</i>
PM _{2.5}	5827	13029	2351	1661
Ag	0.03	0.02	0.03	0.02
Al	0.14	627.6	0.09	41.82
As	0.10	0.04	0.07	0.02
Ba	2.38	5.99	0.67	0.44
Bi	0.05	0.04	0.04	0.02
Ca	15.55	263.9	7.17	18.02
Co	0.05	0.19	0.06	0.13
Cr	0.20	0.71	0.12	2.74
Cu	8.87	2.35	2.55	1.82
Fe	165.2	370.0	55.13	34.90
K	24.34	254.1	7.23	18.85
Li	0.05	0.14	0.05	0.02
Mg	2.34	143.7	2.13	10.88
Mn	1.85	5.32	0.43	0.54
Mo	0.48	0.13	0.19	0.95
Na	4.48	330.6	76.42	15.59
Ni	0.08	0.04	0.09	4.88
Pb	0.80	0.43	0.30	0.28
Rb	0.06	1.22	0.04	0.09
Sb	1.40	0.29	0.39	0.14
Si	656.8	2877	632.6	422.3
Sr	0.05	1.62	0.06	0.09
Th	0.04	0.08	0.04	0.02
Ti	0.45	38.05	0.07	2.07
U	0.03	0.03	0.03	0.02
V	0.68	0.59	0.05	0.40
Zn	5.24	5.18	3.45	2.96
NO _x	24124	5389	111460	6588

Table A1.6 Calculated (based on PMF, 4 factors, G sum normalized, NOx locked towards zero for two factors) source contributions to the measured concentrations in PM_{2.5} samples at Hornsgatan. Units: ng/m³.

	<i>Winter</i>	<i>Road</i>	<i>Exhaust</i>	<i>Brake/ Long-range</i>
PM _{2.5}	2973.76	11142.11	4384.49	4337.48
Ag	0.02	0.02	0.03	0.03
Al	124.71	529.57	0.06	24.45
As	0.03	0.04	0.09	0.07
Ba	1.46	4.87	1.61	1.54
Bi	0.03	0.03	0.04	0.04
Ca	62.05	215.81	7.43	23.05
Co	0.05	0.17	0.05	0.15
Cr	0.18	0.64	0.11	1.31
Cu	1.00	2.45	5.35	6.75
Fe	88.73	306.45	116.47	112.31
K	51.71	209.88	12.46	31.26
Li	0.04	0.13	0.06	0.04
Mg	32.38	106.83	0.44	16.99
Mn	1.21	4.36	1.15	1.44
Mo	0.09	0.13	0.17	1.08
Na	434.24	24.88	34.72	10.30
Ni	0.10	0.08	0.06	1.60
Pb	0.11	0.41	0.56	0.73
Rb	0.24	1.01	0.06	0.08
Sb	0.12	0.32	0.97	0.79
Si	1017.43	2340.53	686.87	547.19
Sr	0.34	1.33	0.09	0.06
Th	0.04	0.06	0.04	0.04
Ti	7.29	31.59	0.13	1.79
U	0.02	0.03	0.03	0.03
V	0.13	0.54	0.05	1.03
Zn	0.75	5.06	5.58	5.23
NO _x	0.00	9027.26	137970.41	0.00

Table A1.7 Calculated (based on PMF, 4 factors, G sum normalized) source contributions to the measured concentrations in PM₁ samples at Hornsgatan. Units: ng/m³.

	Brake	Exhaust	Road	Long-range
PM ₁	2329	3202	1087	1851
Ag	0.02	0.03	0.02	0.03
Al	122.7	4.09	13.85	3.82
As	0.04	0.06	0.03	0.09
Ba	1.07	0.14	0.20	0.36
Bi	0.02	0.03	0.02	0.04
Ca	36.74	4.59	5.06	3.85
Co	0.04	0.05	0.03	0.04
Cr	0.04	0.04	0.48	0.02
Cu	0.75	0.10	2.14	0.47
Fe	104.2	6.40	5.49	26.20
K	42.55	4.89	9.00	6.06
Li	0.04	0.06	0.03	0.09
Mg	27.68	0.14	1.07	0.05
Mn	1.14	0.19	0.23	0.20
Mo	0.14	0.07	0.21	0.04
Na	48.16	0.56	17.85	12.18
Ni	0.01	0.92	0.48	0.01
Pb	0.20	0.36	0.34	0.12
Rb	0.22	0.03	0.03	0.04
Sb	0.10	0.06	0.05	0.11
Si	606.9	425.7	294.0	346.5
Sr	0.19	0.07	0.04	0.07
Th	0.03	0.03	0.02	0.04
Ti	7.80	0.15	0.41	0.08
U	0.02	0.03	0.02	0.03
V	0.12	1.08	0.01	0.04
Zn	2.06	1.71	2.62	1.28
NO _x	4863	34270	3662	96648

Table A1.8 Calculated (based on PMF, 4 factors, G sum normalized, NOx locked towards zero for two factors) source contributions to the measured concentrations in PM₁ samples at Hornsgatan. Units: ng/m³.

	Brake	Exhaust	Road	Long-range
PM ₁	963.9	2376	2365	2776
Ag	0.02	0.03	0.02	0.03
Al	13.29	3.52	123.20	4.45
As	0.03	0.09	0.04	0.05
Ba	0.20	0.40	1.08	0.08
Bi	0.02	0.04	0.03	0.03
Ca	5.19	3.94	36.88	4.67
Co	0.03	0.05	0.04	0.04
Cr	0.39	0.02	0.04	0.06
Cu	2.37	0.22	0.70	0.17
Fe	4.61	29.48	105.70	2.40
K	8.33	6.26	43.20	4.70
Li	0.03	0.09	0.04	0.05
Mg	0.54	0.05	28.23	0.24
Mn	0.22	0.22	1.15	0.17
Mo	0.20	0.04	0.14	0.08
Na	22.67	9.42	47.30	0.39
Ni	0.32	0.02	0.01	1.05
Pb	0.32	0.12	0.20	0.38
Rb	0.03	0.04	0.22	0.03
Sb	0.06	0.11	0.11	0.04
Si	296.6	365.3	611.6	409.3
Sr	0.03	0.07	0.20	0.06
Th	0.02	0.04	0.03	0.03
Ti	0.33	0.09	7.86	0.17
U	0.02	0.03	0.02	0.03
V	0.01	0.08	0.11	1.04
Zn	2.44	1.43	2.09	1.65
NO _x	0.00	131920	7566	0.00

Appendix 2.

**Calculated (COPREM) source contributions to PM₁₀ in
4 cities within the Swedish Urban Air Quality Network**

Table A2.1 Calculated (by means of the COPREM-model) source contributions to the measured concentrations in PM₁₀ samples from Piteå. Units: ng/m³.

	Exhaust	Brake wear	Tyre wear	Road wear	Long-range transport	Residue
PM ₁₀	8929	21.52	17.39	20000	1714	0.00
Ag	0.00	0.02	0.00	0.00	0.01	0.03
Al	0.00	190.7	1.08	1379	22.20	0.00
As	0.27	0.36	0.00	0.00	0.08	0.01
Ba	2.46	0.00	4.15	8.03	0.27	-0.02
Bi	0.06	0.00	0.00	0.00	0.01	0.02
Ca	0.00	456.7	0.05	229.0	32.07	0.00
Cd	0.03	0.00	0.00	0.02	0.02	0.02
Co	0.12	0.00	0.00	0.30	0.02	-0.03
Cr	1.04	1.03	0.00	0.00	0.11	0.00
Cu	6.06	1.07	0.00	0.00	0.24	-0.02
Fe	81.71	297.1	0.00	626.1	21.63	0.00
K	78.98	0.00	501.2	0.00	31.89	0.00
Li	0.00	0.07	0.00	0.95	0.02	0.01
Mg	10.68	0.00	118.02	168.8	20.06	0.00
Mn	0.00	21.62	0.00	0.00	0.71	0.00
Mo	0.25	0.00	0.00	0.00	0.07	-0.06
Na	0.00	0.00	569.2	0.00	110.0	0.00
Ni	0.73	0.00	0.22	0.00	0.56	0.00
Pb	1.57	0.00	0.00	1.09	0.82	0.08
Rb	0.15	1.29	0.46	1.42	0.09	0.01
Sb	0.55	0.15	0.00	0.00	0.06	-0.03
Si	0.00	0.00	4.79	5782	105.7	0.00
Sr	0.48	0.00	1.89	2.24	0.14	-0.01
Th	0.00	0.00	0.00	0.37	0.00	-0.02
Ti	11.34	0.00	0.01	37.10	0.92	0.00
Tl	0.01	0.00	0.00	0.02	0.00	0.08
U	0.00	0.00	0.00	0.16	0.00	0.04
V	0.09	0.00	0.00	1.48	1.06	-0.09
Zn	15.15	0.00	0.61	5.79	4.00	0.00

Table A2.2 Calculated (by means of the COPREM-model) source contributions to the measured concentrations in PM₁₀ samples from Örebro. Units: ng/m³.

	Exhaust	Brake wear	Tyre wear	Road wear	Long-range transport	Residue
PM ₁₀	14362	703.6	798.5	42750	1151	0.00
Ag	0.03	0.01	0.00	0.00	0.01	0.05
Al	0.00	0.00	49.74	2948	14.91	0.00
As	0.12	0.05	0.22	0.00	0.06	0.00
Ba	6.09	9.54	1.35	20.76	0.18	0.00
Bi	0.00	0.16	0.00	0.01	0.01	-0.05
Ca	0.00	602.5	2.28	489.5	21.54	0.00
Cd	0.05	0.00	0.06	0.00	0.02	-0.01
Co	0.15	0.08	0.06	0.87	0.01	-0.01
Cr	1.70	2.26	0.06	0.00	0.08	0.00
Cu	0.00	35.14	0.00	0.00	0.16	0.00
Fe	1234	886.0	21.17	246.6	14.53	0.00
K	1350	0.00	0.00	0.00	21.42	0.00
Li	1.55	0.01	0.05	0.07	0.02	0.01
Mg	7.55	0.00	6.78	686.6	13.47	0.00
Mn	30.94	10.27	0.10	0.00	0.47	0.00
Mo	0.00	1.82	0.00	0.00	0.05	0.01
Na	0.00	0.00	49.72	1294	73.86	0.00
Ni	1.24	0.39	0.11	0.00	0.38	0.00
Pb	0.00	0.00	5.69	2.89	0.55	0.00
Rb	5.24	0.18	0.06	1.65	0.06	0.00
Sb	0.03	5.02	0.00	0.00	0.04	0.00
Si	0.00	0.00	220.1	12359	71.01	0.00
Sr	2.38	0.42	0.00	3.28	0.09	0.00
Th	0.85	0.00	0.00	0.00	0.00	-0.03
Ti	42.77	0.00	0.34	79.30	0.62	0.00
Tl	0.04	0.00	0.00	0.00	0.00	-0.06
U	0.39	0.01	0.00	0.06	0.00	0.02
V	3.37	0.00	0.00	0.00	0.71	-0.02
Zn	0.00	31.57	27.79	12.38	2.69	0.00

Table A2.3 Calculated (by means of the COPREM-model) source contributions to the measured concentrations in PM₁₀ samples from Västerås. Units: ng/m³.

	Exhaust	Brake wear	Tyre wear	Road wear	Long-range transport	Residue
PM ₁₀	4353	441.5	387.6	26815	1345	0.00
Ag	0.01	0.02	0.00	0.00	0.01	-0.09
Al	0.00	73.97	24.14	1849	17.41	0.00
As	0.18	0.00	0.28	0.00	0.07	0.00
Ba	0.53	16.73	3.60	0.00	0.21	0.00
Bi	0.00	0.03	0.04	0.00	0.01	0.03
Ca	0.00	216.0	1.11	307.0	25.16	0.00
Cd	0.11	0.00	0.03	0.00	0.02	-0.02
Co	0.00	0.23	0.32	0.09	0.01	0.00
Cr	0.46	3.14	0.00	0.00	0.09	0.00
Cu	1.81	22.05	0.00	0.00	0.18	0.00
Fe	34.01	801.3	0.00	379.9	16.97	0.00
K	1.47	0.00	885.5	0.00	25.02	0.00
Li	0.00	0.09	0.00	0.54	0.02	-0.01
Mg	12.85	0.00	0.00	274.0	15.74	0.00
Mn	0.00	18.99	0.05	0.00	0.55	0.00
Mo	0.11	0.68	0.72	0.00	0.06	-0.01
Na	0.00	0.00	0.00	772.2	86.25	0.00
Ni	0.41	0.00	1.53	0.00	0.44	-0.01
Pb	1.38	0.00	2.79	0.00	0.64	0.00
Rb	0.00	0.00	1.35	4.12	0.07	-0.01
Sb	0.40	3.15	0.00	0.00	0.05	0.01
Si	0.00	0.00	106.8	7752	82.93	0.00
Sr	0.07	1.53	0.79	0.78	0.11	0.00
Th	0.00	0.00	0.00	0.99	0.00	-0.05
Ti	2.57	0.00	0.17	49.74	0.72	0.00
Tl	0.00	0.00	0.02	0.00	0.00	0.02
U	0.00	0.00	0.00	0.36	0.00	-0.06
V	0.16	0.00	0.00	1.62	0.83	-0.02
Zn	4.54	13.73	13.49	7.76	3.14	0.00

Table A2.4 Calculated (by means of the COPREM-model) source contributions to the measured concentrations in PM₁₀ samples from Jönköping. Units: ng/m³.

	Exhaust	Brake wear	Tyre wear	Road wear	Long-range transport	Residue
PM ₁₀	3820	141.3	645.7	6809	5082	0.00
Ag	0.00	0.00	0.02	0.00	0.02	0.13
Al	0.00	0.00	40.22	469.6	57.82	0.00
As	0.06	0.00	0.25	0.00	0.22	-0.01
Ba	0.55	1.52	0.41	3.76	0.69	0.00
Bi	0.00	0.00	0.02	0.00	0.02	-0.03
Ca	0.00	214.3	1.85	77.96	83.56	0.00
Cd	0.00	0.00	0.19	0.00	0.06	-0.01
Co	0.02	0.07	0.08	0.18	0.04	0.01
Cr	0.30	0.00	0.65	0.72	0.30	0.00
Cu	0.90	7.06	0.00	0.00	0.61	0.01
Fe	16.25	219.2	0.00	266.2	56.35	0.00
K	67.46	0.00	169.9	0.00	83.09	0.00
Li	0.02	0.00	0.07	0.08	0.06	-0.01
Mg	8.78	0.00	0.00	208.5	52.26	0.00
Mn	0.00	8.44	0.08	0.00	1.84	-0.01
Mo	0.00	0.00	0.18	0.00	0.18	-0.09
Na	91.82	0.00	0.00	132.3	286.5	0.00
Ni	0.00	0.00	1.04	0.00	1.47	-0.02
Pb	7.31	0.00	0.00	0.00	0.00	-0.01
Rb	0.00	0.43	0.24	0.10	0.22	-0.01
Sb	0.53	1.01	0.00	0.00	0.16	-0.01
Si	0.00	0.00	178.0	1968	275.4	0.00
Sr	0.19	0.00	0.00	1.77	0.36	0.02
Th	0.00	0.01	0.01	0.02	0.01	-0.06
Ti	9.23	0.00	0.28	12.63	2.40	0.00
Tl	0.01	0.00	0.01	0.00	0.01	-0.03
U	0.00	0.00	0.00	0.01	0.00	0.03
V	0.35	0.00	0.55	0.50	0.60	-0.03
Zn	0.00	0.00	22.48	1.97	10.42	0.00